Construction and Building Materials 470 (2025) 140432

Contents lists available at ScienceDirect

Construction and Building Materials

journal homepage: www.elsevier.com/locate/conbuildmat

Thin spray-on liners (TSLs) as surface support in underground mining: A review

Hyun Jin Kim [a], Kunze Li [b], Selahattin Akdag [b], Chengguo Zhang [b,*], Joung Oh [b], Pengfei Jiang [c], Patrick T. Spicer [a], Per B. Zetterlund [a], Serkan Saydam [b]

[a] Cluster for Advanced Macromolecular Design, School of Chemical Engineering, The University of New South Wales, Sydney, NSW 2052, Australia
[b] School of Minerals and Energy Resources Engineering, The University of New South Wales, Sydney, NSW 2052, Australia
[c] CCTEG Coal Mining Research Institute, Beijing, China

ARTICLE INFO

Keywords:
Thin spray-on liner (TSL)
Surface support
Ground support
Support mechanisms
Mechanical properties
Civil engineering
Underground mining

ABSTRACT

Thin spray-on liner (TSL) is a thin layer of polymeric liner that provides substantial support to the underlying rock mass. TSLs exhibit high tensile, bond, and flexural strengths with short curing time, making them a practical alternative to conventional supporting systems such as shotcrete. Various laboratory tests and field applications have demonstrated that TSLs play crucial roles in underground mines, including prevention of gas leakage, mitigation of rock burst damage, and reduction in weathering of rock masses. However, despite their widespread use over the past decades, TSL applications face limitations due to the lack of standardized testing methods and comprehensive understanding of materials involved. To fully explore the potential of TSL technology, this paper aims to examine the compositions of TSL materials, the chemical and physical interactions during curing, various testing methods for determining TSL properties, and the practical applications of TSL. This review intends to provide valuable insights for researchers and industry professionals, with a focus on enhancing safety and efficiency across a wide range of TSL applications.

1. Introduction

Rock support serves as a fundamental element in both underground mining and various open-cut operations by preventing the movement of excavation boundaries and maintaining overall stability [1]. An integrated ground support system consists of reinforcement and surface support components. Reinforcement support elements, such as rock bolts and cable bolts, improve the rock mass properties and maintain rock mass integrity. Surface support elements, such as mesh, shotcrete, and thin spray-on liner (TSL), provide a reactive force at the excavation boundary to prevent the loosening of fragments and unraveling [2]. Bolts, shotcrete, and TSL provide active support by immediately

Abbreviations: 2-EHA, 2-Ethylhexyl acrylate; 2-HEMA, 2-Hydroxyethyl methacrylate; AA, Acrylic acid; AM, Acrylamide; APTS(, 3-Aminopropyl) triethoxysilane; ASTM, American Society for Testing and Materials; BDMA, Dimethylbenzylamine; C_2S, Dicalcium silicate; C_3A, Tricalcium aluminate; C_3S, Tricalcium silicate; C_4AF, Tetracalcium ferroaluminate; CAH, Calcium aluminum hydrate; CH, Portlandite; CR, Chloroprene rubber; C−S−H, Calcium silicate hydrate; CTS, 3-Chloropropyltrimethoxysilane; DBTDL, Dibutyltin dilaurate; DETDA, Diethyltoluene diamine; DMF, Dimethylformamide; DSS, Double-sided shear strength; EAA, Ethylene acrylic acid; EVA, Poly(ethylene-vinyl acetate); F/C, Fiber/cement ratio; FTIR, Fourier transform infrared spectroscopy; GPTMS, 3-Glycidoxypropyltrimethoxysilane; HEMC, Hydroxyethyl methyl cellulose; HMDI, Hexamethylene diisocyanate; HPMC, Hydroxypropyl methylcellulose; IPDA, Isophorone diamine; IPDI, Isophorone diisocyanate; LS, Lignosulfonates; LVDT, Linear variable displacement transducers; MAA, Methacrylic acid; MAPTAC, 3-Trimethyl ammonium propyl methacrylamide chloride; MBAM, *N-N*'-*M*ethylenebisacrylamide; MDI, Methylene diphenyl diisocyanate; MFFT, Minimum film formation temperature; MMA, Methyl methacrylate; MWD, Molecular weight distribution; *n*BA, *n*-Butyl acrylate; P/C, Polymer/cement ratio; PA, Polyamide; PAE, Polyacrylic ester; PAM, Polyacrylamide; PAPI, Polymethylene polyphenylene isocyanate; PCE, Polycarboxylates; PE, Polyethylene; PEO, Polyethylene oxide; PF, Phenolic formaldehyde; PMS, Polymelamine sulphonates; PNS, Polynaphthalene sulphonates; POEDP, Polyoxyetheylene diphosphonate; PP, Polypropylene; PPE, Personal protective equipment; PVA, Polyvinyl alcohol; RH, Relative humidity; SAE, Poly(styrene-acrylic ester); SBR, Styrene-butadiene rubber; SDBS, Sodium dodecylbenzenesulfonate; SDS, Sodium dodecyl sulfate; St, Styrene; TBP, Tributyl phosphate; TCEP, Tris(2-chloroethyl) phosphate; TCP, Tricresyl phosphate; TDI, Toluene diisocyanate; TEOA, Triethanolamine; TGA, Thermogravimetric analysis; TIPA, Triisopropanolamine; TSL, Thin spay-on liner; VA, Vinyl acetate; VA/VeoVA, Poly(vinyl acetate-vinyl ester); VAE, Poly (vinyl acetate-ethylene); VOCs, Volatile organic compounds; W/C, Water/cement ratio; XSB, Carboxylated styrene-butadiene rubber.

* Corresponding author.
E-mail address: chengguo.zhang@unsw.edu.au (C. Zhang).

https://doi.org/10.1016/j.conbuildmat.2025.140432
Received 4 September 2024; Received in revised form 3 February 2025; Accepted 12 February 2025

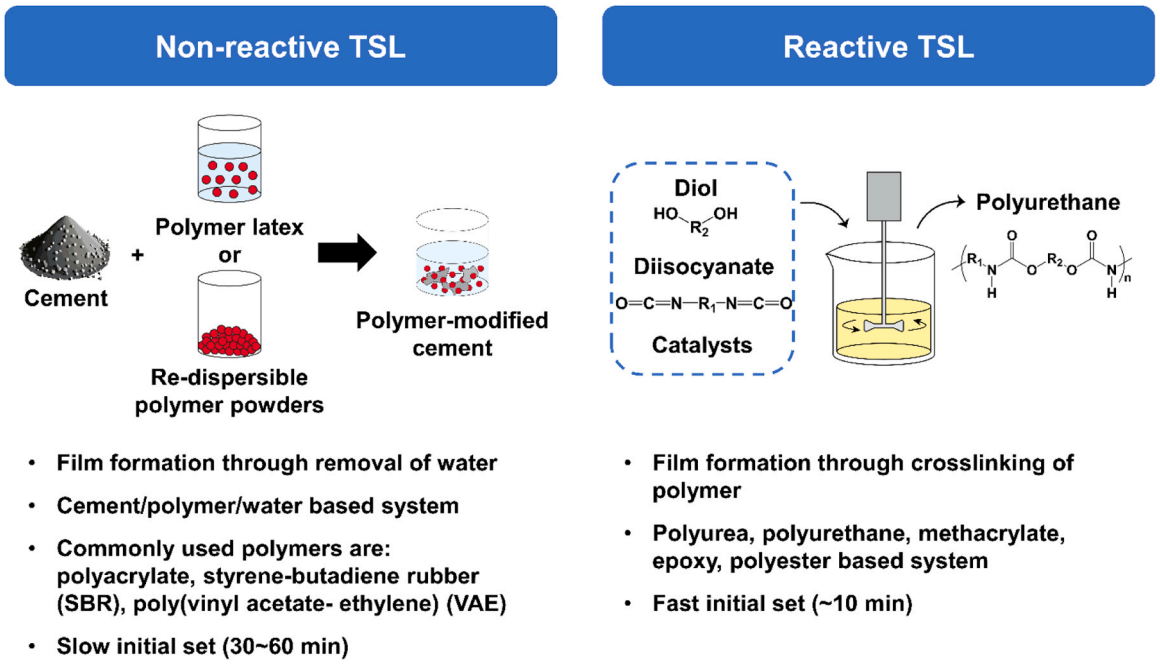

Fig. 1. Schematic illustrations of non-reactive and reactive TSL.

stabilizing the surrounding rock upon installation, thus preventing rock mass deformation and unraveling. On the other hand, mesh serves as a passive support, providing reinforcement when significant rock mass deformation occurs due to disintegration [3].

Conventionally, a combination of reinforcement and surface support utilizing bolts, mesh, or shotcrete has been employed as a high-yielding capacity support system on difficult ground conditions [4]. Shotcrete, which is concrete projected at high velocity, is typically applied at mining excavation with a thickness of a few tens of mm to provide active surface support. However, several problems were encountered when utilizing shotcrete. Shotcrete has a long curing time, and dust generation is often an issue. In addition, shotcrete support structures are susceptible to cracking and spalling, posing severe safety hazards to mining operations. Therefore, significant attention was paid to developing a new cost-effective surface rock support technology that exhibits improved yielding capacity, enhanced strength properties, bond strength, and rapid curing period as an alternative to shotcrete [5,6].

In the late 1980s, the idea of applying TSLs, a thin coat of chemical products on rock mass, as a surface support was first suggested by Archibald of Queen's University in Canada [7]. In the beginning, TSLs were primarily developed as sealants to prevent the further crumbling of rock masses [8]. These liners have been commonly used as sealants in civil engineering projects for many years and were later introduced in the mining industry for surface support. TSLs initially emerged in the extractive industry to improve rock mass integrity and minimize the effects of weathering on rock formations [9].

A TSL, often referred to as a membrane, is a thin layer of liners containing polymeric material that is sprayed onto rock surfaces with a thickness ranging from 3 to 5 mm to provide substantial support to the underlying rock mass [10,11]. TSL often consists of polymer powders or polymer latex with a mixture of sand, cement, and water. Compared to shotcrete, TSL has numerous advantages, including faster curing time, higher tensile, adhesion, flexural strength, and the ability to prevent air infiltration into the rock mass and to penetrate open joints and fractures [4]. Furthermore, TSL is versatile and easy to apply, thus making it considered a substitute for traditional mesh and shotcrete [5,6]. By securely uniting the key blocks, TSL enhances the overall stability and integrity of rock mass, mitigating the risk of structural instability and potential rockfall hazards [5].

Various TSL products have been developed to date and tested to achieve the desired properties such as tensile and adhesion strength, toughness, and elasticity, to support rock mass in mining operations. Numerous laboratory tests and field applications have revealed that TSLs serve multiple functions in underground excavation such as prevention of gas leakage, mitigation of rock burst damage, and reduction in weathering of rock mass in underground mines. However, comprehensive studies are required to fully understand the potential field applications of TSLs, particularly in enhancing the stability and integrity of rock mass and mitigating the risk of potential rockfall hazards in underground mining. While understanding the chemical properties of substances is crucial for designing TSLs with desired properties, the majority of research has focused on determining the mechanical and physical properties of TSLs. The diverse properties of polymers, the complexity of the formulation process, and the potential toxicity represent significant challenges that need to be addressed [12]. To the best of our knowledge, the composition, structure, and chemical/physical interactions during the curing process of TSL materials have not been thoroughly investigated. Hence, this paper focuses on reviewing TSL materials, the chemical and physical interactions that occur during the curing of TSL materials, common testing methods for determining TSL properties, and the general applications and field trials of TSLs in mining and civil engineering.

2. TSL materials

Since the late 1980s, a wide range of TSL materials with diverse physical properties has been developed to provide surface support in various ground and mining conditions. An ideal TSL should exhibit high tensile, adhesive, and shear strength with rapid curing time. The application of TSL should be simple with minimum surface preparation at a low cost. Most importantly, the final product should be self-extinguishable and adhere to health and safety regulations to ensure the safety of operators at mining sites. Numerous products were developed and tested in laboratories and mining sites in an effort to obtain environmentally friendly TSL products that can be produced and applied at a low cost demonstrating ideal mechanical properties [7].

The selection of materials is crucial in designing TSL as it determines the mechanical properties of the final product. Typically, TSL consists of

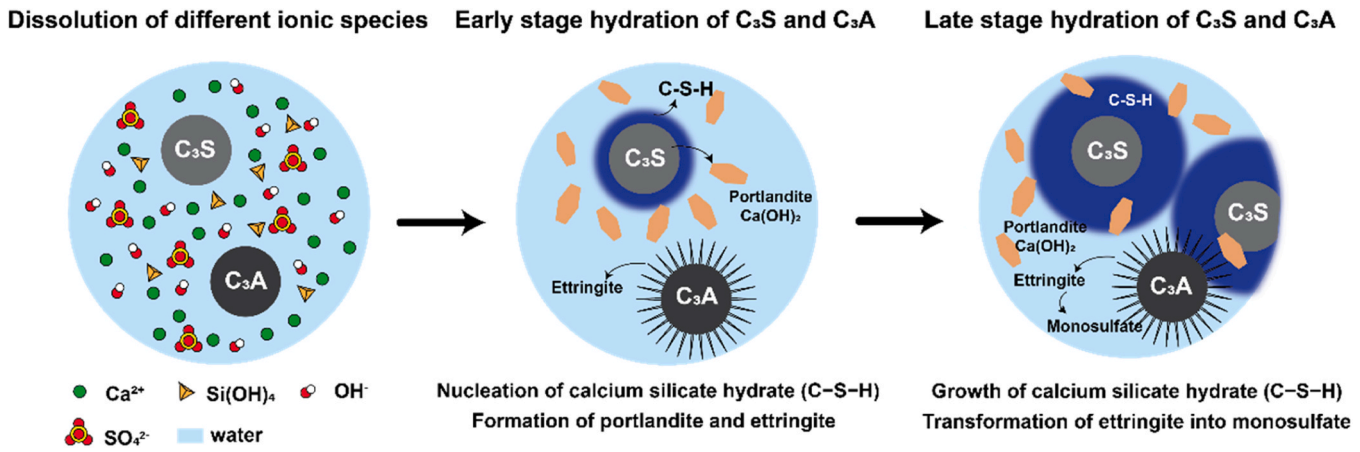

Fig. 2. Schematic illustration of hydration process in ordinary Portland cement.

multiple components such as cement, polymer latex, and other additives, and these components are mixed at the nozzle before they are sprayed onto the rock surface. TSLs can be categorized into single, two, or three-component liners depending on the number of components required to be mixed to form the final product [13,14]. Single-component liners are composed of powders containing cement and polymers that can be mixed with water. Two- or three-component liners can be powder/liquid type consisting of cement, fillers, and polymer latex or liquid/liquid type consisting of pre-polymers, monomers, and catalysts. Throughout the curing process, the components in TSLs react to form a membrane on the surface of the rock mass.

Based on their nature, TSL products can be categorized into two categories *i.e.* non-reactive and reactive TSLs (Fig. 1) [4, 13, 15, 16]. Non-reactive TSLs form membranes through the removal of water as in conventional paint application. Long curing times of 30–60 min are required to acquire significant strength due to the hydration process of cement. They are considered suitable for meeting the desired cycle time conditions in various underground construction applications [16]. On the contrary, reactive TSLs form membranes through exothermic reactions facilitated by a catalyst or an initiator which results in cross-linking of polymers [4]. Curing is rapid and the material attains its strength within a short period of time. Reactive TSLs are usually two-component products based on polyurethane, polyurea, or methacrylate systems [17] Before applying reactive TSLs, occupational health and safety risks need to be thoroughly investigated as isocyanate-based products (polyurethane or polyurea-based products) often cause health and safety issues.

A significant factor to be considered in selecting TSL is the curing time, which provides a primary distinction between non-reactive and reactive TSLs. The performance of the resulting polymer depends on the ratio of the initial components. Any alteration in the ratio of material components can impact the physical properties of the resulting liner [18]. Therefore, it is essential to tailor the properties of the liner when designing a TSL to suit specific rock mass conditions and the type of rock present in the mine. Several commercial TSL products have been utilized to date [4, 13, 19]. With an increasing demand for TSL products, extensive studies have been conducted to design and test TSLs based on different requirements [20–25].

2.1. Non-reactive TSL

Non-reactive TSLs are typically composed of Portland cement and various chemical admixture components, polymers in the form of emulsion or powder, and fillers such as polypropylene fibers. The curing process of non-reactive TSLs is dictated by the hydration of cement. Polymers and chemical admixtures modify rheological behavior and the hydration process, thereby enhancing mechanical properties such as tensile strength, strain at break, and adhesive strength. Hence, it is crucial to understand the polymer film formation and cement hydration processes and the influence of polymers on the fresh and hardened TSLs to successfully design non-reactive TSLs depending on the purpose of application.

2.1.1. Portland cement and chemical admixtures

The amount of Portland cement and chemical admixtures comprise a significant amount of non-reactive TSL and can be up to 50 wt%. Ordinary Portland cement is composed of four minerals – tricalcium silicate C_3S ($SiO2{\cdot}3CaO$), dicalcium silicate C_2S ($SiO_2{\cdot}2CaO$), tricalcium aluminate C_3A ($Al_2O_3{\cdot}3CaO$), and tetracalcium ferroaluminate C_4AF ($4CaO{\cdot}Al_2O_3{\cdot}Fe_2O_3$). In Portland cement, the silicate phase, C_3S and C_2S, makes up 75 wt%, and the aluminous phase, C_3A and C_4AF, makes up to 16 wt%. It also contains minor amounts of magnesia (MgO), free lime, calcium sulfate ($CaSO_4$), pozzolanic materials, and various chemical admixtures. The mixture of minerals and chemical admixtures undergoes a hydration process as it reacts with water [26,27].

The silicate phase (C_2S and C_3S) forms calcium silicate hydrate (C−S−H) and hydrated lime referred to as portlandite CH ($Ca(OH)_2$) upon the addition of water as expressed in Eq.1 (Fig. 1) [26]. Precipitation of an amorphous or poorly crystalline phase C−S−H provides the development strength of cementitious materials as it serves as the main binding phase. C_3S reacts rapidly and contributes to the early strength development within 7 days. On the other hand, C_2S is responsible for the development of strength later due to the slow reaction. Portlandite, large hexagonal crystals, does not enhance the mechanical properties but prevents carbonation-induced corrosion by maintaining high pH in interstitial water. Pozzolanic materials composed of non-crystalline silica are often added to transform portlandite into secondary C−S−H to enhance the durability and strength of cementitious materials as expressed in Eq.2 [27]. These materials are typically fly ashes, silica fume, and calcined clays. The reactivity of Pozzolanic materials depends on the content and fineness of non-crystalline silica which develops a disorganized network due to quenching.

$$C_3S + (3\text{-}x\text{-}n)\ H_2O \rightarrow C_x{-}S{-}H_n + (3\text{-}x)\ CH \quad (1)$$

$$CH + H_4SiO_4 \rightarrow C_x{-}S{-}H_n \quad (2)$$

where n denotes the water-to-silicate ratio in C−S−H.

Although the C_3A content is only 6–8 wt% in Portland cement, it has a significant influence on the mechanical properties as well as the rheological behavior of fresh and hardened products [26]. The reactivity of C_3A is determined by the amount of pure C_3A with a simple cubic structure as it has higher reactivity than C_3A with Na^+ ions trapped which crystallized into the orthorhombic structure in the cement kiln. In Portland cement, gypsum or anhydrite ($CaSO_4$) is added as a set

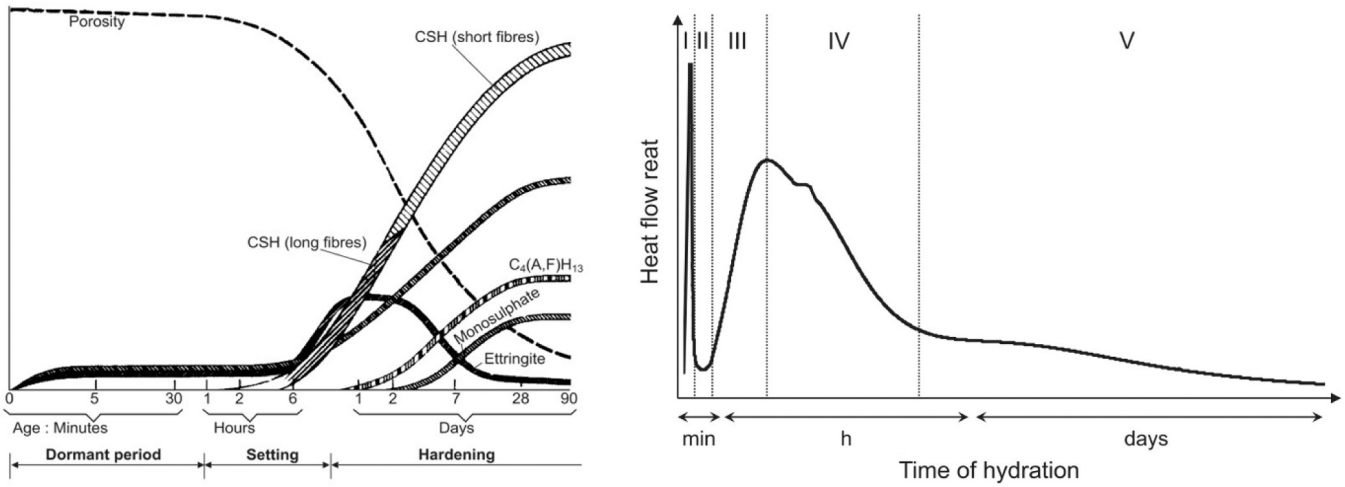

Fig. 3. Schematic representation of the heat release and hydration process at different stages during the hydration of ordinary Portland cement. Adapted with permission from [28]. Copyright 2016 Elsevier. Taken and adapted from [29].

retarder. In the absence of $CaSO_4$, hydration of C_3A occurs rapidly, resulting in the formation of calcium aluminum hydrate (CAH) as expressed in Eq.3. This rapid hydration stiffens the matrix and reduces the workability leading to unexpected rapid setting known as "flash setting".

$$C_3S + n\ H_2O \rightarrow CAH \quad (3)$$

The addition of $CaSO_4$ is crucial to enhance the workability of cement by delaying the setting time. In the presence of $CaSO_4$, C_3A reacts with $CaSO_4$ primarily due to the affinity with sulfate salts and forms ettringite as expressed in Eq.4. Ettringite, which is in the shape of short hexagonal prisms to long needles, effectively blocks the hydration of C_3A in the early stage (Fig. 2).

$$C_3A + 3(CaSO_4{\cdot}2H_2O) + 26H_2O \rightarrow \text{Ettringite}\ (3CaO{\cdot}Al_2O_3{\cdot}3CaSO_4{\cdot}32H_2O) \quad (4)$$

In the early stage, the porosity of the matrix is mostly filled up with ettringite. Ettringite progressively transforms into calcium monosulfate until the final set, occupying the porous spaces within the matrix. This reaction takes place after the first two or three days when it reaches the depletion of $CaSO_4$ for ettringite formation. The crystal structure rearranges as C_3A reacts with ettringite due to the affinity to sulfate ions and transforms into calcium monosulfate as expressed in Eq.5 (Fig. 2).

$$3CaO{\cdot}Al_2O_3{\cdot}3CaSO_4{\cdot}32H_2O + 2C_3A + 4H_2O \rightarrow 3\ (3CaO{\cdot}Al_2O_3{\cdot}CaSO_4{\cdot}12H_2O) \quad (5)$$

Hydration of Portland cement comprises five main stages: (*i*) dissolution of anhydrous phases, (*ii*) induction period with reduced chemical activities, (*iii*) growth of C–S–H due to the hydration of C_3S, (*iv*) depletion of sulfate, (*v*) further growth of C–S–H and transformation of ettringite to calcium monosulfate (Fig. 3) [28–30]. In the first phase, a large amount of heat is released due to the dissolution of anhydrous phases. C_3A reacts with $CaSO_4$ forming ettringite within a few minutes. Then, it moves on to the dormant period as ettringite coating delays further hydration. Formation of C–S–H nuclei also occurs shortly after mixing with water. Nuclei continue to form and grow until they reach critical size during this dormant period. The third phase follows due to the continuous growth and precipitation of C–S–H and portlandite which contributes to the setting and hardening of cement. When the sulfate depletion point is reached, precipitation of ettringite is accelerated and dissolution of C_3A increases. In the last phase, microstructures are densified as C–S–H precipitate and grow slowly. Also, ettringite transforms into calcium monosulfate. Growth and development of C–S–H significantly influences the microstructure of hardened products thereby influencing the durability of cement. In some cases, C–S–H seeds are added to enhance the hydration rate of cement and promote the precipitation of hydrates in the capillary pores. Secondary C–S–H can serve as seeds when nano silica from pozzolanic materials reacts with portlandite. The overall cement hydration process can be affected by the fineness of cement particles as the reactivity of cement powders increases with the specific surface area.

Table 1
Examples of chemical admixtures in ordinary Portland cement (taken and adapted from ref [31–33]).

	Chemical admixtures
Superplasticizers	Polynaphthalene sulphonates (PNS), Polymelamine sulphonates (PMS), Polyoxyetheylene diphosphonate (POEDP), Polycarboxylates (PCE)
Viscosity modifiers	Starch, Welan gum, Diutan gum, Guar gum, Xanthan gum, Alginates, Agar, Polyethylene oxide (PEO), Polyvinyl alcohol (PVA), Cellulose-ether derivatives
Retarders	Lignosulphonates, Sugar derivatives
Accelerators	Triisopropanolamine (TIPA), Triethanolamine (TEOA)
Superabsorbent polymers	Cellulose-based hydrogels, Starch-based hydrogels, Polyacrylamide (PAM), Poly(acrylic acid-acrylamide)
Shrinkage reducers	Monoalcohols, Glycols, Polyoxyalkylene alkyl ethers, *n*-Butylurea, *n*-Butyl acetoacetate
Air entrainers	Vinsol resin, Sodium dodecylbenzenesulfonate (SDBS), Sodium dodecyl sulfate (SDS)
Defoamers	Tributyl phosphate, Dibutyl phthalate, Silicones, Esters, Carbonic acids, Ethylene oxide, Propylene oxide
Fire retardants	Chlorinated paraffin−52, Antimony trioxide, Tricresyl phosphate (TCP), Tri(2-chloroethyl) phosphate (TCEP), Tributyl phosphate (TBP)

In commercial products, numerous chemical admixtures are added to enhance the workability, durability, and strength of fresh and hardened cement [31–35]. The rheological behavior of cement can be adjusted by adding superplasticizers or viscosity-modifying agents. Superplasticizers help maintain good flowability even at a very low water/cement ratio. Viscosity-modifying agents are often used with superplasticizers to enhance the stability, unity, and durability of hardened cement products. Hydration of cement can be modified by adding retarders such as lignosulfonates (LS) and sugar derivatives or accelerators such as triisopropanolamine (TIPA) and triethanolamine (TEOA). Alkali-free admixtures such as aluminum salts, silicate salts, and amorphous aluminum are used as accelerators in shotcrete formulation. Superabsorbent polymer (SAP) hydrogels are used as internal curing agents to reduce volumetric shrinkage and microcrack formation within

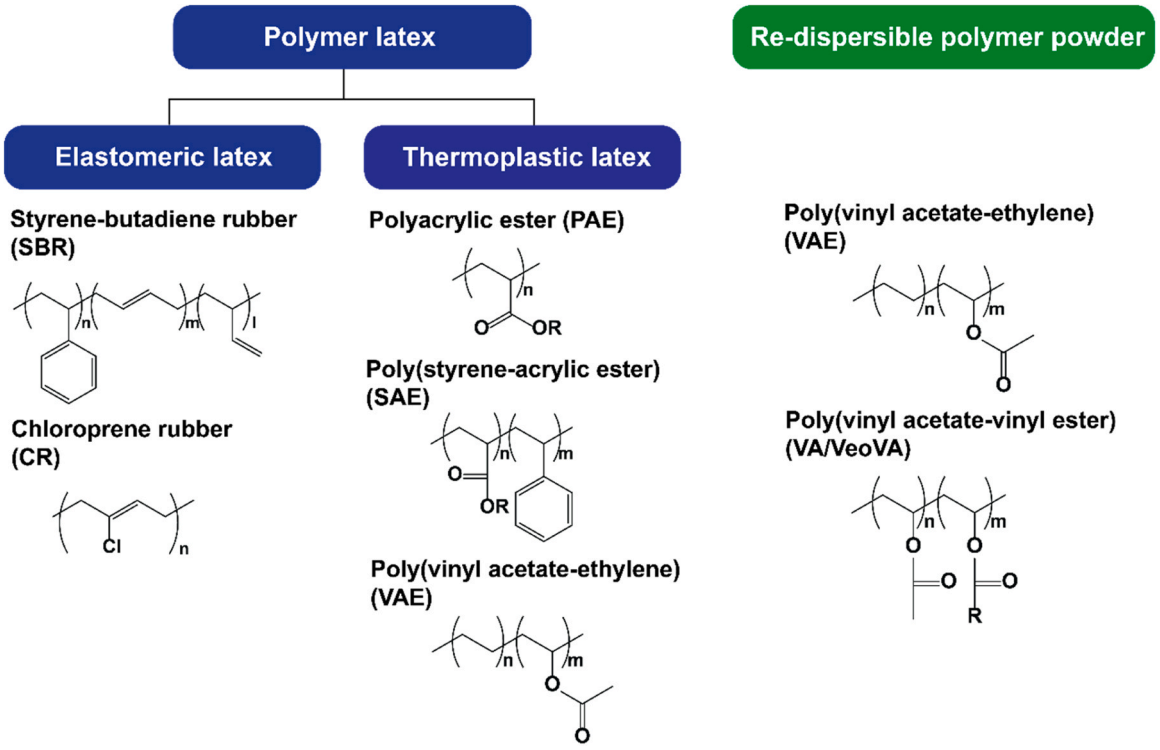

Fig. 4. Classification of polymers used in non-reactive TSLs (R = alkyl group C_nH_{2n+1}).

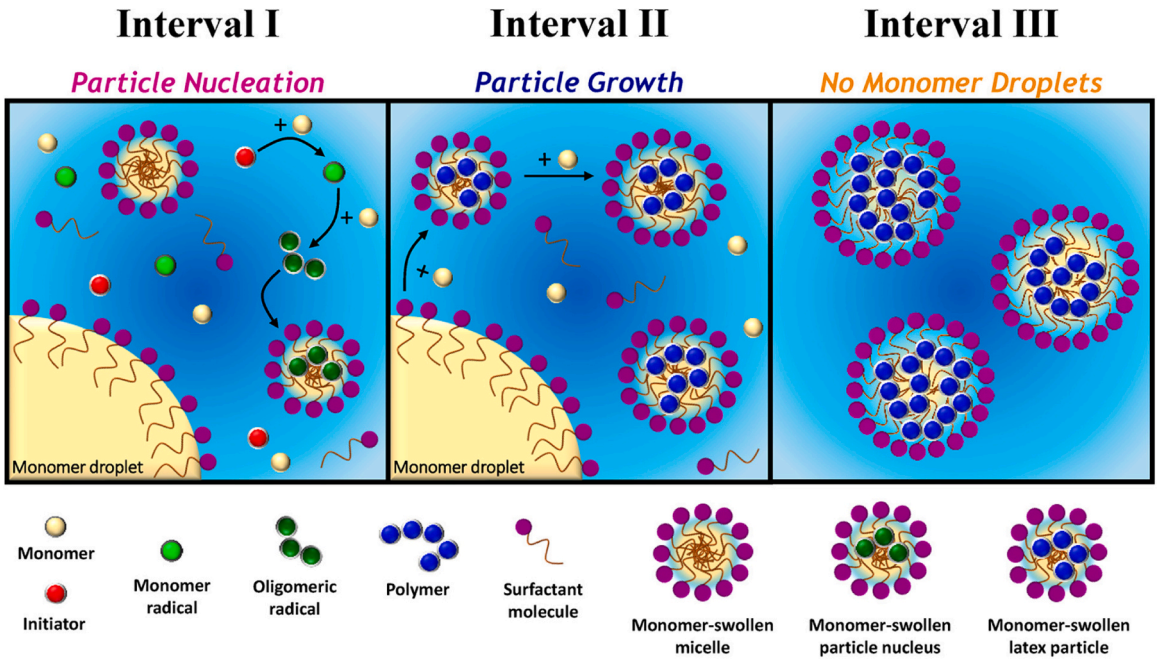

Fig. 5. Schematic illustration of particle formation and growth in aqueous emulsion polymerization. Taken from [39].

cementitious materials. Different types of surfactants are utilized as air-entrainers and shrinkage reducers. Freeze-thaw durability of concrete can be achieved through the addition of air-entrainers as the formation of microscopic air bubbles is facilitated during mixing. Shrinkage-reducing agents effectively decrease the surface tension of solid surfaces covered with water films while drying process of cementitious materials. Defoamers are added to reduce the occurrence of uncontrolled air bubble production during mixing which can reduce the overall strength of cement products. Fire retardants are added to obtain fire-retardant material that can self-extinguish once the flame is removed. Chemical admixtures are effective even at low concentrations and they should be selected upon careful consideration based on the application of cement. Examples of common chemical admixtures are summarized in Table 1.

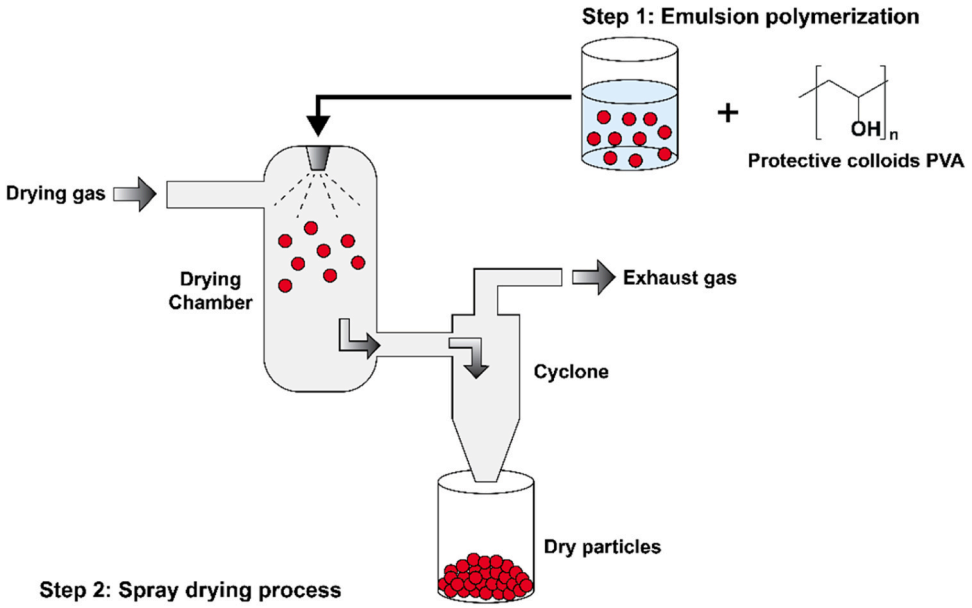

Fig. 6. Schematic illustration of two-step synthesis process for the preparation of re-dispersible polymer powders.

2.1.2. Polymer latexes and re-dispersible polymer powders

Polymers in latex or re-dispersible powder forms are used in non-reactive TSLs to modify or enhance the mechanical properties of cementitious materials (Fig. 4). Several prerequisites for polymers utilized in cementitious mixtures include: (*i*) strong chemical stability to highly reactive cations, Ca^{2+} and Al^{3+}, during the cement hydration process, (*ii*) low air-entraining tendencies, (*iii*) absence of negative impact on the process of cement setting and hardening, (*iv*) low glass transition temperature (T_g) to form polymer films, (*v*) excellent adhesion between polymer films and cement hydrates and aggregates, (*vi*) outstanding ability to withstand water, alkali, and weathering, (*vii*) good thermal and mechanical stability [36, 37].

Latex refers to a dispersion of polymer particles in water with solids content typically ranging from 40 to 50 wt% [38]. Along with polymer particles, latex often contains plasticizers, rheology modifiers, and surfactants. Latexes are typically obtained via emulsion polymerization where polymerization is conducted in water with hydrophobic vinyl monomers, surfactants, and water-soluble initiators (Fig. 5) [39–42]. Low molecular weight ionic or non-ionic surfactants are used to emulsify monomers and stabilize polymer particles. At the beginning of polymerization, oligomeric radicals are formed from monomers in the aqueous phase. These oligomeric radicals enter surfactant micelles swollen with monomer once they become hydrophobic. Particles subsequently grow until all monomer droplets are consumed. Latex with spherical nanoparticles with approximately 100−600 nm in diameter is obtained once polymerization is completed. Monomers such as vinyl acetate, ethylene, and styrene are widely used. Elastomeric and thermoplastic polymers that form continuous film are synthesized and applied in the construction and mining industries. Commercially available polymer latexes include styrene-butadiene rubber (SBR), chloroprene rubber (CR), poly(vinyl acetate-ethylene) (VAE), polyacrylic ester (PAE), and poly(styrene-acrylic ester) (SAE). These commercial products often contain anti-foaming agents and additional anti-foaming agents are not required during the mixing process [36, 37].

Re-dispersible polymer powders are also commercially produced and applied in non-reactive TSLs. Free-flowing re-dispersible polymer powders are produced via a two-step process (Fig. 6) [36, 43]. Firstly, polymer latex is synthesized via emulsion polymerization as described above. Once the latex is obtained, it is mixed with spray-drying agents and biocides to prevent contamination and phase separation of components from microbial attacks. Furthermore, protective colloids such as polyvinyl alcohol (PVA) are added before spray-drying to avoid caking during storage. Secondly, the spray drying method is used to dry polymer latex. Dual or multi nozzles with a nozzle pressure of 4×10^5 Pa, a hot air inlet temperature of 100 – 250 °C, and a hot air outlet temperature of 80 °C are applied for spray-drying. Anti-blocking agents such as clay, silica, and calcium carbonate are added after the drying process. Re-dispersible polymer powders have large particle sizes ranging from 10 to 500 μm as particles aggregate during the spray drying process. The particle size reduces to 100 – 600 nm after re-dispersing polymer powders in water. The obtained polymer powders are mixed with cement and aggregates through dry blending. VAE and poly(vinyl acetate-vinyl ester) (VA/VeoVA) make up the majority of commercially available re-dispersible polymer powders.

Among various types of polymers, VAE copolymers are widely produced and applied as polymer latex or re-dispersible powders in non-reactive TSLs. VAE copolymers demonstrate excellent adhesion to a variety of polar and non-polar substrates, crack resistance, and puncture resistance [44]. VAE copolymers can be synthesized via emulsion polymerization under high pressure [45]. The properties of VAE copolymers are largely determined by the wt% vinyl acetate (VA). Pure low and medium-density polyethylene exhibits 40 – 65 wt% crystallinity. With increasing VA content, the crystallinity of VAE copolymers gradually decreases, and the copolymers become fully amorphous when the VA content reaches 40 – 50 wt%. This also results in an increase in the polarity due to the acetate group in VA. Increased polarity leads to an enhancement in adhesion strength and compatibility with plasticizers and polar solvents such as water. The mechanical properties of thermoplastic VAE copolymers also depend on the VA content. At higher VA content, VAE copolymers behave like a rubbery material. Compared to VA content, molecular weight and molecular weight distribution (MWD) have a minor influence on the properties. High VA content leads to an increase in the amount of chain transfer and results in broader MWDs and increased viscosity. The VA content in VAE copolymers can be easily determined by thermogravimetric analysis (TGA) [46, 47]. Two-step thermal degradation occurs due to the evolution of acetic acid around 350 °C which is followed by main-chain degradation around 460 °C. VA content can be calculated from the weight loss from the first step as acetic acid is produced from VA during thermal degradation.

Understanding the interaction between polymers and Portland cement hydration is crucial to elucidate the enhancement in properties of polymer-modified cement. The cement hydration process is

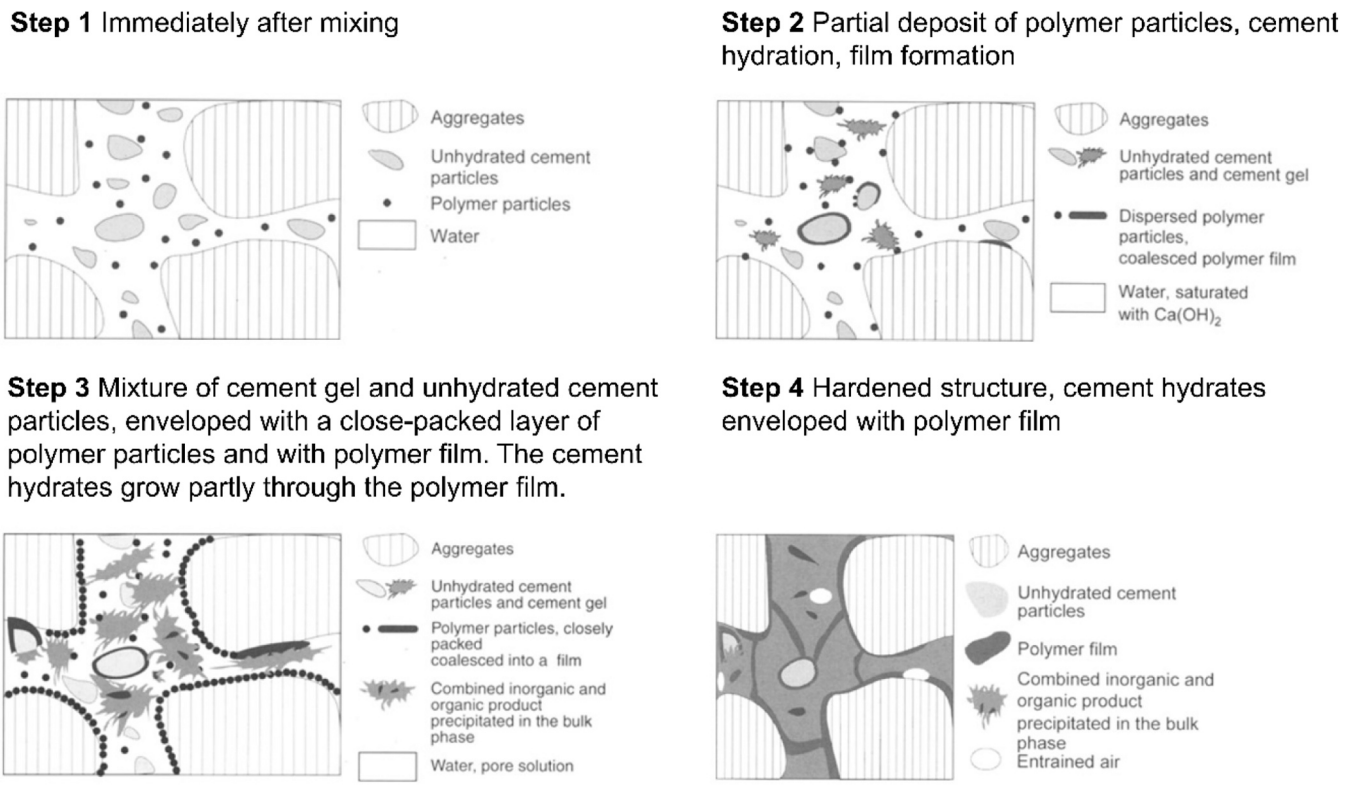

Fig. 7. Schematic illustrations of the cement hydration process in the presence of polymer based on Beeldens-Ohama-Van Gemert's integrated model. Adapted with permission from [48]. Copyright 1969 Springer Nature.

significantly influenced by polymer film formation. There are different proposed mechanisms describing the cement hydration process in the presence of polymer particles. Beeldens-Ohama-Van Gemert's integrated model based on Ohama's three-step model is the most widely accepted mechanism. In Ohama's model [36], cement hydration takes place consuming capillary water and polymer particles create a dense layer on the surfaces of cement after dispersing in water. Over time, a film forms from the coalescence of densely packed polymer particles. Cement hydrates and polymer film form a unified, interconnected network. Beeldens-Ohama-Van Gemert [48] suggested an integrated model with four steps where the mutual influence between the polymer film formation and the cement hydration process was integrated (Fig. 7). In the first step, primary hydration of cement occurs upon dispersing cement particles and polymer particles in water. This results in alkaline capillary water in water-filled pores. Small amounts of polymer particles precipitate on the surfaces of cement particles and aggregate in the second step. Small amounts of polymer particles may also coalesce at the cement hydrate surfaces. This is presumably due to the withdrawal of water during the cement hydration process, resulting in close packing of polymer particles. The hydration process may be retarded as polymer film partially or fully covers cement hydrates. In the third step, cement hydration continues to proceed, and polymer particles coalesce into the film. If the relative humidity (RH) is low, cement hydration and polymer film formation occur simultaneously. This results in the retardation of cement hydration, thereby adversely affecting the overall properties of polymer-modified cement. Depending on the polymer/cement ratio, combined inorganic and organic products precipitate in the liquid phase. Finally, cement hydrates further and the polymer forms a continuous film. The strength development of the material is attributed to the polymer film formed at the interface of aggregate-matrix and the presence of polymer particles in the capillary pores. At a higher polymer/cement ratio, denser polymer film and wider bridges between aggregates are formed. Beeldens *et al.* [48] also investigated the influence of RH on polymer film formation by curing the samples at RH 60 %,

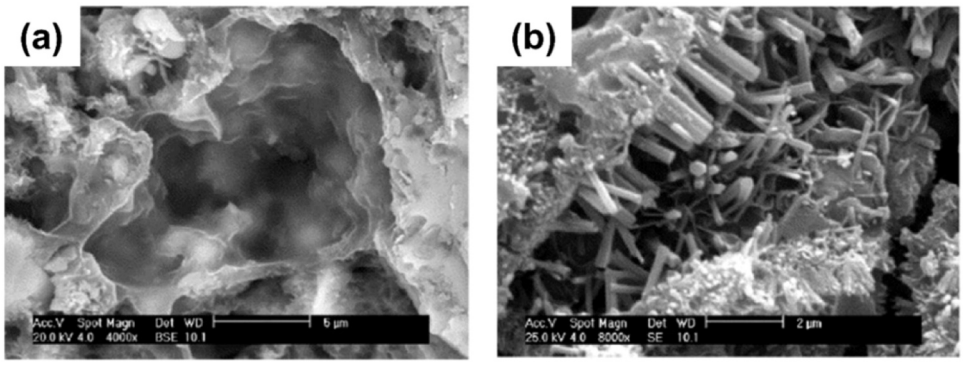

Fig. 8. SEM images of (a) fracture surface and (b) ettringite crystals inside Hadley's grains of VAE-modified cement. Adapted with permission from [50]. Copyright 2002.

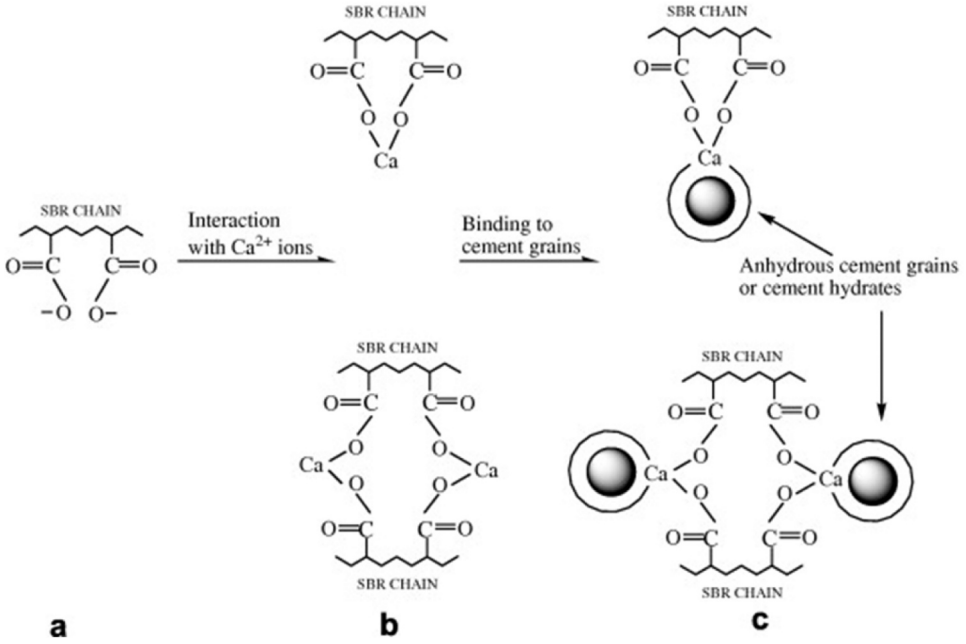

Fig. 9. Schematic illustration of interactions between SBR particles and cement hydrates. Adapted with permission from [65]. Copyright 2009 Elsevier.

86 %, and 98 %. Polymer film formation occurred at a lower temperature than the minimum film formation temperature (MFFT) at high RH due to the close packing of particles during the gradual evaporation of water. These results demonstrated that RH in drying conditions is important in determining the properties of the material.

So far, the cement hydration process in polymer-modified cement has mainly been discussed based on physical interactions between cement and polymer particles. Chemical reactions also play an important role in the cement hydration process. Depending on the polymer, it results in the modification of composition and quantities as well as the formation of complex structures. In the case of VAE copolymers, the vinyl acetate group undergoes hydrolysis due to alkaline capillary water. Acetate anions CH_3COO^- released from the alkaline hydrolysis of VAE copolymers reacts with Portlandite ($Ca(OH)_2$) and produces calcium acetate $Ca(CH_3COO)_2$ as described in Eq.6 [49, 50].

$$Ca(OH)_2 + 2CH_3COO^- \rightarrow Ca(CH_3COO)_2 + 2OH^- \quad (6)$$

Formation of calcium acetate after VAE hydrolysis results in enhanced interfacial bonding and mechanical properties of cementitious materials. Previous studies [50–52] suggest that calcium acetate causes retardation in the cement hydration process. VAE-modified cement developed well-crystallized ettringite due to the retardation in nucleation and growth of crystals. This is potentially due to the sulfate ions being captured in solution as Ca^{2+} ions react with acetate groups from VAE, leading to the formation of portlandite and ettringite at a low rate. Furthermore, retardation of the hydration process can be supported by the formation of Hadley's grains (small hollow hydration grains) which typically appear when the process of precipitating hydrated phases occurs at a lower pace compared to the dissolution of anhydrous phases (Fig. 8) [53]. The extended hydration period can be beneficial as it lengthens the working time. VAE-modified cement exhibits enhanced water resistance and fracture toughness. Although compressive strength and flexural strength are reported to decrease as the amount of VAE increases, this problem can be solved by introducing an adequate amount of methyl cellulose [44, 54, 55]. Baptista *et al.* [56] reported VAE increases the interfacial bonding between cement hydrates thereby resulting in enhancement of overall mechanical properties.

Styrene-butadiene rubber (SBR) is another widely used polymer in polymer-modified cement. SBR-modified cement demonstrates resistance to chloride ion penetration as well as good mechanical properties [57–59]. SBR-modified cement develops a microstructure with reduced porosity and increased density as continuous SBR films seal large pores. The formation of an interpenetrating network between SBR particles and cement hydrates leads to higher flexural and compressive strengths [49, 60, 61]. Reaction of C_3A and gypsum is promoted by SBR latex and enhances ettringite formation and stability. In the presence of chloride ions, some ettringites transform into chloroaluminate by substitution of sulfate anion with chloride anion as shown in Eq.7.

$$3CaO{\cdot}Al_2O_3{\cdot}3CaSO_4{\cdot}32H_2O + 6Cl^- \rightarrow 3CaO{\cdot}Al_2O_3{\cdot}3CaCl_2{\cdot}32H_2O + 3SO_4^- \quad (7)$$

Carboxylated styrene-butadiene latex (XSB) is also often used as it exhibits enhanced compatibility with organic fillers and adhesion properties when compared to SBR latex [62]. XSB latex is synthesized via emulsion polymerization in the presence of butadiene, styrene, and a small amount of carboxylic acid [63]. During the cement hydration process, small amounts of carboxylic acid on the surface of XSB become deprotonated in alkaline capillary water. Deprotonated carboxylic acid interacts with cement hydrates containing Ca^{2+}, which participates during the close packing of polymer particles and behaves like a cross-linking agent. This enhances XSB latex stability and adhesion strength to the substrate (Fig. 9) [64, 65].

Plank *et al.* [66] investigated the influence of polymer particle surface charge on the adhesion of polymer particles on cement hydrates. Anionic and cationic latexes were prepared via semi-batch emulsion polymerization where a mixture of water, monomers, and surfactant was added at a constant rate to the initiator solution. The anionic latex was prepared using styrene, *n*-butyl acrylate, and methacrylic acid in the presence of the anionic surfactant Marlon A375. The cationic latex was prepared utilizing the cationic monomer 3-trimethyl ammonium propyl methacrylamide chloride (MAPTAC) with styrene and *n*-butyl acrylate (*n*BA) in the presence of the non-ionic surfactant Tween 80. Zeta-potential measurements were used to measure the interactions between polymer and cement particles. Anionic latex decreased the zeta potential of cement particles whereas cationic latex led to an increase in zeta potential to positive values. Sedimentation tests were also performed to determine the adsorption of polymer particles on cement.

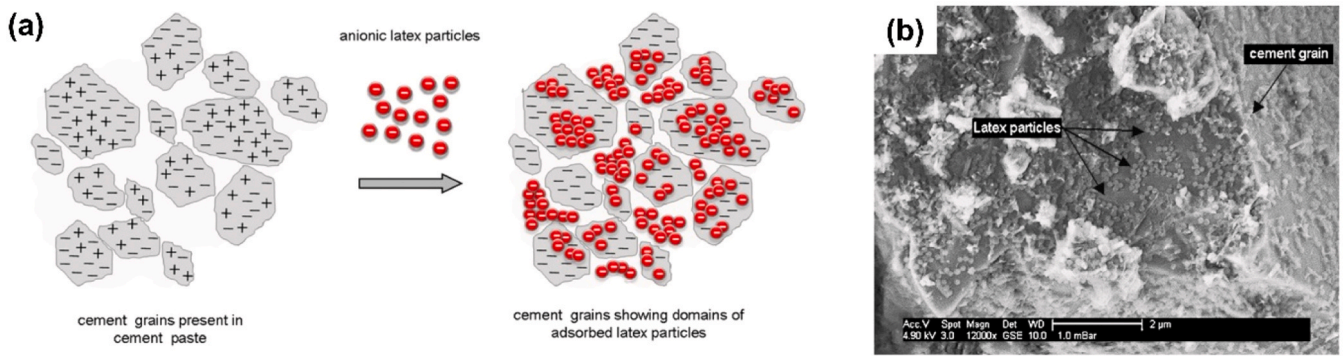

Fig. 10. (a) Schematic illustration of the anionic polymer particle adsorption on cement hydrates, (b) SEM image of cement grain showing domains of anionic polymer particles.
Adapted with permission from [66]. Copyright 2008

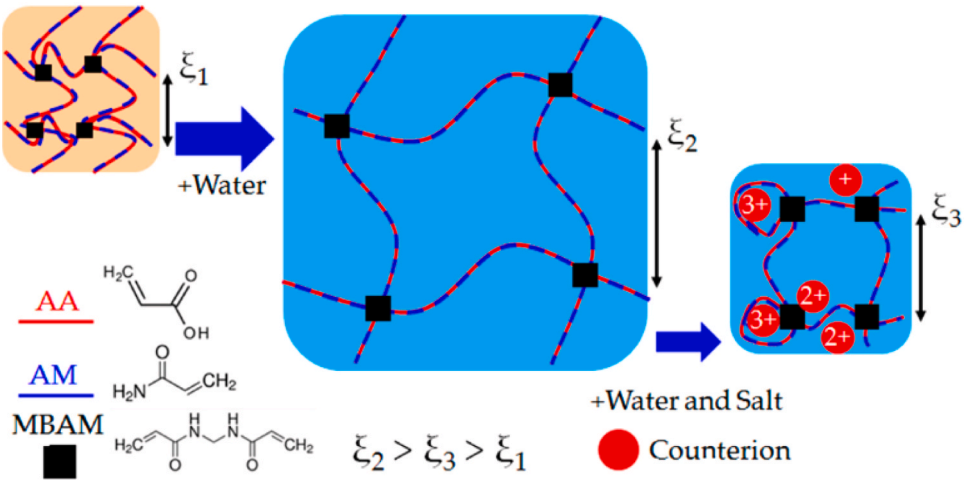

Fig. 11. Schematic illustration of a covalently crosslinked poly(acrylic acid-*stat*-acrylamide) hydrogel network in a dry state (ξ_1), swollen state (ξ_2) after adding water, and deswollen state (ξ_3) upon being exposed to a water and salt solution (acrylic acid (AA) segments = dashed red lines, uncharged acrylamide (AM) = dashed blue lines, covalent crosslinker *N*-*N*′-methylenebisacrylamide (MBAM) = black squares, and counterions = red circles, ξ = mesh size of the gel particles which is the distance between neighboring chains).
Taken from [35].

Approximately 50 mg of anionic particles and 28 mg of cationic particles were absorbed per 1 g of cement. On the surface of cement hydrates, charges are distributed heterogeneously as silicate hydrates provide negative surface charge and aluminate hydrates provide positive surface charge. Cationic or anionic latex can be adsorbed on the cement hydrates due to the heterogeneous charge distribution (Fig. 10). Initially, polymer particles will form domains on the surface of cement hydrates. Then, polymer films will be formed via the coalescence of particles during the hydration and drying process. These results demonstrated the existence of a strong interaction between latex and cement particles. Lu *et al.* [67] reported that adsorption of polymer particles on cement particles causes retardation in the cement hydration process. These retardation effects derive from the inhibition of C–S–H nucleation on the surface of cement particles [68]. Incorporation of a non-charged layer of polyethylene oxide (PEO) on styrene/*n*-butyl acrylate-based anionic latex and modifying polymer particles promoted nucleation of C–S–H and helped mitigate the retardation effect.

Apart from the addition of polymer particles to induce film formation during cement hydration, superabsorbent polymer (SAP) hydrogels are widely used to reduce the occurrence of microcracks and volumetric shrinkage at low water-to-cement ratios [34, 35, 69]. SAP hydrogels absorb water and expand to serve as a water reservoir. This helps control cement hydration to form dense microstructures in high performance concrete (HPC) at a low W/C ratio. Typically, 0.2 wt% of SAP hydrogels by the weight of cement is mixed with cement either in a dry state or wet state after pre-wetting for 24–48 h. When SAP hydrogels are added in a dry state, workability is reduced as SAP particles absorb water and release the water during the cement hydration process. To obtain good workability, an additional 5 wt% water by the weight of cement is added with superplasticizers in the cement mixture.

SAP hydrogels are typically composed of poly(acrylic acid-*stat*-acrylamide) P(AA-*stat*-AM). During the cement hydration process, osmotic pressure gradients drive water to be extracted from the hydrogels. The hydrogel eventually deswells from water extraction and interaction with cations from pore solutions [34, 35, 70–72]. In an alkaline pore solution (pH > 12), the carboxylic acid group –COOH from acrylic acid (AA) undergoes deprotonation. Ionic complexes formed from cations, such as Na^+, K^+, Ca^{2+}, and Al^{3+}, and $-COO^-$ moieties from AA groups behave as crosslinks, which may lead to collapse of polymer network and unexpected deswelling of SAP hydrogels (Fig. 11). Acrylamide (AM) is mostly unaffected as acrylamide has fewer $-COO^-$ moieties from hydrolysis of amide groups forming in alkaline solutions. Ion-induced deswelling is promoted due to the increased amount of anionic sites when the amount of AA is increased in SAP hydrogel. Thus, the stability of SAP particles in the presence of cations needs to be carefully considered when designing an internal curing agent of cement.

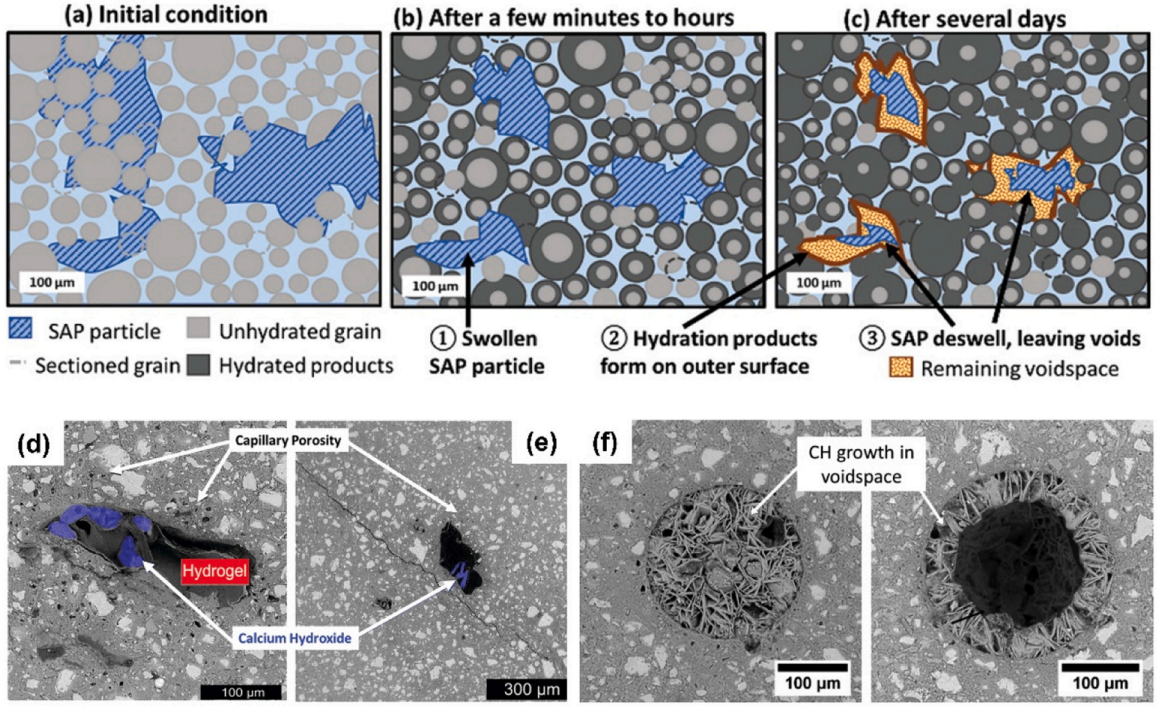

Fig. 12. Cross-section of cement mixture containing SAP hydrogels: (a) immediately after mixing, (b) before final setting of cement, (c) after a few days when a substantial amount of cement has reacted and the hydrogel particles have partially deswollen, SEM images of cement mixture containing SAP hydrogels with (d) 17 % AA, (e) 33 % AA, (f) 100 % acrylamide showing significant CH growth in hydrogel void space.
Taken and adapted from [34] (a-e) and [35] (f)

Deswelling of SAP particles leaves void spaces when the cement hydration process is complete [73]. Nonetheless, previous studies [34, 35, 74] have shown that SAP induced void formation does not compromise the mechanical properties of cement composites as the formation of Portlandite and C−S−H was promoted within the voids (Fig. 12). The internal curing water provided by the SAP particles facilitates a more thorough hydration process and results in a refined microstructure within the cement matrix, which is crucial for enhancing the material's mechanical properties. Additionally, the presence of sufficient water within the hydrogel provides a thermodynamically favorable environment for the cement hydrates to form within the voids. Overall, SAP hydrogels can lead to the enhancement of mechanical properties with less reduction in compressive strength and durability by mitigating microcrack formation at a low W/C ratio.

In general, polymers are known to enhance the strength and durability of cement due to the modification in the microstructure of hardened products [36, 52]. Polymers improve the interfacial bonding between cement hydrates and aggregates and prevent crack propagation as polymer films act as a bridge between microcracks under stress. Polymer films prevent the dry-out of cement and enhance water resistance due to the sealing effect. Furthermore, the long-term strength increases during dry curing by allowing enough time and providing adequate moisture for polymer-modified cement to develop the desired strength. The polymer/cement ratio and types of polymers need to be carefully considered to achieve the desired properties of the final product. Further studies elucidating the chemical and physical mechanisms behind cement hydration and polymer film formation processes are expected to be beneficial in designing non-reactive TSL.

2.1.3. *Polymeric fibers in non-reactive TSL*

Traditionally, steel fibers have been predominantly used to reinforce cement due to the capability of steel fibers to control cracks and absorb energy. However, corrosion of steel fibers has an adverse effect on the durability of such cementitious material. Alternatively, glass fibers and natural fibers have been considered to achieve the desired reinforcement in cementitious products without sacrificing durability. Utilizing these fillers is challenging due to the poor alkali resistance of glass fibers and the low durability of natural fibers. Hence, the use of polymeric fibers has gained attention because of their good corrosion and alkali resistance [37]. Commonly used polymeric fibers are polypropylene (PP) fibers [75–77], polyamide (PA) fibers [78–80], polyethylene (PE) fibers [81], and polyvinyl alcohol (PVA) fibers [82].

The reinforcement efficiency of polymeric fibers depends on the aspect ratio, amount, and the nature of the polymer. Introducing polymeric fibers helps control crack propagation by absorbing energy.

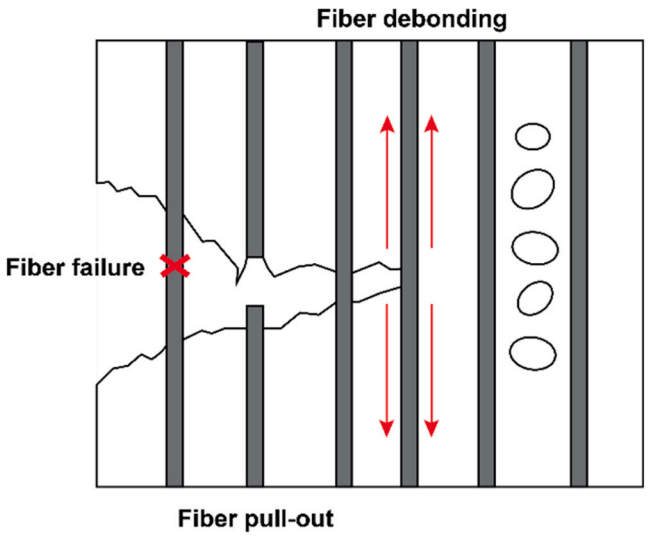

Fig. 13. Schematic illustration of the three main mechanisms of fiber-reinforced cementitious materials.

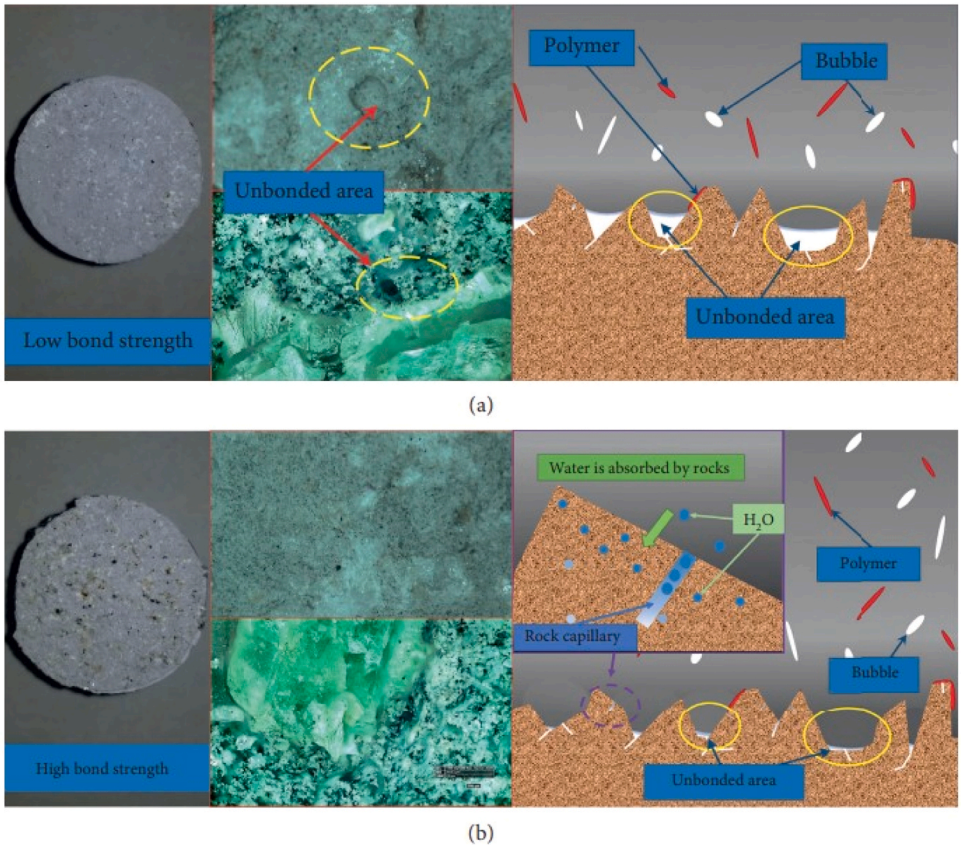

Fig. 14. Schematic illustrations of TSL adhesion on the substrate: (a) TSL with high water content and (b) TSL with optimum water content. Taken from [21].

Significant enhancements in tensile and flexural strength are achieved as fiber-reinforced cementitious material undergoes more complex fracture than normal cementitious material. The three main failure mechanisms involved are: (*i*) fiber failure, (*ii*) fiber debonding, and (*iii*) fiber pull-out (Fig. 13). Among those mechanisms, debonding of fiber from the matrix dissipates the energy the most by creating cracks along the fiber. The presence of fibers in the matrix effectively prevents crack propagation and leads to the formation of small cracks in the cementitious matrix near fibers [83]. Polymeric fibers of 5 – 30 mm in length and diameter of 5 – 100 μm have been reported to improve resistance to shrinkage cracking of cementitious materials [81, 84].

Having adequate interfacial bonding between hydrophobic polymeric fibers and hydrophilic cement matrix is crucial to obtaining cementitious materials with desired properties. Fiber-cement adhesion can be improved via surface modification of polymeric fibers. Lopez-Buendia *et al.* [85] performed alkaline treatment on PP fibers. Treated PP fibers became more hydrophilic than untreated fibers as the contact angle reduced from 120° to 96°. The surface roughness of PP fibers was significantly increased because of the residual sodium on the fiber surface. The growth of ettringites on the surface of PP fibers was facilitated by sodium precipitation on the surface as sodium takes part in regulating the formation of ettringite. Micro roughness as well as the formation of ettringite on the surface contributed to the modification in mechanical properties. Enhancement in interfacial bonding between PP fibers and cement resulted in an increase in flexural strength by 14 %. Hernandez-Cruz *et al.* [86] modified the surface of PP fibers by coating a thinlayer of ethylene acrylic acid (EAA). Uniform distribution of modified PP fibers was observed within cementitious material as the carboxylate group of EAA enhances the interfacial bonding. Signorini *et al.* [87] have coated PP fibers with rapid-acid catalyzed silica using the sol-gel technique. Silica coating significantly enhanced the bonding between PP fibers and cement matrix. It was found that silica-coated fibers enhanced the dissipation of energy without sacrificing ductility, whereas ductility decreased significantly as strength developed for uncoated fibers during the curing process. These studies demonstrate that the mechanical properties of cementitious materials can be significantly enhanced in the presence of polymeric fibers, and appropriate surface modification of the fibers can further enhance the properties. Hence, the selection of polymeric fibers needs to be carefully considered based on the desired properties of non-reactive TSLs.

2.1.4. *Recent developments of non-reactive TSLs*

Until now, various non-reactive TSLs based on polymeric materials have been developed and tested. Chen *et al.* [21] developed TSL products by mixing polyacrylate emulsion, Portland cement, and other additives to prevent weathering on mine tunnels. Different amounts of fillers such as calcium carbonate ($CaCO_3$), PP fibers, and hydroxyethyl methyl cellulose (HEMC) were used to optimize the recipe. HEMC was used as a tackifier to moderate the viscosity of TSL. The influence of the amount of each component on TSL properties was investigated by varying the water/cement (W/C), polymer/cement (P/C), and fiber/-cement (F/C) ratios. The initial setting time increased with increasing water and polymer content due to the presence of large gaps between cement particles and the hindered hydration process by polymer particles. At an optimum P/C ratio, polymer particles would enhance the formation of Portlandite and absorb onto the cement hydration products. Also, the gaps between fibers and cement were filled as a result of polymer film formation, which led to an increase in bending strength. The adhesive strength of TSL on both wet and dry surfaces was improved by utilizing polymer as it helps glue onto the substrate (Fig. 14). When the amount of polymer increased up to 14 wt%, the bending strength of TSL reduced as it led to incomplete cement hydration. Adhesive strength

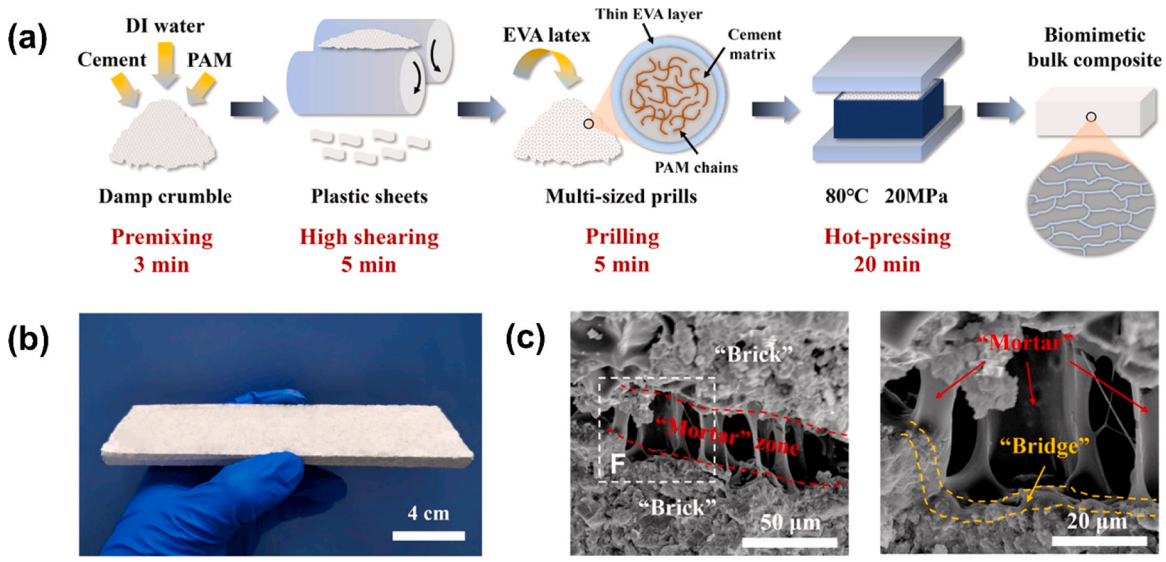

Fig. 15. (a) Schematic illustrations of the fabrication process of "brick-bridge-mortar" cement composite, (b) image of fabricated cement composite, (c) SEM images of polymer films represented as "mortar" and cement matrix represented as "brick".
Adapted with permission from [92]. Copyright 2020 American Chemical Society.

was also reduced as observed by the separation of TSL from the substrate. Overall, W/C and P/C ratios were the two main factors that influenced the mechanical properties of TSL.

Chen *et al.* [25] designed a TSL product consisting of VAE emulsion, aluminate cement, and other additives such as hydroxypropyl methylcellulose (HPMC) as tackifier and organic silicone defoamers. High compressive, flexural, tensile, and adhesive strengths of 12.4, 5.1, 2.7, and 1.5 MPa, respectively, were reached at a relatively low cost. A single-component non-reactive TSL was designed by Nanjing Coal Science & Technology Research Co. Ltd [24] for anti-weathering, anti-rust, and gas sealing purposes in coal mines. The exact formula of the product was not provided, but high tensile strength (3.5 MPa) was developed after 56 days, and the adhesive strength reached between 1 and 2 MPa. Kim [88] studied the influence of types of polymers on the mechanical properties of cementitious material. VAE led to the largest enhancement in compressive and flexural strength by 33 % and 63 % compared to polyacrylates, PVA, and SBR. This suggests that utilization of VAE would be ideal in obtaining non-reactive TSL with desired properties.

The brittleness of cement-based materials arises from the ionic bonds, covalent bonds, and physical adhesion forces between cement hydration products [89–91]. This makes cement-based materials susceptible to plastic deformation, thereby resulting in low flexural strengths, toughness, and resistance to crack propagation. Microcrack formation significantly affects the durability of cement-based materials by facilitating corrosion due to the penetration of ions. To enhance the mechanical properties of cement-based materials, polymers in the form of powder or latex have been commonly added to cement that undergoes a film formation process during cement hydration [36, 48]. Polymer films within cementitious materials form an interpenetrating network within cement hydrates and reduce the occurrence of microcrack formation. The flexural strengths of the materials enhance significantly in the presence of polymers. However, cement hydration is often delayed

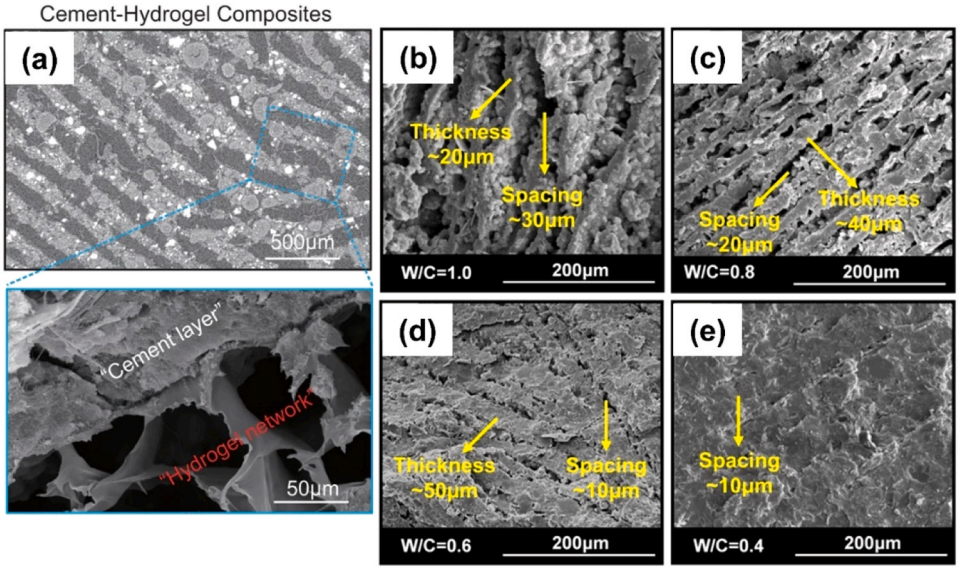

Fig. 16. (a) X-ray computed tomography and SEM image of cement-PVA hydrogel composite, and SEM images of cement-PVA hydrogel composites at (b) W/C = 1.0, (c) W/C = 0.8, (d) W/C = 0.6, (e) W/C = 0.4.
Taken and adapted from [93].

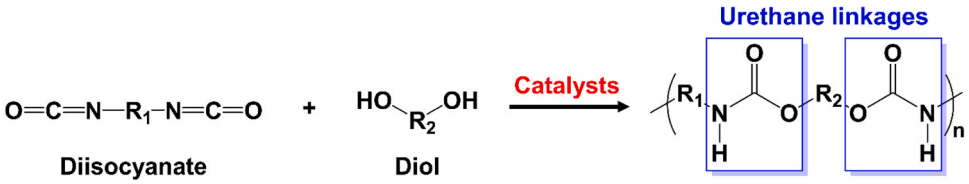

Fig. 17. Schematic illustration of polyurethane synthesis.

which is accompanied by the reduction of compressive strengths. Thus, different structure designs of cementitious materials have been developed and investigated to enhance mechanical properties without sacrificing compressive strengths.

Pan *et al.*[92] proposed the formation of a three-dimensional "brick-bridge-mortar" cement composite structure through prilling and compaction via hot press method (Fig. 15). Damp crumbles of cement and polyacrylamide (PAM) were first obtained by using a double-roll mill. Then, EVA latex was thoroughly mixed with damp crumbles which were hot pressed to obtain cement composite. Cement matrix served as a rigid brick, polymers as a mortar, and interfacial interaction between cement and polymers as a bridge within the composite. Two different types of polymers, PAM and EVA, were involved in toughening mechanisms. Crosslinking occurred between Ca^{2+} ions from cement hydrates and carboxylate groups from hydrolysis of PAM. Furthermore, energy was dissipated by the creation of filaments between EVA polymer film and cement hydrates. Toughening mechanisms along with a unique "brick-bridge-mortar" structure led to a significant enhancement in the toughness of the cement composite in the presence of 4 wt% polymers.

Chen *et al.* [93] employed ice-template methods to synthesize cement composites with PVA hydrogels filled into the unidirectional pores. Depending on the W/C ratio, the toughness of cement-hydrogel varied as cement gaps were too small at a low W/C ratio and too big at a high W/C ratio which affected the incorporation of PVA hydrogels within the pores (Fig. 16). The enhancement in toughness can be attributed to the formation of a lamellae structure with alternating soft and hard phases as well as the high interface affinity between C–S–H from cement hydrates and PVA hydrogel. The high interface affinity occurred from the strong attraction between Ca^{2+} ions and oxygen atoms from hydroxyl groups of PVA and hydrogen bonding between C–S–H and PVA hydrogel. In ice-templated cement composite, the appearance of multiple cracks effectively dissipated stress in the overall structure through the bond failure process between cement and hydrogel. This led to the enhancement in toughness, increase in compressive strength, and low thermal conductivity compared to pure cement paste.

Recent studies conducted by Pan *et al.* [92] and Chen *et al.* [93] demonstrated that interfacial interaction between cement hydrates as well as the cement composite structure is crucial in enhancing durability

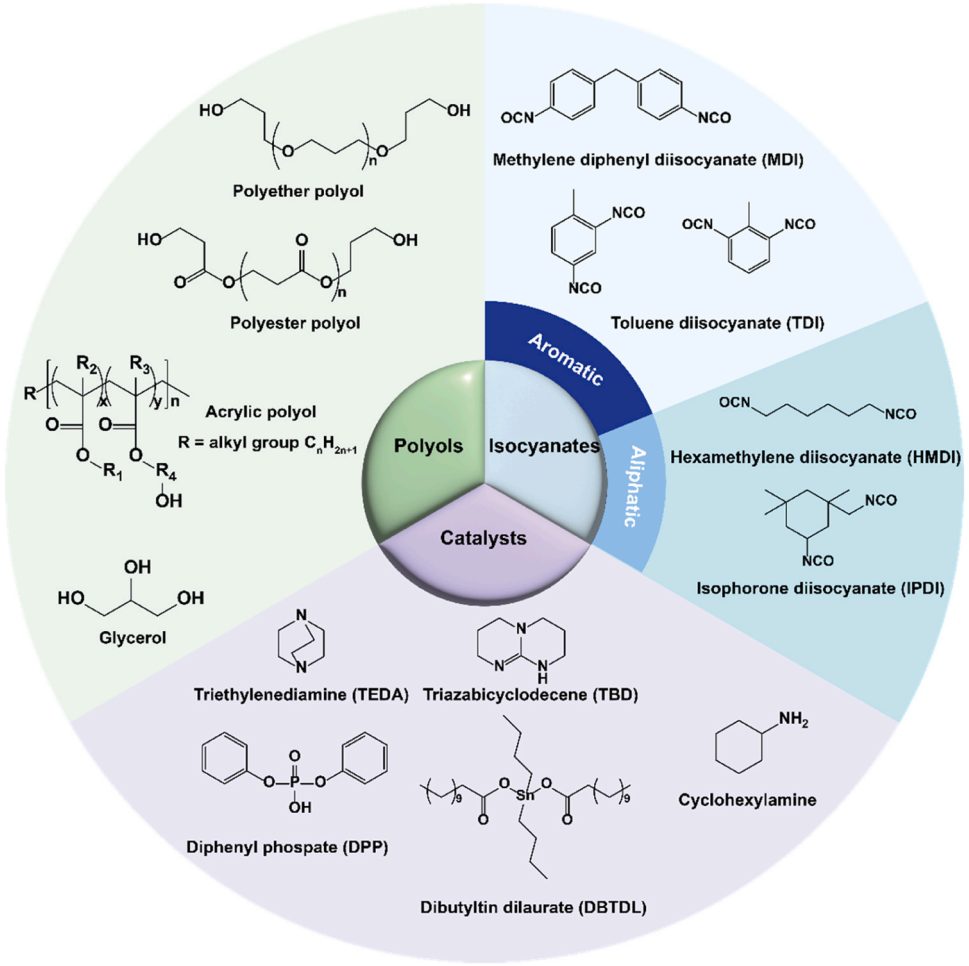

Fig. 18. Examples of polyols, isocyanates, and catalysts used in polyurethane synthesis.

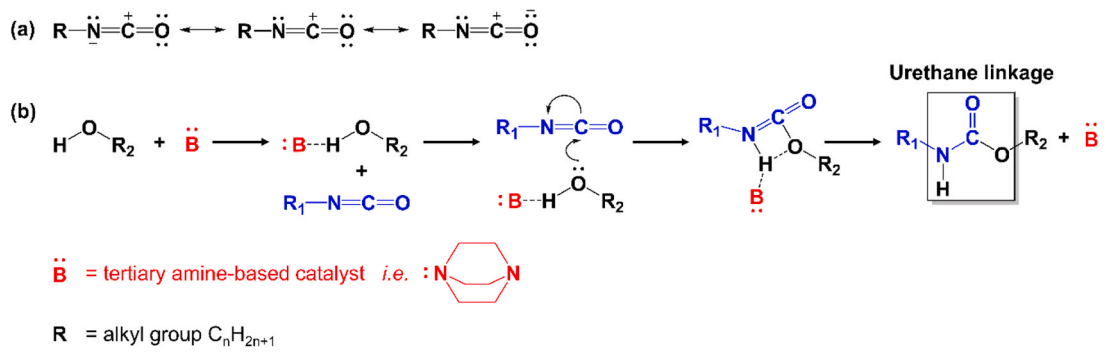

Fig. 19. Schematic illustrations of (a) resonance structures of isocyanate and (b) urethane addition reaction between isocyanates and hydroxyl groups in the presence of tertiary amine-base catalysts.
Adapted with permission from [96]. Copyright 2021 American Chemical Society.

of cementitious materials. This can provide a facile solution to overcome the limitation of enhancement in mechanical properties of non-reactive TSL which is typically applied by physical mixing between cement and polymer. Further research needs to be conducted to simplify the synthesis process of these cement composites to be utilized as TSL to support roof and ribs of the excavation site.

2.2. Reactive TSLs

Reactive TSLs are typically two-component polymer-based liners that require combinations of liquid/liquid or liquid/powder. Setting times of reactive TSLs are much shorter than cementitious TSLs as the film formation process occurs through chemical reactions rather than the evaporation of water. The utilization of two-component reactive TSL systems has gained significant attention because of ease of application, longer shelf lives, and short curing times [4, 7]. In the beginning, materials such as phenolic/phenolic formaldehyde (PF) resins and acrylate/methacrylate-based resins were developed. However, the brittleness and low strength limited the utilization of these materials as reinforcement in ribs and roofs of underground mining sites [94, 95]. Currently, the majority of reactive TSLs available in the market are polyurethane/polyurea-based resins as strong, durable, and elastic coatings can be formed with enhanced fire-retardant properties by adding fillers such as sodium silicate (waterglass) to the resin. Hence, this section will focus on the reactive TSL based on polyurethane/polyurea systems and their curing process.

2.2.1. Isocyanate-based TSLs

Polyurethanes are synthesized by the addition reaction of isocyanate groups (R−N = C═O) and hydroxy groups (-OH) which creates urethane linkages (Fig. 17) [96–99]. An extensive variety of polyurethanes can be synthesized as desired properties are achieved by simply altering the structure of the polyols and isocyanates. The elasticity of polyurethanes is enhanced by utilizing high molecular weight linear polyol with low functionality, whereas rigid polyurethanes are obtained by using low molecular weight polyol with high functionality. Despite their benefits, the application of polyurethane/polyurea-based TSLs has been limited due to the toxicity and high flammability of the material. Occupational health and safety risks mainly originate from the toxicity of isocyanates releasing volatile organic compounds (VOCs) at high temperatures. This can be solved by employing polymeric isocyanates with high vapor pressures or utilizing non-isocyanate based syntheses. In addition, adding fire retardants such as sodium silicate and chlorinated paraffin-52 can reduce the flammability of polyurethanes.

The main materials used for polyurethane synthesis are polyols, isocyanates, catalysts, and additives such as chain extenders and crosslinkers. The elasticity of polyurethanes is determined by the molecular weight and functionality of polyols (Fig. 18). Polyols can be divided into high or low molecular weight polyols and commonly used polyols are polyether polyols, polyester polyols, and acrylic polyols. High molecular weight polyols such as polyethylene oxide polyether polyols have long alkyl segments. The flexibility of polyurethanes derives from the free rotation of these linear chains that have low functionality and crosslinking density. On the other hand, rigid polyurethanes are prepared from polyols with low molecular weight that have high functionality. These polyols provide a large number of hydroxyl groups, thereby leading to the formation of highly crosslinked polyurethanes with multiple urethane linkages. Polyester-based polyurethanes are known to exhibit good fire resistance, high crystallinity, and good thermostability. Rigid polyurethanes can be prepared by utilizing polyether or polyester polyols. However, polyether-based polyurethanes are often preferred due to their low cost and chemical versatility. Another type of polyols is acrylic polyols containing monomers with a hydroxyalkyl group *i.e.* acrylic acid (AA), methacrylic acid (MAA), and 2-hydroxyethyl methacrylate (2-HEMA). Polyurethanes with different properties can be prepared depending on the monomers used in acrylic polyols. The elasticity of polyurethanes can be enhanced by utilizing monomers such as *n*-butyl acrylate (*n*BA) or 2-ethylhexyl acrylate (2-EHA) in the backbone. Also, employing monomers such as methyl methacrylate (MMA) and styrene (St) as backbone can improve water resistance and hardness. Recently, glycerol obtained from corn and soybean oils is gaining attention as an alternative renewable material to conventional polyols in synthesizing flexible polyurethanes [96–99].

Isocyanates can be categorized into two types: aromatic and aliphatic isocyanates (Fig. 18). Aromatic isocyanates, toluene diisocyanate (TDI) and methylene diphenyl diisocyanate (MDI), are often used in the formation of rigid polyurethanes and have the advantages of low cost and high reactivity. However, discoloration of polyurethane surfaces occurs upon exposure to UV lights. On the other hand, aliphatic isocyanates such as hexamethylene diisocyanate (HMDI) and isophorone diisocyanate (IPDI) are insensitive to UV lights and maintain glossiness without discoloration. This enables aliphatic isocyanates to be used in polyurethane coatings. It is important to optimize the amount of polyols and isocyanates to design polyurethanes with desired properties as an excess amount of polyols results in soft and hydrophilic polyurethanes whereas an excess amount of isocyanates leads to the formation of rigid and hydrophobic polyurethanes.

Catalysts enable polyurethane synthesis to occur at ambient temperature by increasing the rate of reaction between polyols and isocyanates (Fig. 18). Organometallic compounds, bismuth and zinc, and tertiary amine-based compounds are commonly used to enhance the reaction rates. Additives such as chain extenders and crosslinkers are also added to enhance the thermal and mechanical properties of polyurethane. Low molecular weight amine or hydroxyl terminated compounds are used as chain extenders to introduce rigid segments in polyurethane. Strong polyurethanes with high thermostability are prepared by utilizing crosslinkers with high functionality. Crosslinkers allow the formation of densely interconnected networks by creating

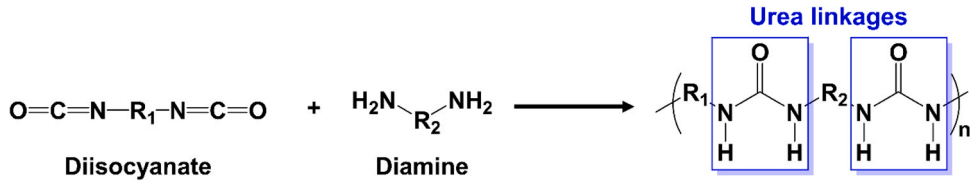

Fig. 20. Schematic illustration of polyurea synthesis.

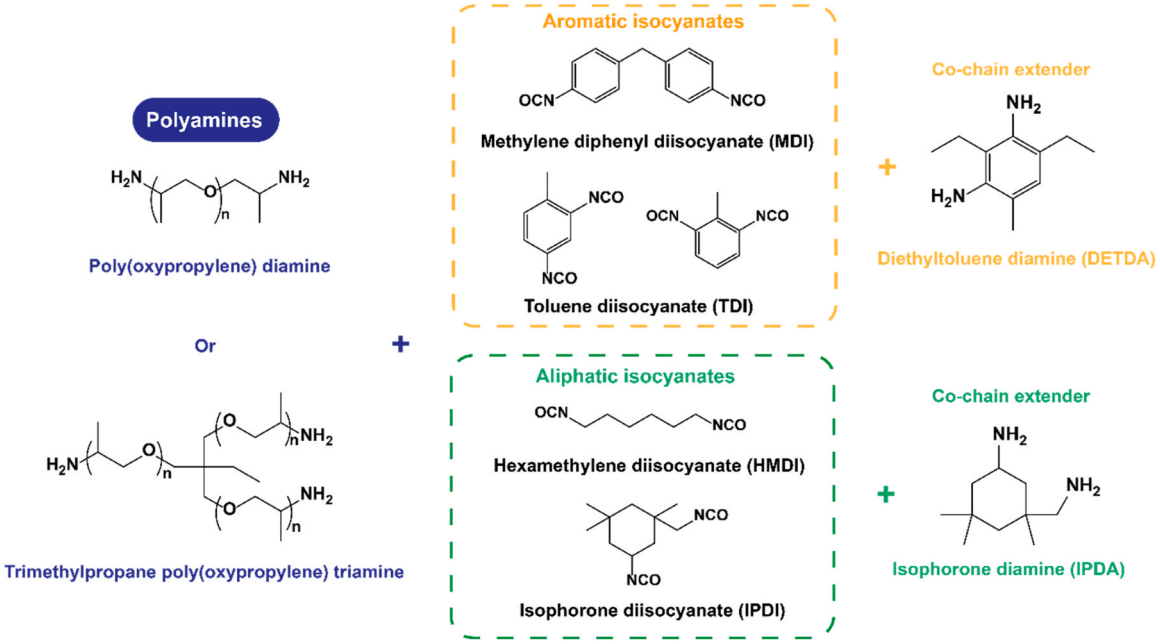

Fig. 21. Examples of polyamines and isocyanates used in polyurea synthesis.

covalent bonds between polymeric chains. Aromatic crosslinkers help developing stronger and more thermally stable polyurethanes than aliphatic crosslinkers. Furthermore, other additives are often used to reduce cost and enhance fire retardancy, resistance to UV lights, and enhance mechanical properties.

The versatility of polyurethanes originates from a rapid curing process at ambient temperature [96]. High reactivity between isocyanates and polyols allows rapid curing as the carbon center in isocyanates carries partial positive charge due to the electronegativity difference and becomes vulnerable to nucleophilic attack from polyols with hydroxyl group (−OH) (Fig. 19). The presence of electron-withdrawing aromatic groups in aromatic isocyanates, MDI and TDI, leads to faster reactions with polyols than aliphatic isocyanates. The reactivity of polyols also needs to be considered as higher reactivity results in shorter curing time. Depending on the application, polyols can be selected by the reactivity of hydroxyl groups (primary hydroxyl groups > secondary hydroxyl groups > tertiary hydroxyl groups > aromatic hydroxyl groups). In the presence of tertiary amine-based catalysts, catalysts with a free pair of electrons in the nitrogen induce nucleophile attacks of oxygen atoms in polyols on partially positive carbon (Fig. 19). This reduces reaction times by promoting the formation of urethane linkages. Overall, the properties of polyurethanes rely on the amount of catalysts and the selection of polyols, isocyanates, and additives such as chain extenders and crosslinkers.

Two-component polyurea-based systems differ from polyurethane-based systems by achieving rapid curing without utilizing catalysts [100–102]. Polyurea is synthesized via a reaction between isocyanate groups (R−N = C═O) and amine groups (-NH_2) from polyamine which forms urea linkage (Fig. 20). Typically, isocyanate prepolymer with 8–16 % isocyanate content is mixed with resin blend component by 1:1 vol ratio as in two-component polyurethane systems. Compared to polyurethanes, polyurea can endure extreme environments such as low temperatures and where high humidity is present. Furthermore, polyurea exhibit a rapid initial curing time of typically 2–3 s which is beneficial to underground mining as reinforcement can be quickly provided upon spraying on fresh excavation sites. In the application of polyurea, temperature of the substrate needs to be considered as it is required to be 5 °C above the dew point.

The main materials used for polyurea synthesis are similar to polyurethane synthesis. Isocyanates, polyamines, and additives such as chain extenders and crosslinkers are utilized to synthesize polyurea in the absence of catalysts (Fig. 21). Aromatic isocyanate-based polyurea uses isocyanate prepolymers prepared from the polymerization of aromatic isocyanates such as MDI and polyether polyols to lower the overall isocyanate content. This enables the isocyanate component to be mixed with the resin blend component with a 1:1 vol ratio. Resin blend contains high and low molecular weight components. A high molecular weight component, polyoxypropylene diamine or polyoxypropylene triamine, contributes to the flexibility and initial set in the polyurea system. A low molecular weight amine-terminated chain extender controls the overall time required for the drying process. Diethyltoluene diamine (DETDA) is the most commonly used chain extender. A co-chain extender, a secondary amine, is often utilized along with a chain extender to achieve enhanced substrate adhesion by extending the drying process. In addition, additives such as UV stabilizers can be added to reduce the occurrence of discoloration due to its sensitivity to UV lights. Aliphatic isocyanate-based polyurea utilizes isocyanate such as IPDI which is stable under UV lights. It is also blended with resin blend which contains polyoxypropylene diamine as a high molecular weight component to introduce flexibility and develop the initial set. However,

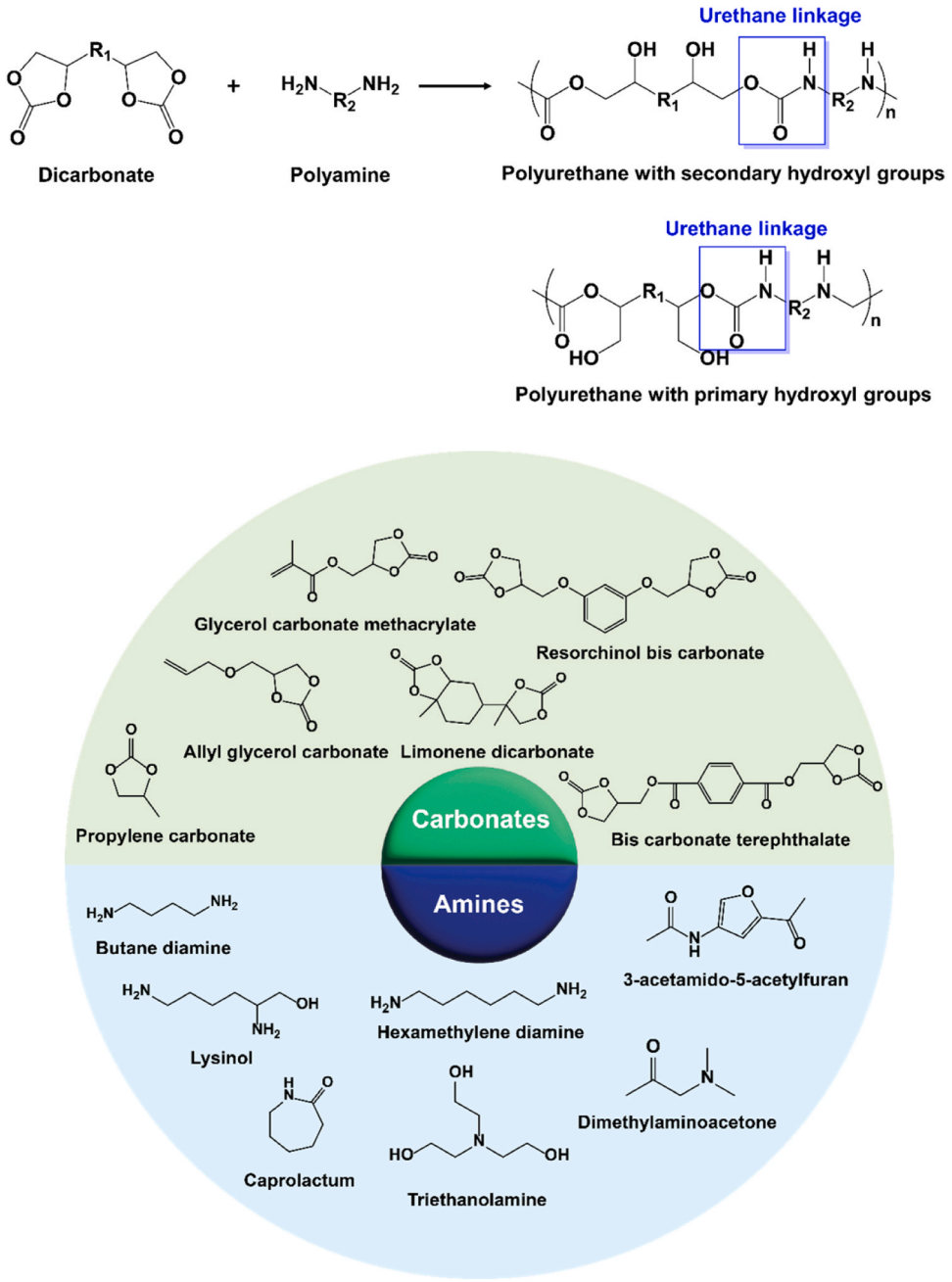

Fig. 22. Schematic illustration of non-isocyanate polyurethane synthesis and examples of carbonates and biobased amines used in non-isocyanate polyurethane synthesis.

the chain extender used in this system differs from aromatic polyurea systems as isophorone diamine (IPDA) is commonly used with a co-chain extender.

Polyurethane, polyurea, and polyurethane/polyurea hybrid systems exhibit outstanding durability, elasticity, and adhesion to different substrates. Properties of polyurethanes or polyurea can be easily tuned by selecting starting materials with different functionalities. This enables these materials to be utilized in various applications *i.e.* sealants, adhesives, and coatings to reinforce the excavation sites. However, the main drawbacks originate from the toxicity of isocyanates. Inhalation of isocyanate aerosols, dust, or vapors during the process of spray coating or curing process can cause irritation to the respiratory system upon short-term exposure. Long-term exposure can cause asthma, dermatitis, and chronic lung damage. Proper ventilation and personal protective equipment (PPE) are required to minimize occupational health and safety risks [103–105]. To ensure the safety of workers, utilization of polymeric isocyanates or non-isocyanate based polyurethane syntheses were developed.

Non-isocyanate polyurethanes can be synthesized via a polyaddition reaction between polycyclic carbonate oligomers derived from vegetable oils, lignin, and terpene and aliphatic or cycloaliphatic polyamines with primary amino groups that act as a curing agent (Fig. 22) [106, 107]. These polyurethanes are environmentally safe due to the absence of isocyanates. Furthermore, they are less sensitive to moisture with high chemical and thermal stabilities when compared to conventional polyurethanes. These properties can be enhanced mainly by the crosslinker type and the addition of difunctional hydroxyalkyl urethane glycols with urethane bonds as additives. A stable crosslinking network in conventional polyurethanes restricts them from exhibiting self-healing properties. On the other hand, non-isocyanate

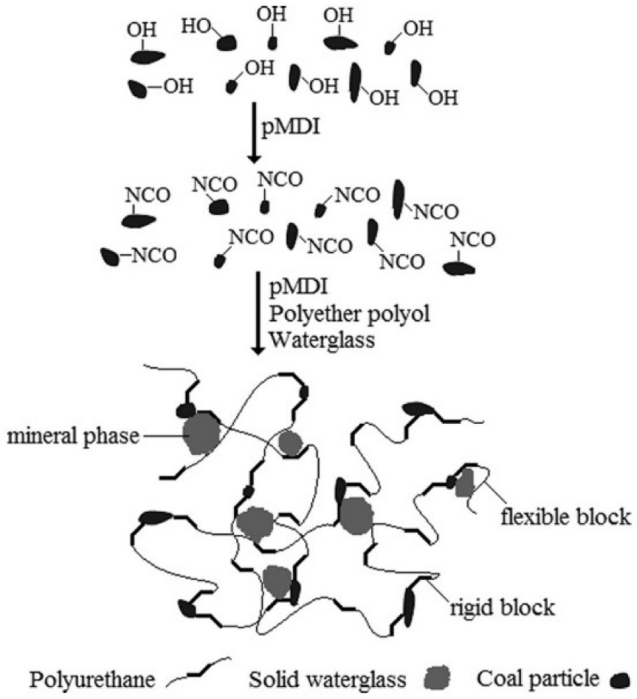

Fig. 23. Schematic illustration of bonding mechanism between waterglass-polyurethane composite and coal.
Adapted with permission from [111].

polyurethanes have self-healing and excellent shape memory properties depending on the formulation. Although non-isocyanate polyurethanes possess tremendous potential with versatile applications, commercial products based on non-isocyanate synthesis routes have not been able to replace conventional polyurethanes due to several challenges that need to be overcome.

The biggest challenge faced in producing non-isocyanate polyurethanes at present is producing highly reactive cyclic carbonates on an industrial scale. Due to the simplicity of industrial-scale production, 5-membered cyclic carbonates are widely produced on an industrial scale by simply inserting CO_2 into epoxides. However, syntheses of non-isocyanate polyurethanes using 5-membered cyclic carbonates require high temperatures and long reaction times due to their low reactivity. This significantly increases the occurrence of side reactions, resulting in low molecular weight non-isocyanate polyurethanes. Reactivity can be enhanced by using two different approaches: (*i*) utilization of 8-membered cyclic carbonates or (*ii*) utilization of cyclic carbonates reacted with different secondary or primary amines. Production of activated and larger cyclic carbonates on an industrial scale is not achievable because of the low stability and yields. Extensive research also needs to be conducted in designing catalysts and more reactive hydroxylamines to enhance the reactivity. Hence, it remains challenging to achieve rapid curing and curing at room temperature. The outstanding challenges also include hydrolysis of cyclic carbonates during polymerizations in aqueous medium, lack of appropriate polyamines in preparation of thermoplastic polyurethane elastomer with soft and hard segments, and difficulties in large-scale synthesis. Addressing these issues through further studies will lead to the development of safe and sustainable reactive TSL.

2.2.2. Recent development of reactive TSLs

Reactive TSLs based on polymeric materials should demonstrate properties such as high strength, strong durability, excellent adhesive strength to the substrate, and rapid curing. Film formation should occur at low reaction temperatures without releasing toxic substances during or after the curing process. Fire accidents can cause serious occupational health and safety issues, thereby it should contain flame retardants such as expandable graphite, dimethyl methylphosphate, aluminum hydroxide, and chlorinated paraffin. Also, the flash point of each component should be lower than the reaction temperature in order to avoid fire accidents [108]. Currently, materials such as waterglass (sodium silicate), fly ash, and graphene are often added to polyurethanes to improve their thermal stability and flame resistance.

Waterglass that contains silicon dioxide (SiO_2) and sodium oxide (Na_2O) is a glassy solid which can dissolve in water [109, 110]. Guan *et al.* [111] first introduced waterglass to enhance the thermal stability of polyurethane. Waterglass-polyurethane composites were synthesized by mixing polyether polyol with waterglass under a constant stirring rate. Consequently, polymeric MDI was introduced and mixed vigorously for several minutes. Fourier transform infrared spectroscopy (FTIR) of coal surface, waterglass/polyurethane, and waterglass/polyurethane/coal surface revealed that hydroxyl groups on coal surface initially react with isocyanate groups in polymeric MDI. These modified isocyanate groups further react with polyether polyols and waterglass during the curing process. It was proposed that there is an adhesion mechanism between coal and waterglass/polyurethane, whereby waterglass is uniformly dispersed in a polymer network and coal is connected to the polymer chain (Fig. 23). This would result in an enhancement in adhesive strength between coal and waterglass-polyurethane composite.

He *et al.* [112] later reported that incompatibility of waterglass with polyurethane due to the presence of water on waterglass, Si-O^-, and Si-OH groups, can be overcome by employing chloropropyl-based silane coupling agent 3-chloropropyltrimethoxysilane (CTS). A two-component polyurethane system was prepared: component A with waterglass, CTS, glycerol, and cyclohexylamine as catalyst and component B with polymethylene polyphenylene isocyanate (PAPI), polyether polyol, chlorinated paraffin-52, and dioctyl phthalate as plasticizer. Pre-treatment of waterglass with 2.5 wt% CTS for 30 min before mixing significantly enhanced the compatibility between inorganic waterglass and organic polyurethane matrix, which resulted in the uniform distribution of silicate particles. The authors proposed a reaction mechanism between waterglass-polyurethane composite and CTS (Fig. 24). First, unstable silanol from the reaction of CTS with water on the surface of waterglass and Si-O^- and Si-OH groups from the waterglass create hydrogen bonding after condensation. The gathering of chloropropyl groups from hydrolysed CTS enables uniform distribution of waterglass and reduction of interfacial tension between waterglass and polyurethane. Second, unstable amine groups created from the reaction between the isocyanate group in PAPI and water from waterglass and hydrolysed CTS react with isocyanate groups and form urea linkages. Finally, the hardening of waterglass occurs in the presence of water and CO_2. This results in the formation of Na_2CO_3 crystals which fill the interphase region, thereby reducing the hydrophobicity of the cavities present in polyurethane surfaces. Liang *et al.* [113] also reported that the addition of CTS enhanced the curing process by distributing waterglass uniformly in polyurethane. A two-component polyurethane system was employed: component A with waterglass, CTS, and cyclohexylamine and component B with polyisocyanate, polyether polyol, and chlorinated paraffin-52. The chemical interactions between CTS and isocyanate groups led to a significant enhancement in compressive strength, flexural strength, flexural modulus, and fracture toughness of these polyurethane composites.

Zhang *et al.* [114] further investigated the influence of different catalysts on the properties of waterglass-polyurethane composites. Two different types of catalysts, dimethylbenzylamine (BDMA, tertiary amine catalyst) and dibutyltin dilaurate (DBTDL, organotin catalyst), were employed in a two-component polyurethane system. Component A contained waterglass, glycerin, and a certain amount of catalyst, and component B contained PAPI, polyether polyol, chlorinated paraffin-52, and dioctyl phthalate. Overall, the addition of an organotin catalyst accelerated the curing process more effectively than a tertiary amine

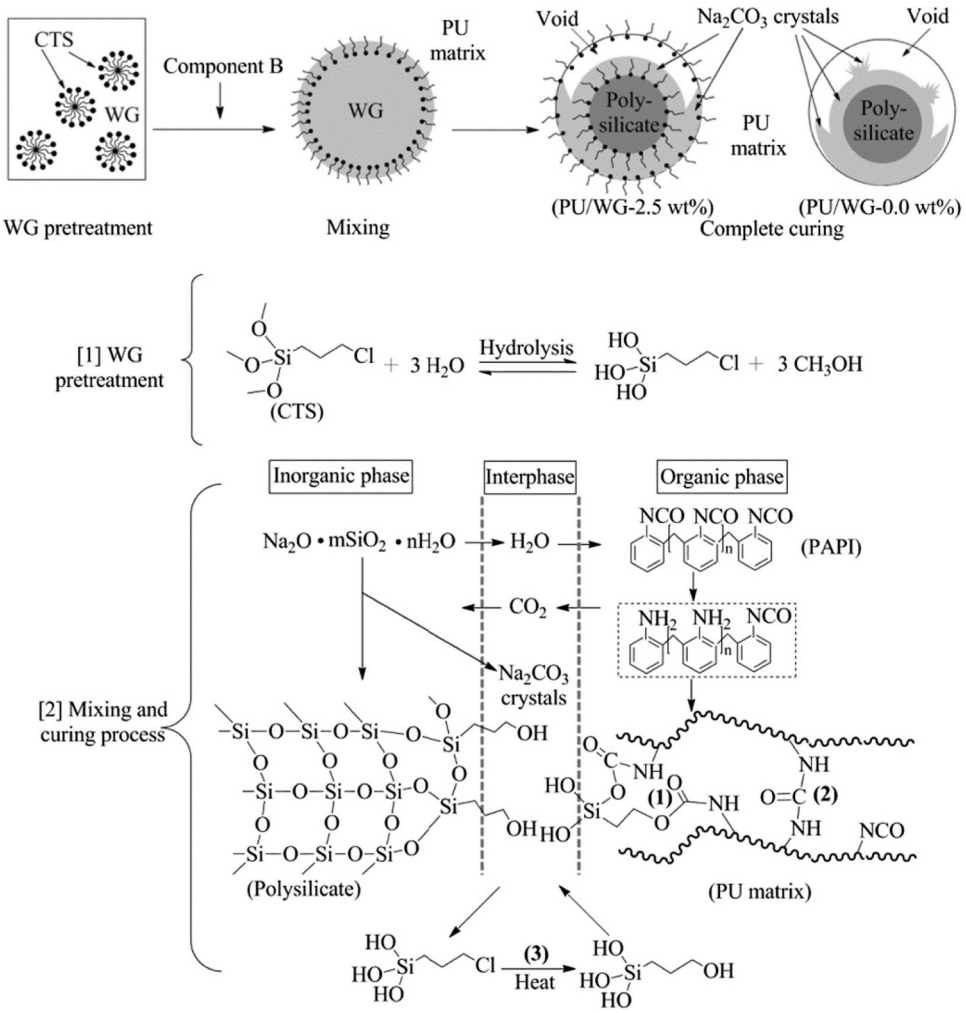

Fig. 24. Schematic illustration of reaction mechanism between waterglass-polyurethane composite in the presence of CTS.

catalyst. The combination of 0.1 wt% BDMA and 0.1 wt% DBTDL resulted in excellent fluidity, rapid curing, and enhanced thermal stability.

Coal combustion in thermal power plants produce wastes called fly ash containing silica (SiO_2), alumina (Al_2O_3), iron oxide (Fe_2O_3), and calcium oxide (CaO). The utilization of fly ash from coal wastes as fillers has drawn attention as it can reduce production costs and pollution [115–117]. Qin *et al.* [118] studied the effect of fly ash treatment with silane coupling agents on the mechanical properties of polyurethane composites. Pre-treatment of fly ash with the silane coupling agent 3-glycidoxypropyltrimethoxysilane (GPTMS) increases the hydrophobicity of fly ash particles, thereby increasing the compatibility between fly ash and polyurethane. When GPTMS reacts with fly ash particles, alkoxy group from GPTMS hydrolyzes and forms silanol group (Si-OH). Silanol molecules are condensed by the hydroxyl group present on the surface of fly ash. Furthermore, the crosslink density increases by ring-opening reaction between epoxy functional group at GPTMS and polyurethane (Fig. 25). At optimum GPTMS concentration, the fracture toughness and flexural strength increased by 10 % and 19 %, respectively, due to the increase in crosslink density. Zhang *et al.* [119] investigated the influence of fly ash in thermal properties of polyurethane composites. The surface of fly ash was modified by mixing with silane coupling agent (3-aminopropyl) triethoxysilane (APTS) at high stirring rate for 15 min. Pre-treatment of fly ash effectively reduced the interfacial tension between fly ash particles and polyurethane, thus resulting in uniform distribution within the polyurethane. Fly ash serves as a barrier that inhibits the release of VOCs from degradation of polyurethane [120]. Furthermore, thermally stable oxides in fly ash prevent diffusion of heat and gas, leading to significant enhancement in thermal stability of fly ash-polyurethane composites [121].

Graphene has been widely incorporated as a reinforcement filler in polymer nanocomposites due to its excellent electrical and thermal conductivities and high strength [122–125]. Thiyagu *et al.* [126] investigated the influence of graphene on the thermal and mechanical properties of polyurethane composites. Graphene-polyurethane composites were prepared by solvent casting method [88, 127, 128]. Graphene was dispersed in dimethylformamide (DMF) and mixed with dried polyurethane powder at 125 °C for 45 min. Incorporating graphene delayed the formation of VOCs by forming a fire barrier at high temperatures. Also, the grafting of polyurethane to the functionalized graphene nanosheets with hydroxyl groups contributes to the enhancement of thermal stability. The addition of graphene nanosheets enhanced the load-carrying capacity with increasing amounts of graphene. However, the elasticity is significantly reduced in the presence of excessive graphene due to the agglomeration of graphene nanosheets. At optimum graphene concentration, desired mechanical properties can be achieved. Graphene has great potential to be applied as a filler in polyurethane-based reactive TSLs to enhance thermal and mechanical properties. Further studies would be essential in synthesizing graphene-polyurethane composites in mild conditions where high temperatures and organic solvents are not required.

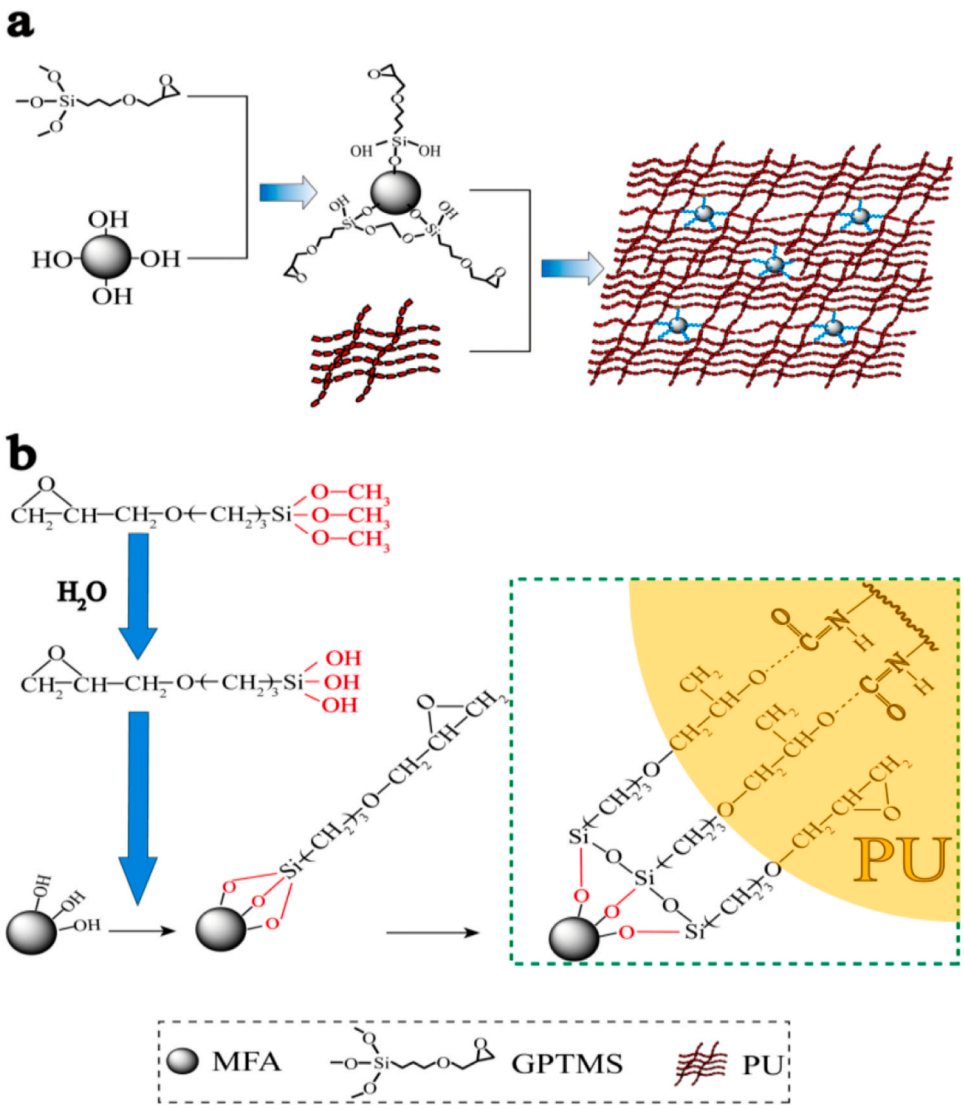

Fig. 25. Schematic illustration of (a) the synthesis of fly ash-polyurethane composite, and (b) crosslinking mechanism between surface modified fly ash and polyurethane matrix.
Taken and adapted from [118].

2.3. *Commercially available TSL products*

With the rapid advancements in the materials and chemical industries, TSL products are continually being updated and replaced. Table 2 summarizes TSL products that have been listed in the literature or have been utilized commercially in recent years. All products are listed with the name of the manufacturer, mix base, material type, and application purposes.

The material performance and functional emphases of these commercial TSLs vary in response to market demands, local regulations, and industry standards specific to different regions. A summary of some mechanical properties of commercial TSLs, based on available technical data sheets, is presented in Table 3. The majority of TSL products are non-toxic, non-flammable, and self-extinguishing. Antistatic properties required in coal mines are only mentioned in a few products. In the technical data sheet of ZMKJ in China and Minova's Tekflex LP, which is available in Europe and Africa only, the description of the antistatic properties of products is stated as 'antistatic' and 'dissipative', respectively. Silcrete TSL, sold in Australia and New Zealand, specifically highlights its antistatic properties, which comply with the electrical resistance requirements outlined in MDG3608, published by the Mine Safety Operation Branch in New South Wales to minimize the health and safety risks associated with the utilization of non-metallic materials in underground coal mines. Certain commercial TSL products require the use of dedicated spraying equipment or adherence to special spraying process due to their complex application conditions and material composition. Minova Tekflex pumping equipment is utilized to apply Tekflex. Silcrete TSL is applied through a suitable plural component pump system directly to the rock face either by handgun or robotic arm application. For the same product, different spraying times and thicknesses can be set, depending on the purpose of application. Min *et al.* [24] conducted an experimental study on a non-reactive TSL product designed by Nanjing Science & Technology Coal Research Co., Ltd., demonstrating that spraying can be performed with a thickness of 2–5 mm at a time for weathering and rust prevention. However, three to four rounds of re-spraying are required resulting in a total spraying thickness of 10–20 mm when TSL is applied for a sealing purpose, particularly in challenging refuge chambers for gas control.

3. Support and loading mechanisms

TSLs can effectively 'lock' rock blocks together, minimizing relative

Table 2
List of the currently available TSL products.

Product	Manufacturer	Mix Base	Material Type	Purposes	Reference
AERO SEAL	Genrock Mining - South Africa (SA)	Cementitious polymer	Powder	Support	Ozturk and Guner [19]
BluSeal TF05	Bluey Technologies - Australia (AU)*	Cement polymer	Powder/ liquid	Sealing/ Support	\
Chryso TSL LP	Chryso - SA	Cement/polymer	Powder/ liquid	Support	Ozturk and Guner [19], Tweefontein coal mine in Ogies, South Africa [129]
Chryso TSL SP	Chryso - SA	Cementitious polymer	Powder	Support	Ozturk and Guner [19]
Ekopur LS/G**	Minova Europe - EU	Two-component polyurethane	Liquid/ liquid	Sealing/ Support	\
GeoFlex**	Minova USA - United States (US)	Silicate resin	Liquid/ liquid	Sealing	\
MasterRoc TSL 865**	Master Builders Solutions - AU*	Single-component polymer	Powder	Sealing/ Support	Ozturk and Guner [19]
NJBP**	CCTEG Nanjing Design & Research Institute Co., Ltd. – China (CN)	Cement-based	Powder	Sealing/ Support	[130]
Non-reactive TSL-MB**	Jiangsu Kehang Mining Technology Co., Ltd. - CN	Cement/resin	Powder/ liquid	Sealing/ Support	
Polyshield HT SL	SPI - US	Polyurea	Powder	Sealing	\
Rock Guard SS50	Rock Support Systems Mining Supplies - US	Cement/polymer	Powder/ liquid	Sealing/ Support	\
RockWeb TSL	Spray-on Plastics - Canada (CA)	Two-component polyurea	Liquid/ liquid	Sealing/ Support	Gold mine in Quebec, Canada [131]
Silcrete TSL**	Polymer Group - New Zealand (NZ)*	Polyurea-silicate	Liquid/ liquid	Support	Roache, Jardine and Sainsbury [18], Hill [132]
Tamcrete SSL	Normet - Finland	Acrylic resin and graded fillers	Powder/ liquid	Sealing/ Support	Ozturk and Guner [19]
TamPur 116T**	Normet - Finland*	Silicate modified polyurea	Liquid/ liquid	Support	\
Tekflex Black AP**	Minova USA - US	Cement-based	Powder	Sealing/ Support	\
Tekflex Black**	Minova USA - US	Cement-based	Powder/ liquid	Sealing/ Support	Ozturk and Guner [19]
Tekflex Dry Spray**	Minova USA - US	Cement-based	Powder	Sealing/ Support	\
Tekflex DS-W**	Minova Europe - EU	Polymer-based	Powder	Sealing	\
Tekflex LP**	Minova Europe - EU	Cement/polymer	Powder/ liquid	Sealing	Ozturk and Guner [19]
Tekflex White AP**	Minova USA - US	Cement-based	Powder	Sealing/ Support	\
Tekflex White**	Minova USA - US	Cement-based	Powder	Sealing/ Support	Ozturk and Guner [19]
Tekflex**	Minova Australia - AU*	Cement-based	Powder/ liquid	Sealing/ Support	Ozturk and Guner [19]
TL−40**	Jennmar - AU*	Polymer-modified	Powder/ liquid	Sealing/ Support	\
Tunnel Guard	ZETACHEM - SA*	Cementitious mix & latex liquid	Powder/ liquid	Sealing/ Support	\
Tunnel Guard SS	Altecrete - SA	Cement-based	Powder	Sealing/ Support	Ozturk and Guner [19]
V-SEAL TSL	Carbontech - SA	Polymer-based cement	Powder/ liquid	Sealing/ Support	Burnstone mine, Tau Lekoa mine, and a diamond mine in Kimberley, South Africa [133]
ZMKJ**	Zhong Mei Science - CN	Polymer	Powder	Sealing/ Support	\

*: Products available in Australia.
**: Products that can be used in coal mines.

block displacements between them. This locking mechanism contributes to the stabilization of the rock mass around excavations, acting as a preventive measure against minor rockfalls [16, 134]. The ability of liners to adhere to the rock surface plays a crucial role in preventing the fragmentation or loosening of individual rock fragments. This is due to the intimate contact between the liner and rock surface, which helps reduce the magnitude of stress and strain energy resulting from distortion, displacement, and rotation at the interface [16, 135]. The adhesion of TSLs can be influenced by several environmental and rock characteristics, including surface roughness, surface moisture, surface contamination, rock strength, and weathering conditions. Ozturk and Tannant [136] demonstrated that contaminants tend to decrease the bonding between the TSL and rock substrate, while larger grain sizes increase the bond strength. They also found that surface roughness does not significantly influence the bonding behavior.

It may be challenging to restrain relative displacements in circumstances where rock mass conditions, stress levels, and excavation geometry result in significant rock deformations or convergence. This could lead to the formation of an unstable rock zone. In such situations, the primary function of the liner shifts to retaining loose rock in place between the rock bolts [16, 134]. Thus, the volume of rock involved and the magnitude of relative displacements between adjacent rock blocks need to be considered to ensure TSL provides adequate support. Furthermore, it is crucial that the rock mass is intact and tightly compacted before the liner is applied [16]. If the rock mass is already fractured, the self-supporting capability of a significant portion of the rock may be reduced before the application of the liners. The effectiveness of TSLs in stabilizing the rock mass around excavations depends on both the rock mass conditions and the rock surface. Proper assessment and preparation of the rock surface are essential to achieve the desired

Table 3
Mechanical properties of some currently available TSL products.

Product	Tensile strength (MPa)	Elongation (%)	Bond strength (MPa)	Setting time	Toxicity	Flammability
AERO SEAL	Not available (NA)	NA	NA	3 h (25°C)	Non-toxic	Non-flammable, self-extinguishing
BluSeal TF05	5 (28d)	50 (28d)	1.5	50–60 min (initial set)	Low (liquid part)	Non-flammable
Chryso TSL LP	NA	NA	NA	2 h (25°C)	Non-toxic	Non-flammable, self-extinguishing
Chryso TSL SP	NA	NA	NA	2 h (25°C)	Non-toxic	Non-flammable, self-extinguishing
Ekopur LS/G	NA	NA	NA	NA	Non-toxic	Low flammability, self-extinguishing
MasterRoc TSL 865	> 0.2 (4 h) > 0.4 (1d) > 2.0 (7d) > 5.6 (28d)	> 100 (4 h) > 50 (1d) > 60 (7d) > 30 (28d)	1.7 (on concrete), coal failure	Fast setting (within 5 min)	Non-toxic	Self-extinguishing
NJBP	> 0.5 (4 h) > 1.0 (1d) > 2.6 (7d) > 3.5 (56d)	> 150–50	1–2	NA	Non-toxic	Complies with fire resistance requirements of MT113–1995
Non-reactive TSL-MB	> 2.5	10–100	> 3.0	< 6 h	NA	Complies with fire resistance requirements of MT113–1995
Rock Guard SS50	6.8	NA	3.2	NA	Non-toxic	Non-flammable
Silcrete TSL	7.8	5–10	> 3.7 (substrate failure)	10–15 min	Part B is a diisocyanate, inhalation must be avoided	Non-combustible, complies with fire resistance requirements of MDG3608
Tamcrete SSL	1.0 (1 h) 2.2 (7d)	NA	NA	4 s−4 min (gel time)	Non-toxic	NA
Tekflex LP	> 1.0 (1d) > 10 (28d)	> 20 (1d)	NA	30–70 min (gel time)	Non-toxic	Low flammability, self-extinguishing
Tekflex	4–5	60–100	NA	50–70 min (initial set)	Non-toxic	Non-flammable
TL−40	> 3.5 (7d)	60	> 1.7 (on concrete), coal failure	NA	Non-toxic	Self-extinguishing
Tunnel Guard	2.5–8	NA	1.7	1 h (initial set)	Non-toxic	Non-flammable
Tunnel Guard SS	13.78	NA	3.56	45 % strength after 6 h	Non-toxic	Non-flammable
V-SEAL TSL	2.0 (1d) 3.0 (3d) 3.5 (7d) 4.0 (14d) 4.5 (28d)	NA	0.8 (1d) 1.2 (3d) 1.5 (7d) 2.5 (14d) 3.0 (28d) 3.5 (72d)	40 min	NA	Non-flammable
ZMKJ	8.5	NA	4.5	< 40 min	Non-toxic	Flame retardant

stabilization effect with sprayed liners. Therefore, understanding the support and loading mechanisms provided by TSLs is important when determining appropriate testing methods to ensure the successful application of TSL on mining sites.

3.1. Support mechanisms

The primary function of TSLs is to help maintain excavation stability. The support mechanism of liners mainly depends on good adhesion and tensile properties between the sprayed layer and the surface of the rock mass [137]. Tannant [16] suggests that thin liners help maintain the excavation stability by simply gluing or bonding loose pieces of rock to adjacent competent rock. Additionally, high shear strength of the sprayed layer is also essential to ensure effective areal support between the bolts installed around an excavation. Stacey [138] summarized the support mechanisms of TSL and categorized them into ten categories, which may occur individually or in combinations, as shown in Fig. 26.

In a considerably unloosened condition, the *promotion of block interlock* is expected to preserve the rock mass. The mechanisms involved in the *promotion of block interlock* can be subdivided into four categories.

i. The promotion of interlock relies on the bonding between the liner and rock and the tensile strength of the liner, which helps prevent shear at the interface and restricts the rotation of blocks (Fig. 26a).
ii. The irregularity of the interface surface leads to the development of shear strength between the liner and the rock (Fig. 26b).
iii. The penetration of the liner into joints and cracks restricts the block movement (Fig. 26c). When the thin liner is applied to the rock surface in the early stages of fracturing development, it can withstand the movements of fractured rocks (Fig. 26d).
iv. Block movement is prevented due to shear resistance (Fig. 26e) and tension resistance provided by the liner (Fig. 26f).

In addition to the four mechanisms involved in the *promotion of block interlock*, Stacey [138] also described several other support mechanisms, including *air tightness*, *structural arch*, *basket mechanism*, *slab enhancement*, *extended 'faceplate'*, and *durability enhancement*.

Air tightness: The dilation of joints and fractures is a contributing factor to rock mass failure. Hence, potential failure can be mitigated by preventing dilation. TSL acts to prevent the ingress of air into joints and fractures (Fig. 26g), thereby effectively limiting rock mass dilation [139].

Structural arch: A rigid liner can restrict further deformation of the

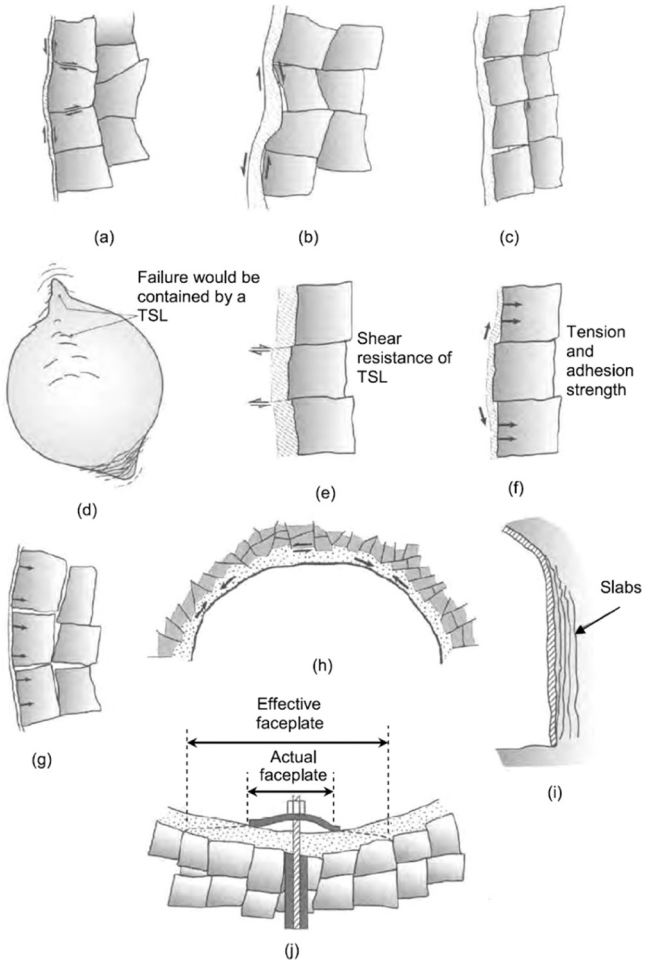

Fig. 26. Schematic illustration of support and loading mechanisms of TSL. Taken from [138].

rock mass (Fig. 26h). However, this support provided by TSL is limited compared to shotcrete [3].

Basket mechanism: TSL forms a basket to support the loosening rocks or unstable blocks. Three key factors influence the performance of the TSL during the formation of the basket. First, the flexural properties or ductility of the TSL determine its ability to bend during the basket formation. Secondly, the tensile strength of the material is crucial, providing support to the basket when it begins to form. Lastly, both the tensile strengths of the fibers and the polymer have an impact on the performance in the case of fiber-reinforced TSL. If the interfacial bonding between reinforcing fiber and TSL materials is insufficient, there will be a decrease in the loading capacity [140].

Slab enhancement: Rock slabs are formed under high stress during the initial stage of excavation. These slabs are prone to failure and collapse due to buckling caused by increased deformation. The thickness of rock slabs increases through the application of liners to the rock surface (Fig. 26i). This reduces the slenderness of the slabs and enhances their resistance to buckling. Furthermore, the formation of tensile cracking due to bending is reduced, consequently enhancing the tensile strength of the slabs [4].

Extended 'faceplate': TSL increases the influenced area where rock bolts and cable faceplates are installed (Fig. 26j).

Durability enhancement: The application of TSL can enhance durability by preventing the deterioration of rocks when exposed to wetting and drying. The mechanical and corrosion protection provided by TSL enhances the safeguarding of other support elements. It absorbs energy from mechanical impacts and acts as an impermeable barrier against corrosion and weathering [3].

3.2. Loading mechanisms

A range of loading mechanisms can occur under both static and dynamic loading conditions [138].

Wedge and block loading: The displacement of a wedge or block of rock applies load to the liner locally. This induces shear stresses in the TSL along the perimeter of the block on bonded liners. If the bond fails, tensile stress is induced in the TSL and bond stress develops at the interface (Fig. 26f).

Distributed surface loading: Distributed load may result from failed rock (due to gravity), high-stress-induced squeezing or swelling of rock (static), and dynamic loading caused by rock bursts. Distributed loading activates a basket support mechanism in the TSL. In this case, TSL will experience localized deformation at the rock joint.

Stress-induced loading: When the TSL support is well-bonded to the rock surface, it deforms along with the rock mass. Shear, bending, buckling, tension, or more complex failure mechanisms may occur, leading to stress-induced spalling of the TSL.

Water and/or gas pressure loading: Water and/or gas pressure is a distributed pressure that can weaken the surface support in undrained conditions. When TSLs are employed for coal mine gas management, the gas pressure must be considered in the design of TSL support [3].

Bending loading: Bending loads on the TSL support occur particularly in the haunch areas, where floor level convergence is greater than roof level convergence.

4. Testing methods

TSL underground trials in operating mines were first performed in Canada in 1990 at Inco's Copper Cliff North and Kidd Creek Mines. During the 1990s, Inco focused on laboratory and field trials using Mineguard and RockGuard. In the mid-1990s, there was a significant increase in interest in utilizing TSL as surface support within the South African mining industry where experiments were conducted with the Everbond product. However, challenges were faced in the utilization of TSLs due to the absence of standardized procedures or guidelines for determining the mechanical properties of the product. As a result, Yilmaz *et al.* [141] highlighted the necessity to develop standardized guidelines for testing TSLs to enhance the reliability of performance quality.

In rock engineering, the design of surface support relies on the material properties of the liner product, as they directly influence the load-bearing capacity of the membrane for support. The design of liner material properties for ground support relies on the geological conditions of the rock mass [142]. The following tests are considered to be most relevant in measuring TSL properties and the research effort so far has been mainly spent on these tests: tensile strength (elongation) [15, 25, 143, 144], adhesion (bond) strength [3, 25, 145, 146], shear strength [9, 147, 148], tear strength, creep behavior, the effect of temperature, the effect of water/humidity [149], acid and base resistance, flammability, impact strength (abrasion) and toxicity [147].

Previous studies [3, 23] recommended that the testing methods to determine mechanical properties of TSLs should have the following attributes: simplicity (easily prepared samples), cost-effectiveness, repeatability, practicality, representativeness of relevant properties, correlation with *in-situ* performance, and generation of statistically valid data. Testing should be conducted to examine the TSL material itself or/and estimate the interaction between the TSL and the substrate. Large-scale tests are often time-consuming, expensive, and difficult to perform in the laboratory. Standardizing large-scale tests is challenging as these tests are often conducted individually by the manufacturers that develop TSL materials [150]. Furthermore, it is difficult to interpret the data to determine TSL properties and behaviors. This can be problematic in designing TSL materials by utilizing large-scale test results. On the

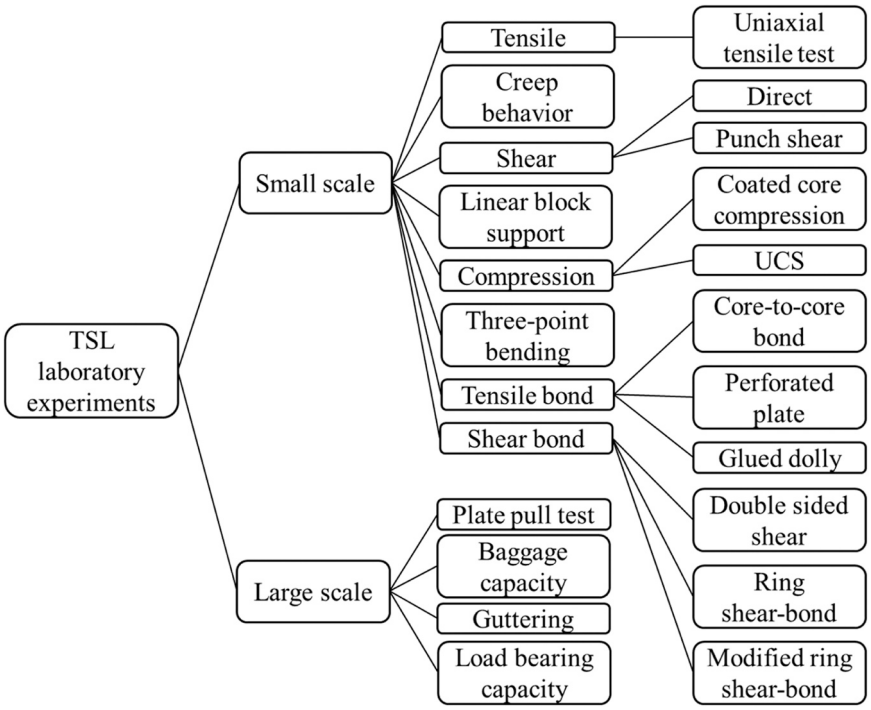

Fig. 27. Schematic illustration of laboratory TSL experiments in literature.

Table 4
Relevant updated standards for TSL testing methods (taken and adapted from ref [3]).

Test type	Standard	Description
Tensile strength and Elongation	ASTM D638–22	Tensile Properties of Plastics
	ASTM D1708–18	Tensile Properties of Plastics by Use of Micro-tensile Specimens
Tear strength	ASTM D1004–21	Tear Resistance (Graves Tear) of Plastic Film and Sheeting
	ASTM D1922–23	Propagation Tear Resistance of Plastic Film and Thin Sheeting by Pendulum Method
	ASTM D5884/ D5884M−04	Determining Tearing Strength of Internally Reinforced Geomembranes
	ISO 34–1: 2022	Rubber, vulcanized, or thermoplastic — Determination of tear strength — Part 1: Trouser, angle, and crescent test pieces
	ISO 34–2: 2022	Rubber, vulcanized, or thermoplastic — Determination of tear strength — Part 2: Small (Delft) test pieces
Compressive strength	ASTM D7012	Compressive Strength and Elastic Moduli of Intact Rock Core Specimens under Varying States of Stress and Temperatures
Shear strength	ASTM D732–17	Shear Strength of Plastics by Punch Tool
Bond strength	ASTM D4541–22	Pull-Off Strength of Coatings Using Portable Adhesion Testers
Toxicity	ASTM E1619–11	Chronic Oral Toxicity Study in Rats
Flammability	ASTM E162–22	Surface Flammability of Materials Using a Radiant Heat Energy Source
	ASTM E84–23	Surface Burning Characteristics of Building Materials
	CAN/ULC S102	Surface Burning Characteristics of Building Materials and Assemblies
Water absorption	ASTM C827/ 827M−23	Change in Height at Early Ages of Cylindrical Specimens of Cementitious Mixtures
	ASTM D570–22	Water Absorption of Plastics
Abrasion	ASTM D4060–19	Abrasion Resistance of Organic Coatings by the Taber Abraser

other hand, small-scale laboratory tests have been more successful in generating controlled results [151]. Up until now, only direct tensile and adhesion strength tests have gained widespread acceptance, as they are easy to operate and provide direct results of TSL properties. Potvin, Stacey, and Hadjigeorgiou [7] proposed a classification of mechanical tests based on the scale of the test. Fig. 27 summarizes laboratory studies that have been done to measure the mechanical properties of TSL materials.

Although many scholars have conducted laboratory and *in-situ* tests on the strength characteristics of TSLs, there are currently no corresponding international standards for testing the mechanical properties of TSLs. Even these commonly applied testing methods are adapted from the testing standards of other materials like plastics or shotcrete. To the best of our knowledge, there is a limited number of reports that provide specifications and guidelines for TSLs used in the mining and tunneling industries [152]. Table 4 summarizes current testing standards and the relevant testing methods that could be used for testing TSLs either directly or with modifications [3]. Governments may also produce specifying requirements for material characteristics based on local conditions. For example, the New South Wales government (Mine Safety Operations Branch) in Australia has issued MDG 3608, which provides appropriate testing requirements for non-metallic materials used in underground coal mines to minimize safety and health risks.

The boundary conditions and loading mechanisms for the strength tests are shown in Fig. 28 [9]. The tensile, compressive, shear, tear, and bend strength tests only measure the properties of TSL materials, whereas bond strength tests demonstrate the interaction between TSL and the substrate. In bond strength testing, bond failure can occur at any location within the TSL and substrate. Failure that occurs at the interface is referred to as adhesion failure, while failure that occurs within the substrate or TSL is referred to as cohesion failure. In some cases, a combination of adhesion and cohesion failure can occur.

4.1. Tensile strength testing

Measuring tensile strength and elongation at the break of TSL materials is crucial to determine the maximum support capacity of loads

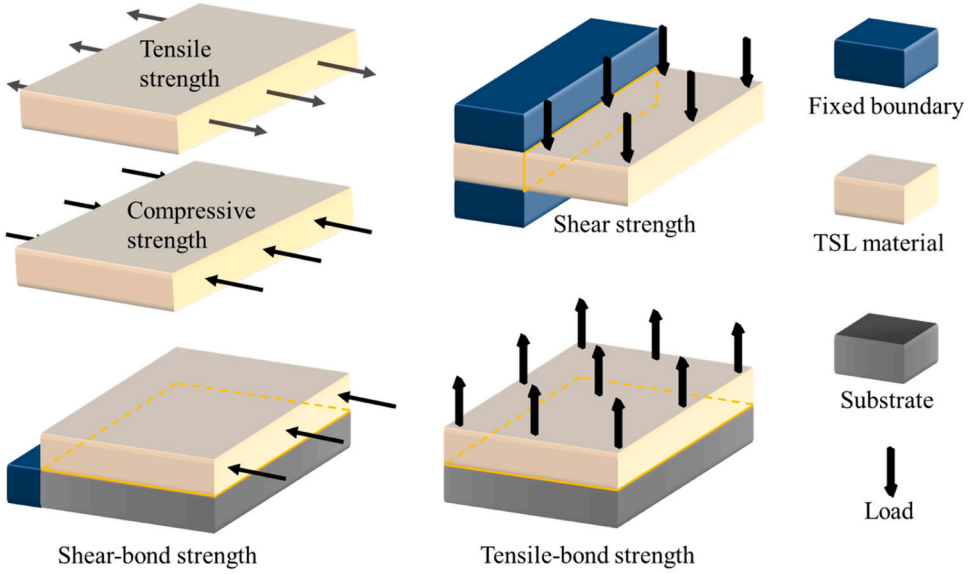

Fig. 28. Schematic illustration of boundary conditions and loading mechanisms for mechanical tests of TSL. Taken and adapted from [9].

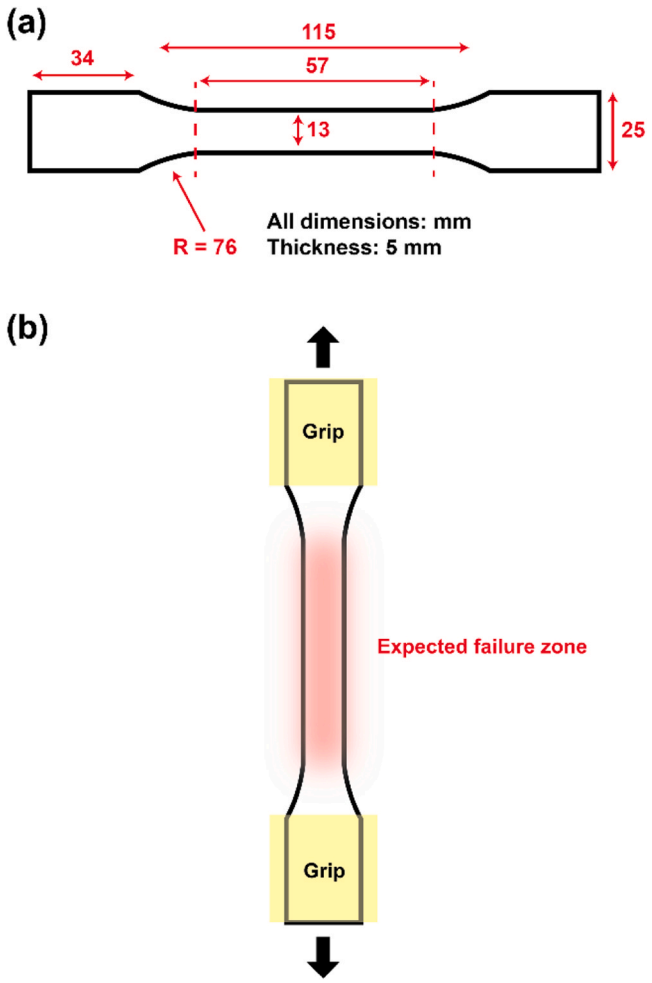

Fig. 29. Schematic illustrations of (a) ASTM D638-Type 1 specimen and (b) failure location for valid uniaxial tensile testing.

and long-term support resistance to prevent the unraveling of loose rocks in the roof and sidewalls of excavations [7]. Tensile test specimens should be prepared under temperature and humidity conditions that represent those at mining sites. Tensile testing is often carried out 3, 7, 14, and 28 days after mixing as the tensile strength of TSL develops over time. This testing schedule helps estimate when the workers can safely resume work after TSL application [14].

Uniaxial tensile tests for TSLs are adapted from the ASTM D638 standard test method for tensile properties of plastics. Both early and recent studies followed the ASTM D683 standard for examining liner characteristics of tensile strength, elastic modulus in tension, and elongation capacity [14, 21, 134, 143, 144, 151, 153, 154]. For uniaxial tensile testing, dog-bone-shaped samples are prepared by following ASTM D638 Type 1 (Fig. 29). These samples can be prepared by stamping using die-cutting machine, molding from Perspex plastic, or silicone molds. Stamping methods are found to be suitable for ductile TSLs but not for cementitious-based TSLs due to their brittleness. The machining process using a lathe machine or laser cutting adds significant costs to sample preparation [3]. As an alternative, Yilmaz [14] proposed using Perspex molds to prepare the dog-bone-shaped samples. A 5 mm Perspex sheet with five ASTM D638 Type 1 shapes was prepared by laser cutting. A mold release agent was applied to the Perspex mold, and TSL materials were applied using a spatula. A plastic sheet was then applied on top of the TSL material to obtain samples with uniform thickness and remove air bubbles (Fig. 30). This approach is simple, cost-effective, and applicable to brittle TSL materials. Additionally, the molding process ensures uniform thickness, making it a favorable option for sample preparation [7]. The thickness of samples is determined depending on the field application which is typically around 5 mm. The results of the test conducted by Archibald [151] indicated that the thickness of the liner has an influence on its load-deformation behavior *i.e.* thin liners have a lower tensile strength than thicker liners. Samples were cured over 28 days for the samples to develop full strength as improvements in tensile strength and modulus of the TSL were observed with increasing curing time [14, 143].

For TSL samples, loading rates should be adjusted from the ASTM D638 standard so that failure occurs within the minimum test duration of 30 seconds as suggested by Ozturk and Tannant [14, 135]. At least five samples should be tested, and only the samples that fail within the narrow section in the middle are considered valid for tensile strength testing. Nominal stress (σ_n) and strain (ε_n) values can be calculated from

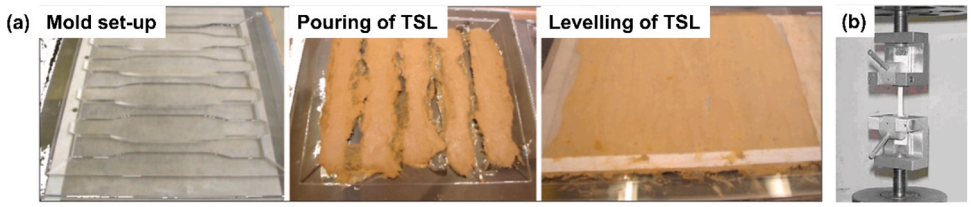

Fig. 30. Schematic illustration of (a) preparation of dog-bone specimens and (b) uniaxial tensile testing apparatus. Taken and adapted from [7, 14].

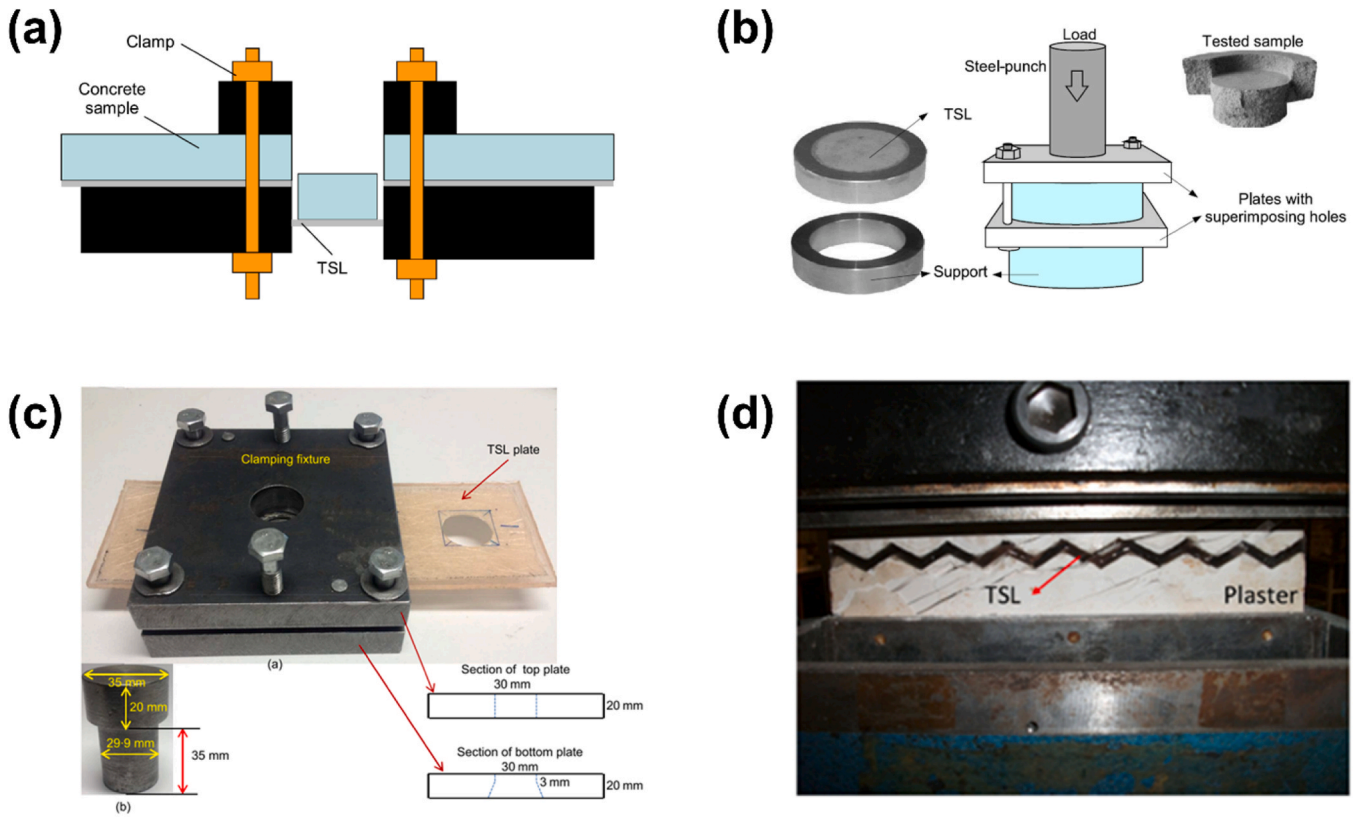

Fig. 31. Schematic illustration of different set-ups of shear strength tests. Taken and adapted from (a) [150], (b) [154], (c) [146], (d) Adapted with permission from [157].

the force (F) and elongation in the tensile direction.

Stress (σ_n, MPa) was determined by Eq.8:

$$\sigma_n = \frac{F}{A} \tag{8}$$

where F (N) is the load applied perpendicular to the cross-sectional area of the specimen, and A (m^2) is the original cross-sectional area of the specimen before a load is applied.

Strain (ε_n, %) was determined by Eq.9:

$$\varepsilon_n = \frac{\Delta l}{l_0} \times 100 \tag{9}$$

where Δl is the absolute increase in length and l_0 is the initial length of the specimen before a load is applied.

Furthermore, Young's modulus (E) and toughness of the material can be calculated by calculating the slope of the elastic region of the stress-strain curve and integrating the total area under the stress-strain curve, respectively.

4.2. Shear strength testing

The shear strength of TSL is considered one of the most crucial properties that significantly contribute to the reinforcement quality. Although some studies focus on the shear strength of TSL, no standardized test method currently exists for evaluating this property.

Hadjigeorgiou and Grenon [155] assumed that the shear strength of TSL is almost equal to its tensile strength when evaluating the supporting capacity. EFNARC [152] introduced a shear testing method for evaluating the shear bearing capacity of TSLs, which involves using three concrete blocks and a clamp fixture (Fig. 31a). Yilmaz [156] developed a punch test composed of a steel ring, a steel punch, and a clamping fixture to evaluate the shear strength of TSL (Fig. 31b). Qiao *et al.* [148] modified Yilmaz's method to determine the shear strength of glass fiber-reinforced TSL (Fig. 31c). The same group [157] conducted direct shear tests on artificial rock joints filled with TSL materials (Fig. 31d). In these tests, shear failure within the plaster resembled typical failure in intact rock, as shear failure did not occur at the TSL-plaster interface. The results suggested that the bond strength between the TSL and plaster exceeded the shear strength of the plaster.

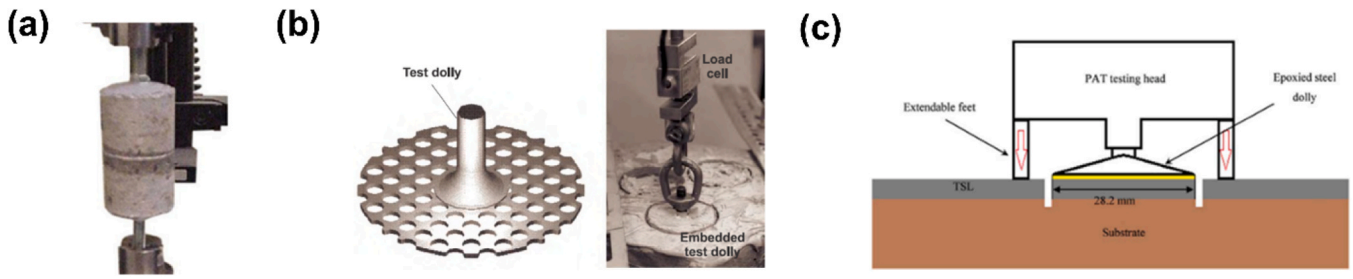

Fig. 32. Schematic illustration of tensile-bond strength tests; (a) core-to-core bond test. Taken and adapted from [7], (b) perforated plate pull test. Taken and adapted from [153], and (c) glued dolly test. Taken and adapted from [3].

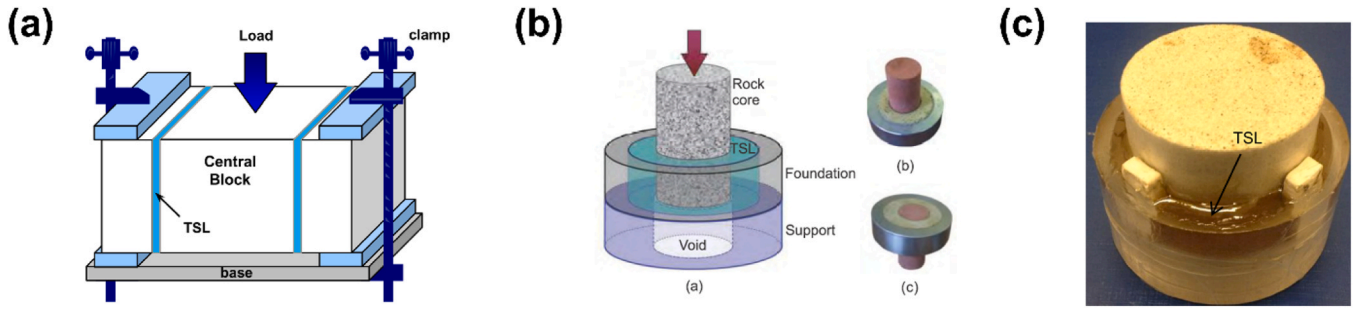

Fig. 33. Schematic illustration of shear-bond strength tests; (a) DSS test. Taken and adapted from [163], (b) ring shear-bond strength test. Taken and adapted from [9], (c) modified ring shear-bond test sample. Adapted with permission from [164].

This test clearly demonstrated a strong bond between the TSL and the plaster.

4.3. *Bond strength testing*

Determining the bond strength of TSL is crucial as loss of adhesion is the most common form of rock support failure in underground excavations [10, 158]. When engaged in the support process, TSL establishes a close bond with the rock surface immediately after spraying [4]. High bond strength enables TSL material to transmit the loads from gravity-induced rockfalls or unstable substrates, to the stable geological units, enhancing the self-supporting capacity of the loosened strata [25, 140].

Analytical and numerical techniques are utilized to determine the bond strengths of TSL [159,160]. There are mainly two types of bond strengths: tensile-bond strength and shear-bond strength. Tensile-bond strength measures the capability of TSLs to withstand the stress perpendicular to the rock-TSL interface, while shear-bond strength measures the ability of TSLs to withstand stress parallel to the rock-TSL interface. Typically, the rock-TSL interface experiences a combination of tensile and shear stresses [3].

Tensile-bond strength testing: Previous studies proposed three methods to measure the tensile-bond strength, the core-to-core bond test, the perforated plate pull test, and the glued dolly test (Fig. 32). In the core-to-core bond test, two core pieces are bonded together using TSL and subjected to a uniaxial pull test until failure occurs at the TSL-rock interface. The center line of the cores must align with the pull direction during sample preparation and testing to prevent failure caused by eccentric loading [3]. The two-layer spraying method is used for perforated dolly tests, where a perforated steel test dolly is embedded within the TSL and pulled after curing. However, this method may introduce internal defects, potentially leading to inaccurate results. The glued dolly test is adapted from ASTM D4541, which provides guidelines for conducting adhesive strength tests, using a dolly adhered to the coated surface. Glued dolly test specimens are prepared by gluing the steel dolly to the top surface of TSL with epoxy. The tensile bond strength is measured by gradually pulling the dolly after the epoxy has cured. The pull-off testing machines were designed for glued dolly tests to ensure a consistent displacement rate, avoid eccentric loading, providing reliable load-deformation data [17, 135, 136, 161].

Shear-bond strength testing: Shear-bond strength quantifies the bond resistance of TSLs against shear stress, particularly when TSL penetrates fractured rock. Two methods are used to measure shear-bond strength: the double-sided shear strength (DSS) test proposed by Saydam *et al.* [147] and the ring shear-bond strength test proposed by Yilmaz [9]. In DSS tests, three substrate blocks are bonded using TSL, and a load is applied to the middle block until failure occurs [162, 163], as shown in Fig. 33a. Yilmaz [9] devised a shear-bond strength test consisting of a steel ring, a steel base, and a rock core, specifically designed to determine the shear-bond strength of TSL (Fig. 33b). The sample was positioned on a base that provided support to the steel ring rather than the rock core. A compressive load was then applied to the rock core, causing it to displace towards the void in the supporting base. In some tests, failure occurred within the rock mass rather than at the TSL-rock interface, suggesting that the shear-bond strength of TSL can exceed the shear strength of certain rock types.

Qiao [140] performed DSS tests and ring shear-bond tests on TSL material using sandstone and coal. The tested samples did not fail along the TSL-rock interface; instead, many cracks appeared on the sandstone. When soft rock is used in DSS tests, the experimental results may not accurately reflect the shear bond strength of TSL. Since failure occurs within the rock mass, these results may suggest that the shear-bond strength of TSL is higher than the shear strength of the tested rock. Additionally, ring shear-bond tests on sandstone and coal were inaccurate due to the shrinkage of TSL during the curing process. The measured shear-bond strength increased as the TSL ring applied normal stress to the interface. Consequently, the ring shear-bond testing method was modified to obtain accurate shear-bond strength by placing four pieces of rubber around the sample in the ring test to separate the TSL and mitigate the influence of shrinkage (Fig. 33c).

The overall bond strength of TSL depends on several factors: the material compositions, thickness, curing time, surface roughness, and strength of the substrate [25]. Li [3] investigated the influence of curing time on the bond strength of TSL by performing pull-off tests on liner

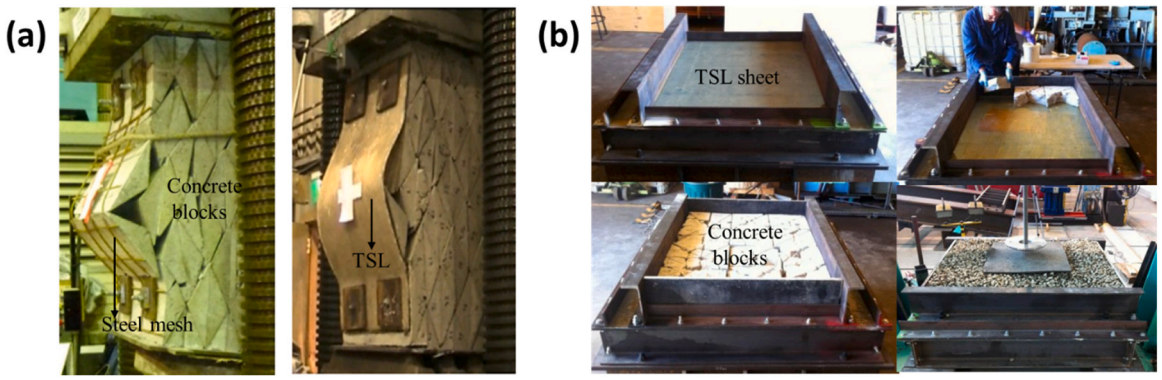

Fig. 34. Large-scale test setup; (a) State of guttering for the two tests after 80 mm deflection. Adapted with permission from [167]. Copyright 2014 Elsevier, (b) Large-scale loading test setup. Adapted with permission from [168].

materials adhered to both complete and fractured coal, reporting a direct correlation between curing time and adhesive strength. A significant increase in adhesive strength was observed as curing time increased. Moreover, when comparing a complete coal area to a fractured coal area, it was evident that the former exhibited notably higher adhesive strength. Chen *et al.* [165] conducted direct pull-off tests to investigate the influence of humidity on the bond strength of TSLs. Their findings indicated that low humidity environments increase dry shrinkage in TSLs, promoting crack formation and reducing bond strength. Li *et al.* [10] explored the influence of surface roughness and substrate strength on the bond strength of the liner. Bond strength initially increased with increasing substrate strength and higher bond strength was achieved when using a substrate with a rough surface. Ozturk and Tannant [135] revealed an inversely proportional relationship between bond strength and the square root of liner thickness. In addition, it was reported that the surface of excavation sites needs to be properly cleaned as contaminated substrate surfaces can lead to low bond strengths [136].

4.4. Large-scale testing

Conducting large-scale tests on TSL contributes to understanding its load-bearing capacity and ensuring quality and performance in practical engineering applications. However, there are only a few reports on large-scale tests of TSL due to the challenges associated with conducting these tests in the laboratory.

Tannant *et al.* [153] designed large-scale plate pull tests to replicate the load generated when a small block of rock experiences relative movement with the surrounding rock. In these tests, a circular steel plate was positioned on a concrete slab or a rock surface, and TSL was uniformly sprayed over the plate and surrounding substrate instead of being applied between the plate and the substrate, as the objective was not to assess TSL bond strength. Espley *et al.* [166] also conducted large-scale plate pull tests to measure the load-carrying capacity of TSL. Boeg-Jensen and Swan conducted large-scale pull tests on underground and blasted wall surfaces to evaluate the toughness and blast resilience of 3 M polymeric composite membrane (PCM) [145].

Shan *et al.* [167] conducted large-scale laboratory tests comparing TSL with welded steel mesh as confinement elements in coal mines. They utilized triangular concrete prisms and concrete blocks embedded with plastic sheets to simulate rock material and weak bedding planes. Each concrete block measured 400 mm × 400 mm × 800 mm (Fig. 34a) and was anchored by four bolts. One side of the block was reinforced with either mesh or TSL, with the latter applied at a thickness of 5 mm and reinforced with glass fibers. The results demonstrated that the TSL-reinforced block with a bedding plane exhibited a higher peak load compared to the control specimen. Building upon their previous research, Shan *et al.* [168] conducted tests on larger specimens

Fig. 35. Large-scale test configuration.
Adapted with permission from [23].

measuring 1.4 m × 1.4 m. They artificially fractured a concrete slab and bonded it to prepared TSL (Fig. 34b). The TSL materials tested included three different types of fiber-reinforced polymer composites and fiber-reinforced polymer-concrete composites. Results indicated that TSL specimens demonstrated greater stiffness compared to the tested steel mesh and provided higher support loads at smaller displacements.

Du Plessis and Malan [23] conducted large-scale surface tests using a 1.5 m × 1.8 m test rig loaded with an external mass across a 1.5 m × 1.5 m support spacing. An artificial rock surface was created using reinforced cement blocks. Fifteen blocks were placed on a 2 m high steel framework and coated with TSL. TSLs, with an average thickness of 8 mm, were applied below the cement blocks (Fig. 35). Four different types of two-component polymer-modified TSL materials were tested. Among these, only one type of TSL was self-supporting for both the cement blocks and the TSL layer after the rig was removed. Conversely, the other types of TSLs caused shear failure at the block joint interface when the clamping force was reduced.

4.5. Other testing methods

In addition to the testing methods discussed above, various other testing methods have been employed by researchers to assess TSL properties. Richardson *et al.* [163] conducted bending tests on sandstone blocks, where a strip of TSL was applied to the bottom side to measure the indirect tensile strength of the rock. This approach facilitated the measurement of both the load and displacement that TSL can withstand while providing secondary support to the fractured rock. Qiao *et al.* [169] and Ozturk and Guner [170] conducted coated compression tests on different types of rock. The rock samples were positioned on a bench, and a plastic mold was centrally placed around each sample, leaving a 5 mm annular gap to accommodate the TSL material. A syringe/silicone cartridge gun was then used to inject the mixed TSL into the space between the rock sample and the mold. Results showed that cylindrical rock samples reinforced with 5 mm thick TSL were significantly stronger than unreinforced samples.

Guner and Ozturk [144, 171] researched the creep behavior of TSL, revealing an inverse relationship between the elongation capability and rupture time parameters with curing time. The creep testing setup was designed to perform eight tests simultaneously according to the ASTM D2990 testing standard. A large test frame was securely fixed to the ground to avoid disturbance from falling weights. The top grip, connected to the table by screws and nuts, and the bottom grip, loaded with dead weights, were designed to minimize eccentric loading and prevent specimen sliding. Linear Variable Displacement Transducers (LVDT) and dial gauges on the bottom grips were used to measure elongation resulting from the total applied forces.

Chen *et al.* [21] conducted a series of tests, including the viscosity test, setting time test, permeability test, bond test, three-point bending test, and compressive test, to evaluate the properties of polymer-modified TSL in mine tunnels. The results demonstrated that the addition of an appropriate amount of polyacrylate emulsion enhanced the reinforcement effects of fibers. Roache *et al.* [18] conducted the core-to-core bond test and linear block support test to determine the suitable TSL product for specific applications in face support at the Kanmantoo Copper Mine in South Australia. The TSL linear block support test was introduced in EFNARC [150] to simulate the loading situations at the development face. Two aluminum plates were placed between three concrete blocks, with two large concrete blocks (8 cm × 4 cm × 3 cm) on the sides and a small concrete block (4 cm × 4 cm × 3 cm) in the middle. The mixed TSL was evenly applied to the bottom surface of the concrete blocks. After curing, the entire test block was positioned on the loading device, and the load was applied to the middle concrete block until failure occurred. The investigation illustrated that the preferred TSL product at a 4 mm thickness not only offers adequate face support but also presents a cost-effective alternative per meter, thereby offering the potential to replace mesh and bolts on development faces at the Kanmantoo Copper Mine.

The testing and evaluation of TSL products for underground mines still present several challenges, as field support behavior often does not align with laboratory test results [23, 172]. Due to limitations in performing large-scale tests, only a few studies have been conducted to assess the *in-situ* behavior of TSLs once applied to the excavation sites. The effectiveness of TSL in supporting rock masses depends on the number of mobilized blocks and the extent of rock mass displacement. To improve their performance, laboratory simulations should more accurately replicate mine conditions and consider the tensile and bond strength of TSL to enhance its energy absorption capabilities. The preparation and application of TSL can significantly impact its performance. Therefore, the mixing process and thickness of TSL need to be carefully planned and executed. It is also essential to explore the impact of varying rock conditions on TSL performance by testing different types of rocks. Numerical modeling, particularly using distinct element methods (DEM) could provide valuable insights by simulating the liner's effects and block assembly behavior. Further research is required to better understand TSL behavior by incorporating both small-scale and large-scale tests. This research will be crucial to optimize TSLs for reinforcing fractured rock surfaces and providing reliable support in underground mining environments.

5. Spraying equipment and methods

Due to space constraints, most laboratory experiments are small-scale because it is impractical to employ professional nozzleman or specialized spraying equipment to apply TSL materials to the substrate. As a result, TSL is typically applied by directly mixing and pouring into the molds or substrates in most laboratory experiments [10, 22, 144, 164, 170, 173]. Guner and Ozturk [144] used a food mixer to blend the two-component cement-based Tekflex LP TSL and injected into molds using a silicone cartridge gun. They discovered that the mixing time and speed influences the mechanical properties of TSL. When mixed at high speeds, air bubbles were generated and trapped within the TSL batch mixture, which could potentially weaken the material. Ozturk and Guner [19] also conducted laboratory tests on two different TSL products: a flexible liner (MasterRoc TSL 865) and a rigid liner (Tunnel Guard). When preparing cylindrical specimens, they recommended pouring TSL into a mold for flexible liners and using the coring technique for rigid liners. To simulate the actual field application conditions, high-pressure pumps and spray guns have been designed and employed for spraying TSL [21, 25]. Cementitious TSL is added to the spray gun, and then sprayed onto the rock substrate at a distance of 1 m using an air pressure of 0.6 MPa. Dong *et al.* [174] employed a similar spraying device, applying TSL at a distance of 0.4 m with an air pressure of 0.4 MPa. Zhao *et al.* [175] used a sprayer to prepare dog-bone-shaped specimens of two-component TSL for tensile strength testing. However, there is limited research on how different spraying equipment and methods influence the performance of TSL when applied to the rock surfaces in the laboratory.

In field applications, using high-pressure air to spray the TSL material onto the rock surface results in the formation of different internal structures compared to the casting. Tibbs *et al.* [176] indicated that autonomous TSL technology ensures consistent lining thickness, enhancing safety and productivity in coal and metalliferous mining. Spraying TSL material allows it to penetrate cracks within the rock surface, increasing the contact area. High-pressure sprayers can apply TSL rapidly and uniformly, significantly reducing time and operation costs. Thus, employing suitable spraying equipment to spray the TSL material shortly after mixing is crucial to prevent it from setting in the mixing containers. Roache *et al.* [18] reported that the liquid/liquid Silcrete product was tested at Kanmantoo Copper Mine in South Australia. The nozzleman prepared the spraying equipment on a light vehicle, ensuring the proper storage and temperature control of TSL components. Subsequently, the nozzleman sprayed the development heading using a one-person, on-foot process, with resin mixing occurring at the spray gun's static mixer. This enabled the efficient spraying within 30 min. In northern Shanxi of China, specific spraying equipment, namely a TJX3.2 portable spraying machine, was used to spray inorganic TSL (TSBP/3.0 type) in a buried coal seam [177]. Min *et al.* [24] reported that Nanjing Coal Science & Technology Research Co., Ltd designed a new single-component TSL for application in coal mines. To enhance work efficiency, a spraying system comprising a rear vehicle and a front vehicle was designed and developed. The rear vehicle was responsible for mixing the slurry and outputting it to the front vehicle, which sprayed the TSL onto the walls. The non-reactive TSL from the same manufacturer was installed using a wet-spray machine in the Fankou Lead-Zinc Mine [165]. The installation of TSL typically involves three workers: one spray worker, one operator, and one assistant. In comparison, the dry shotcrete application requires 7–8 workers to spray the same area in a mine, taking more time to complete the installation [165]. Mukhopadhyay [178] emphasized that the spraying hose should have a diameter of 32 mm and the nozzle should have an 18-hole water

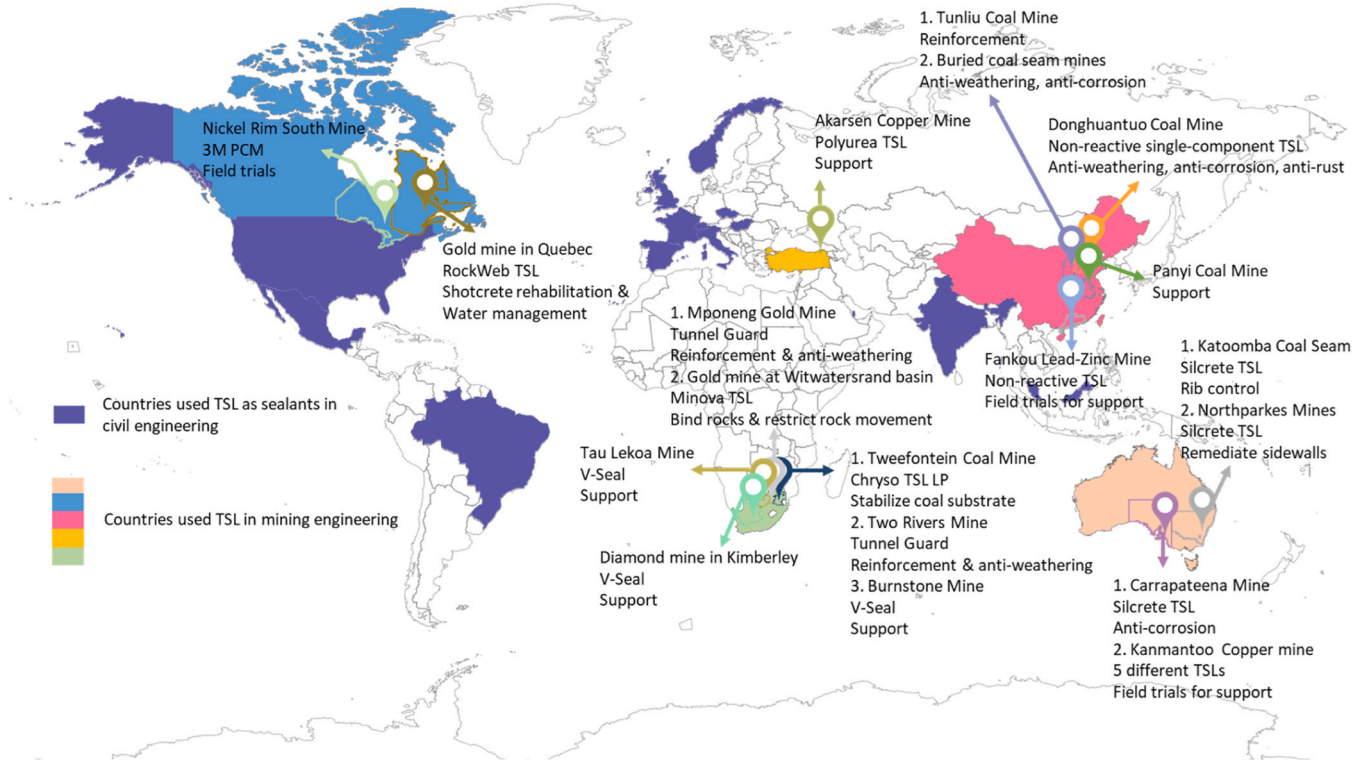

Fig. 36. Some field trials and applications of TSL in recent years.

ring to ensure controlled and uniform mixing between water and the powder when spraying a polymer-based cementitious Masterseal 845 A. Zhang *et al.* [165] indicated that compared to shotcrete, TSL offers several advantages during installation, including requiring less labors, resulting in a safer and more cost-effective operation. Additionally, TSL application creates a brighter working environment, potentially reducing energy consumption for underground lighting. Furthermore, the process generates minimal rebound material and achieves faster installation times.

In addition to the laboratory and on-site spraying methods mentioned above, technical data sheets for some TSL products also briefly mention the requirements for the spraying process or equipment. BluSeal TF05 is a two-component powder/liquid TSL consisting of cementitious powder and poly (ethylene-vinyl acetate) (EVA) liquid kit. Special mixing and pumping equipment are required for BluSeal TF05, which is applied as wet spraying. MasterRoc TSL 865 is a single-component polymer powder suitable for dry spraying. The spraying system recommended by the manufacture consists of a rotor with an 18-pocket feed bowl, a rotor dust collector, a double bubble nozzle with an 18-hole water ring, a spraying hose with a diameter of 32 mm, and a water separator on the air supply. Silcrete is a two-component urea-silicate liquid/liquid TSL and can be applied through a plural component spray unit with compressed air assisted spray direct to the rock surface, either by handgun or robotic arm application.

6. Field trials and applications

Liner technology has been widely adopted in projects such as tunnel support and construction sealing. Before being employed as a surface support system in the mining industry, TSLs had been used for many years as sealants in civil engineering and construction [134]. TSL materials were initially designed for rock cementing and to prevent further weathering of rocks. In the current mining market, various commercial TSL products are available, selected based on the applications. Extensive research has been conducted to develop TSL materials for desired objectives. This section summarizes a few reports on TSL field trials and applications. Fig. 36 demonstrates a global overview of TSL applications over the past few years [4, 8, 18, 24, 165, 179–185].

Liner technology plays a key role in controlling fluid movement and stabilizing soils. These specialized materials, typically composed of geosynthetics or sprayed-on membranes, offer a range of benefits, including waterproofing, containment, and erosion control. According to Khan and Singh [179], geosynthetics encompass a broad category of polymer materials widely utilized in construction and civil engineering, where they come into contact with soil, rock, land, or other geo-materials. By providing an impermeable barrier, geosynthetic liners prevent water infiltration, protecting structures from moisture damage. Geomembranes serve as containment liners in applications like landfills, preventing the release of harmful contaminants into the environment. In bridge construction and maintenance, geosynthetic liners prevent lubrication failure by averting the detrimental consequences of excessive hydrostatic pressures.

TSLs find extensive applications in tunnel engineering and underground structures such as hydropower construction, waterways, and passageways. In tunnel construction and underground facilities, the stability of the foundational structure is required to be ensured by employing conservative design approaches. Liners are commonly incorporated as part of surface control measures during underground excavation. At optimum thickness, the liner can mitigate the negative influence of surface irregularities, especially in poor rock conditions. The applied thickness needs to be carefully selected as it influences the stiffness and flexibility of the liner [183]. Liners also serve as continuous waterproof layers to prevent section disintegration, water seepage, and shear failure that can arise from poor geological conditions or highly weathered strata [185]. Additionally, the liners serve as fire insulation material in tunnels, reducing the temperature transmission to existing concrete slabs [186]. Liners effectively secure weathered tunnel surfaces, contributing to the stability of underground excavation. Previous studies have demonstrated the feasibility of employing TSLs through spray applications onto blasted tunnel surfaces. TSL application

Fig. 37. TSL provides a protective barrier for the mesh and bolts in the Carrapateena mine.
Taken from [188].

Fig. 38. Underground application of TSL material in Northparkes Mines.
Taken from [188].

moderates the impact of blasting on surrounding rock formations, thereby enhancing stability and minimizing displacements of fractured rock within tunnel structures [163, 181, 182].

Shotcrete, mesh, and rock bolts have been widely used in underground mines for stabilizing and repairing mine roadways as surface support systems. However, the time and associated cost taken to mesh and bolt the surface as well as the long curing time required for shotcrete was problematic in fast-advancing mines. Mesh and rock bolts are prone to corrosion and require significant labor for installation [18]. In the challenging mining environment, ground support elements such as rock bolts are susceptible to severe corrosion due to factors like high stress, high temperature, high humidity, and continuous ventilation. Shotcrete and sprayed mortar are commonly utilized as sealants after installing the bolts to maintain the reinforcement strength. However, shotcrete may pose safety hazards due to its susceptibility to detachment caused by bond failure. Additionally, the ventilation system can introduce dust generated during spraying into the tunnel. The ingress of dust-laden airflow into the excavation zone poses a serious threat to miner safety [21, 22]. Faced with increasing mining operations and environmental challenges, there was an urgent need for a rapid, efficient, and high-strength spraying material to provide secondary reinforcement and safeguard the tunnel from weathering, corrosion, and self-ignition. Some reports [18, 24, 165, 187] have pointed out that in engineering projects, TSLs are more efficient, economical, and environmentally friendly compared to shotcrete during spraying because they require less labors, are faster with minimal rebound and produce less dust during spraying. Due to their higher tensile-bond strength, tensile strength, and deformation capacity, TSLs can provide surface support performance that meets or even exceeds that of traditional support elements in some cases.

Many field trials have been conducted mostly in Australia, Canada, China, and South Africa. In Australia, Silcrete was the first TSL material to be applied and tested for rib control in an underground coal mine, although it has been used and tested for several civil and mining applications [132]. The viability of replacing mesh and bolts with TSL on development faces was investigated at hard rock mines in Kanmantoo, South Australia [18]. The findings indicated that the preferred TSL product, with a thickness of 4 mm, offers adequate face support while also reducing the cost per meter of development. The Northparkes Mines also used TSL material to remediate the convergence of sidewalls and to form a barrier on the lower walls to reduce cable damage from steel fibers in shotcrete [188]. In Carrapateena Mine, a two-component urea-silicate spray liner was used to provide a surface barrier for mesh and bolts to protect them from corrosive water. This TSL product was also applied to the walls and backs of the mine in several declined areas [188]. Another commercial TSL product was tested at the Nickel Rim South Mine in Canada, demonstrating promising potential to substantially enhance the effectiveness of ground support systems at depth while also improving the illumination within the mine [139]. A gold mine in northern Quebec, Canada utilized polyurea-based TSLs to line a new cone sump at a depth of 2.8 km, primarily due to transportation challenges and cost considerations, rather than choosing shotcrete [131]. In China, a TSL material was tested in the Donghuantuo Coal Mine of the Kailuan Group and demonstrated better properties than shotcrete [24]. Zhang *et al.* [165] compared a non-reactive TSL and shotcrete on a roadway subjected to blasting in the Fankou Lead-Zinc Mine. In an underground copper mine in Türkiye, 5 mm thick polyurea-based TSL was applied to prevent large displacements and facilitate the strata in supporting themselves [189]. Several mines in South Africa, including the Burnstone mine, the Tau Lekoa mine, and a diamond in Kimberley have applied a polymer-based cement spray liner to provide support in localized areas [133]. A liquid polymer TSL was applied over 1400 m^2 of highwall to effectively stabilize against geological disturbances at the Tweefontein coal mine central pit near Ogies in Mpumalanga, South Africa [129].

Initially, TSL was employed in the construction of mine roadways as a sealing material, offering a superior gas and water barrier to prevent the corrosion of mesh networks (Fig. 37). Gas leakages from rocks are common in underground coal mine environments. Methane and other

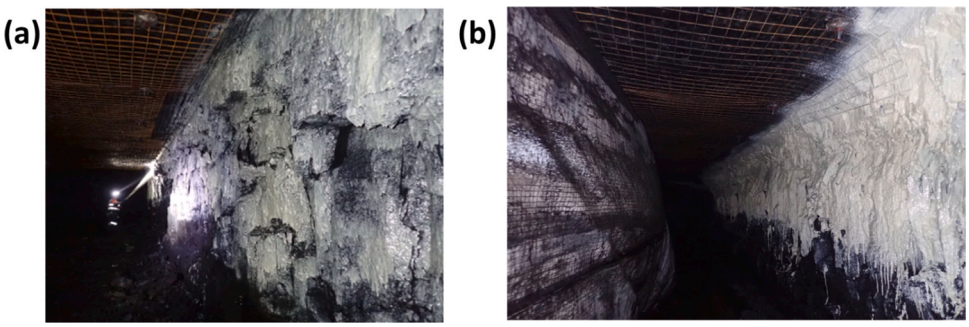

Fig. 39. (a) Spraying of the first coat, (b) final appearance of the ribs after application of TSL. Taken from [132].

toxic gases are generated from active and abandoned underground and surface coal mine environments due to mining activities. In most cases, gases from the coal seams escape into the mining area, leading to gas disasters and outbursts, such as spontaneous combustion, gas explosions, and coal gas combustion. Gas explosions and coal spontaneous combustion are primary threats in coal mines [3, 24, 154]. TSL materials based on polymers or cement are preferred in underground coal mines for their significantly low permeability properties. When applied to coal surfaces, TSL can effectively control gas movement by reducing gas leakage and water penetration. Spraying the TSL liner enhances the integrity of the strata, roof, and supports. This helps hinder spontaneous combustion caused by insufficient oxygen in the coal seams. Moreover, the application of TSL as a sealant in gaseous mines improves the gas extraction yield and purity [3].

TSL typically exhibits higher bond strength with the rock surface compared to shotcrete, contributing to enhanced structural support and reducing the risk of roof collapses and rib spalling [190]. The stability of underground excavations depends on the geological conditions of the rock mass. Instability arises when the rock mass cannot adequately support its weight. Spray-on lining technology provides proactive support through adhesion, rendering it an effective support system for controlling instability. In both hard and soft rock mining applications, fluctuations in humidity and temperature can adversely affect weak strata, potentially leading to rockfalls and rib degradation. The sufficient tensile strength of TSL enables it to transfer loads, generated by gravity or loose rocks, onto a stable or continuous substrate surface. thereby preventing potential injuries from falling loose strata. Hepworth and Lobato [191] documented an example of TSL applications in a highly weathered rock mass. TSL can prevent further weathering and rehabilitate highly stressed strata to stabilize the loosened rocks [192]. A TSL product was applied to the rough and uneven rock surface on the roof and sidewalls to prevent wedge-type failures caused by the intersection of fractures and joint sets during excavation [193]. Fig. 38 shows that TSL was applied to sidewalls to remediate the convergence. This capability allows for repairing damaged mine tunnels and supporting efficient transportation operations. Three mechanisms can be summarized through which TSL enhances rib stability [132]: (*i*) TSL prevents or minimizes weathering of the rock mass, (*ii*) TSL enhances the resistance to buckling by improving tensile strength to the immediate skin of the rib, (*iii*) TSL penetrates dilated discontinuities and glues blocks together to create larger stable blocks.

Field trials of a polyurea silicate TSL product for rib control were conducted in an underground coal mine at Katoomba Seam in Australia, as shown in Fig. 39 [132]. One of the panel trials aimed to assess the performance of the TSL in a secondary extraction/abutment loading environment, where a section of rib had remained unsupported for over 2 years before sealing. The results indicated that the TSL provided satisfactory rib support during the lifting process in the panel and remained effective despite the magnitudes of deformation experienced. Another trial area involved two sections of cut-through driven within the previous 24 h, experiencing limited deformation. A re-spray was conducted on the margin area near the first spraying section because this region had developed tiny cracks due to rib buckling during drivage. The operators working in the trial area reported a safe working environment and expressed confidence in the rib support. Sufficient information and experience from field trials have concluded that the TSL material is capable of replacing the existing rib support system under normal conditions (Trigger Action Response Plan Level 1) at the mine. Further research is required to achieve significant surface support by applying TSL in abnormal conditions.

Another advantage of TSL is its excellent energy absorption capacity due to its high deformability. Rock bursts, triggered by stress redistribution in rocks, can cause large deformations in excavations and pose serious risks to the safety of underground mining operations [194]. TSL has exhibited promising capabilities in ensuring the stability of underground excavations, particularly in mitigating impact damage and other rock-related risks resulting from blasting operations [182]. Boeg-Jensen and Swan [145] reported that a polyurethane TSL product can support rock under highly deformable conditions and in areas influenced by rock burst. A case study performed by Komurlu [181] suggested that the elastomer TSL has the advantages such as good ductility, high elastic deformation limits, and a short curing time, making it suitable for withstanding rock bursts. Zhang *et al.* [165] provided a detailed comparison of the performance of TSL and shotcrete in a roadway subjected to blasting. Through comparative field experiments, they demonstrated that TSL not only outperforms shotcrete in terms of installation efficiency and environmental impact, but also exhibits superior resistance to blast-induced damage due to its higher tensile bond strength, tensile strength, and deformation capacity.

While TSLs have achieved comparable mechanical properties and support performance to shotcrete in certain laboratory and field tests, additional factors must be considered for a comprehensive evaluation. Both laboratory and field tests for TSL rarely take into consideration the variable and complicated geological conditions on-site, with most field tests conducted in areas with stable geological conditions. For example, Zhang *et al.* [165] tested TSLs in the roadway with rock mass rating (RMR) values reaching 68. Hill [132] evaluated the TSL product in the Katoomba seam, where the compressive strength of coal samples averaged 44 MPa. Researchers recommended increasing the thickness of TSL in mines with low RMR values [189], while caution should be exercised when applying TSL in rock masses with cracks, structural damage, or excessive loose conditions [165]. Moreover, the temperature and humidity in the field may significantly affect the performance of TSL. Chen *et al.* [149] examined the effect of humidity on two reactive TSLs in the laboratory. They found that increased humidity decreases the mechanical and sealing properties of TSLs; however, it leads to an increase in bond strength due to the weakened dry shrinkage effect of TSLs. Therefore, before applying TSL in underground projects, it is essential to have a comprehensive understanding of the sensitivity of environmental factors, such as moisture, temperature, and acidity, to the TSL product.

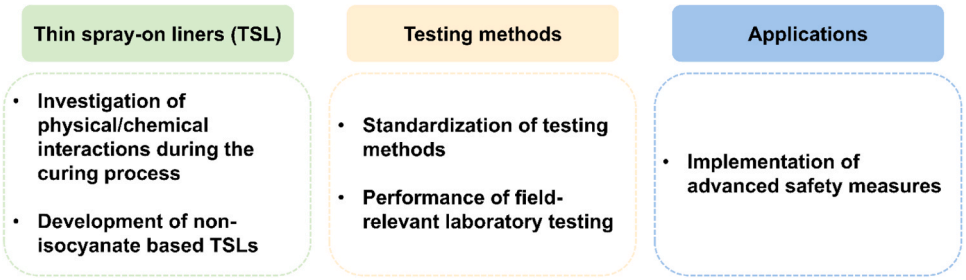

Fig. 40. Future research directions.

7. Future research directions

TSL technology demonstrates the potential to support unstable rock masses, as evidenced by numerous tests and practical applications. Compared to shotcrete, TSL provides a more efficient and cost-effective alternative while also offering a better working environment. The use of less labor-intensive and automated spraying equipment provides an efficient and secure solution for TSL applications. Economic benefits arise from reduced support installation time and simplified material processing, despite the potentially higher costs of TSL products compared to bolts and mesh. However, the mining industry faces practical challenges in fully realizing the potential of TSL due to a lack of understanding of materials, uncertainties regarding its capabilities, and the health and safety risks associated with the technology [4, 172].

To enhance the efficiency of TSL application, it is crucial to understand the materials and physical/chemical interactions during the curing process to achieve desired properties. For cementitious TSLs, several factors, *i.e.,* the influence of T_g of polymers, surfactants, particle sizes, *etc.*, influencing polymer film formation upon cement hydration need to be elucidated. For isocyanate-based TSLs, future studies should focus on the development of non-isocyanate based TSLs to ensure occupational health and safety. Currently, there is no comprehensive standard for evaluating the properties and performance of TSLs, both in the laboratory and *in-situ*. This lack of standardized testing methods makes it challenging to assess TSL properties and behavior for practical applications. Also, multiple factors, such as mixing ratios, spraying methods, and environmental conditions, can influence the properties of TSL, making it difficult to obtain consistent material performance in the field [145, 146, 149]. To resolve this, testing conditions in laboratories should mimic the real mining environments, including temperature, relative humidity, and other factors with a comprehensive understanding of the sensitivity of TSLs to environmental factors which is crucial for optimizing their performance and ensuring their effectiveness in the field. Lastly, future studies should focus on implementing advanced safety measures in the application of TSL. These include the design of improved ventilation systems and the provision of enhanced protective equipment to ensure the health and safety of workers. Fig. 40 summarizes the suggested future research directions.

8. Conclusions

The evolution of TSLs over the past decades highlights their growing importance for enhanced performance and improved safety in mining operations. These developments have resulted in a diverse range of TSL products with distinct physical properties and chemical compositions designed to address specific challenges in surface rock excavations and stability support. Since the concept's introduction in the late 1980s, TSL has shown a potential to provide retaining and holding functions, as well as a level of reinforcement to the unstable rock masses. Their effectiveness is characterized by substantial adhesive bonding with the rock and the liner, along with their intrinsic high tensile strength. TSL has gained wide recognition for its substantial benefits in enhancing productivity, profitability, and safety within the mining industry. It offers advantages such as rapid application and curing times, reduced material handling, high tensile strength with extensive area coverage, strong bond strength, and the ability to penetrate fractures and joints, ultimately contributing to safer underground mining environments. Experiments conducted so far indicate that TSL can withstand minor rock displacements and prevent rock displacements by penetrating cracks. However, the lack of standardized testing methods and comprehension of the materials significantly limits TSL applications. This review examines TSL materials, testing methods, and field applications to explore the potential of TSL technology while also providing future research directions to improve safety and efficiency of TSL applications.

CRediT authorship contribution statement

Oh Joung: Writing – review & editing, Supervision, Methodology, Conceptualization. **Jiang Pengfei:** Writing – review & editing, Funding acquisition. **Zhang Chengguo:** Writing – review & editing, Methodology, Conceptualization. **Li Kunze:** Writing – original draft, Methodology, Formal analysis, Conceptualization. **Akdag Selahattin:** Writing – review & editing. **Kim Hyun Jin:** Writing – original draft, Methodology, Formal analysis, Conceptualization. **Saydam Serkan:** Writing – review & editing, Supervision, Methodology, Funding acquisition, Conceptualization. **Spicer Patrick T.:** Writing – review & editing, Supervision, Methodology, Conceptualization. **Zetterlund Per B.:** Writing – review & editing, Supervision, Methodology, Conceptualization.

Declaration of Competing Interest

The authors declare that they have no known competing financial interests or personal relationships that could have appeared to influence the work reported in this paper.

Data availability

Data will be made available on request.

References

[1] J.A. Hudson, J.P. Harrison, Engineering rock mechanics: an introduction to the principles, Elsevier, 2000.
[2] C.R. Windsor, Rock reinforcement systems, Int. J. Rock. Mech. Min. Sci. 34 (6) (1997) 919–951.
[3] Z. Li, Use of thin spray-on liners for gas management in underground coal mines, UNSW Sydney (2016).
[4] P. Kolapo, M. Onifade, K.O. Said, M. Amwaama, A.E. Aladejare, A.I. Lawal, P. O. Akinseye, On the application of the novel thin spray-on liner (TSL): a progress report in mining operations, Geotech. Geol. Eng. (2021) 1–33.
[5] V. Lau, S. Saydam, Y. Cai, R. Mitra, Laboratory investigation of support mechanism for thin spray-on liners, Proceedings of the 12th International Conference of International Association for Computer Methods and Advances in Geomechanics (IACMAG), Goa, India (2008) 1381–1388.
[6] C.C. Clark, M.A. Stepan, L.A. Martin, Mining publication: early strength performance of modern weak rock mass shotcrete mixes, Min. Eng. 63 (1) (2011) 54–59.
[7] Y. Potvin, D. Stacey, J. Hadjigeorgiou, Surface support in mining (2004).

[8] A. Spearing, G. Borejszo, A. Campoli, The application of a structural thin support liner (TSL) on mines. ARMA US Rock Mechanics/Geomechanics Symposium, ARMA, 2009. ARMA-09-032.
[9] H. Yilmaz, Shear-bond strength testing of thin spray-on liners, J. South. Afr. Inst. Min. Metall. 107 (8) (2007) 519–530.
[10] Z. Li, B. Nocelli, S. Saydam, Effect of rock strength and surface roughness on adhesion strength of thin spray-on liners, Int. J. Rock. Mech. Min. Sci. 91 (2017) 195–202.
[11] S. Saydam, Y. Docrat, Evaluating the adhesion strength of different sealants on Kimberlite. ISRM Congress, ISRM, 2007. ISRM-11CONGRESS-2007-131.
[12] E.Y.E.Y. Baafi, ACARP Project C17004: Polymer based alternative to steel mesh for coal mine strata reinforcement, Australian Coal Association Research Program, 2011.
[13] S. Jjuuko, D. Kalumba, Application of thin spray-on liners for rock surface support in South African mines–a review, Int. J. Innov. Res. Adv. Eng. 3 (7) (2016) 42–56.
[14] H. Yilmaz, Tensile strength testing of thin spray-on liner products (TSLs) and shotcrete, J. South. Afr. Inst. Min. Metall. 110 (10) (2010) 559–569.
[15] H. Yilmaz, Development of testing methods for comparative assessment of thin spray-on liner (TSL) shear and tensile properties, University of the Witwatersrand, 2011.
[16] D.D. Tannant, Thin spray-on liners for underground rock support, Proceedings of the 17th International Mining Congress and Exhibition of Turkey-IMCET (2001) 57–73.
[17] H. Ozturk, Work of adhesion of thin spray-on liners, Rock. Mech. Rock. Eng. 45 (2012) 1095–1102.
[18] B. Roache, J. Jardine, B. Sainsbury, Thin spray liners for face support at Kanmantoo, Underground Operators Conference 2023, Brisbane, QLD (2023) 176–187.
[19] H. Ozturk, D. Guner, Laboratory and distinct element analysis of the deformability behaviour of thin spray-on liners, Int. J. Rock. Mech. Min. Sci. 123 (2019) 104118.
[20] S. Chang, S. Choi, C. Lee, T. Kang, J. Kim, M. Choi, Performance comparison between thin spray-on liners with different compositions, UMT 2017: Proceedings of the First International Conference on Underground Mining Technology, Australian Centre for Geomechanics (2017) 79–85.
[21] L. Chen, X. Jiang, Z. Liu, X. Cui, G. Liu, Z. Zhou, Q. Dong, Synthesis and properties of a polymer-modified material for thin spray-on liners in mine roadways, Adv. Mater. Sci. Eng. 2020 (2020) 1–19.
[22] G. Zhou, S. Li, Y. Ma, J. Ding, M. Zhang, Synthesis and properties of a reinforcing dust-cementing material for thin spray-on liners in mine roadways, Adv. Mater. Sci. Eng. 2019 (2019).
[23] M. Du Plessis, D.F. Malan, Investigating the use of polymer-modified cementitious thin spray-on liners as stope face support, Int. J. Rock. Mech. Min. Sci. 142 (2021) 104728.
[24] F. Min, K. Chen, X. Li, S. Pang, Research on thin spray-on technology and equipment of coal mine. IOP Conference Series: Materials Science and Engineering, IOP Publishing, 2020 012095.
[25] L. Chen, Z. Zhou, G. Liu, X. Cui, Q. Dong, H. Cao, Effects of substrate materials and liner thickness on the adhesive strength of the novel thin spray-on liner, Adv. Mech. Eng. 12 (2) (2020), 1687814020904574.
[26] P.C. Aïtcin, Portland cement, Science and Technology of Concrete Admixtures, Elsevier, 2016, pp. 27–51.
[27] P.C. Aïtcin, Supplementary cementitious materials and blended cements. Science and technology of concrete admixtures, Elsevier, 2016, pp. 53–73.
[28] D. Marchon, R.J. Flatt, Mechanisms of cement hydration. Science and technology of concrete admixtures, Elsevier, 2016, pp. 129–145.
[29] N. Bhanumathidas, N. Kalidas, Dual role of gypsum: set retarder and strength accelerator, Indian Concr. J. 78 (2004) 1–4.
[30] J.W. Bullard, H.M. Jennings, R.A. Livingston, A. Nonat, G.W. Scherer, J. S. Schweitzer, K.L. Scrivener, J.J. Thomas, Mechanisms of cement hydration, Cem. Concr. Res. 41 (12) (2011) 1208–1223.
[31] S. Mantellato, A.B. Eberhardt, R.J. Flatt, Formulation of commercial products. Science and Technology of Concrete Admixtures, Elsevier, 2016, pp. 343–349.
[32] G. Gelardi, S. Mantellato, D. Marchon, M. Palacios, A.B. Eberhardt, R.J. Flatt, Chemistry of chemical admixtures. Science and technology of concrete admixtures, Elsevier, 2016, pp. 149–218.
[33] D. Marchon, R. Flatt, Impact of chemical admixtures on cement hydration. Science and technology of concrete admixtures, Elsevier, 2016, pp. 279–304.
[34] K.A. Erk, B. Bose, Using polymer science to improve concrete: Superabsorbent polymer hydrogels in highly alkaline environments, Gels and Other Soft Amorphous Solids, ACS Publications, 2018, pp. 333–356.
[35] M.J. Krafcik, N.D. Macke, K.A. Erk, Improved concrete materials with hydrogel-based internal curing agents, Gels 3 (4) (2017) 46.
[36] Y. Ohama, Polymer-based admixtures, Cem. Concr. Compos. 20 (2-3) (1998) 189–212.
[37] W. Kujawa, E. Olewnik-Kruszkowska, J. Nowaczyk, Concrete strengthening by introducing polymer-based additives into the cement matrix—a mini review, Mater 14 (20) (2021) 6071.
[38] J.L. Keddie, Film formation of latex, Mater. Sci. Eng. R. Rep. 21 (3) (1997) 101–170.
[39] A. Czajka, S.P. Armes, Time-resolved small-angle x-ray scattering studies during aqueous emulsion polymerization, J. Am. Chem. Soc. 143 (3) (2021) 1474–1484.
[40] S.C. Thickett, R.G. Gilbert, Emulsion polymerization: state of the art in kinetics and mechanisms, Polymer 48 (24) (2007) 6965–6991.
[41] P.B. Zetterlund, S.C. Thickett, S. Perrier, E. Bourgeat-Lami, M. Lansalot, Controlled/living radical polymerization in dispersed systems: an update, Chem. Rev. 115 (18) (2015) 9745–9800.
[42] P.A. Lovell, F.J. Schork, Fundamentals of emulsion polymerization, Biomacromolecules 21 (11) (2020) 4396–4441.
[43] N. Tarannum, K.M. Pooja, R. Khan, Preparation and applications of hydrophobic multicomponent based redispersible polymer powder: a review, Constr. Build. Mater. 247 (2020) 118579.
[44] V. Balagopal, J.P. Raju, A.A. Kumar, M. Sajeev, P. Veena, Effect of ethylene vinyl acetate on cement mortar–a review, Mater. Today.: Proc. (2023).
[45] A.M. Henderson, Ethylene-vinyl acetate (EVA) copolymers: a general review, IEEE Electr. Insul. Mag. 9 (1) (1993) 30–38.
[46] Z. Wenwei, Z. Xiaoguang, Y. Li, Z. Yuefang, S. Jiazhen, Determination of the vinyl acetate content in ethylene-vinyl acetate copolymers by thermogravimetric analysis, Polymer 35 (15) (1994) 3348–3350.
[47] K.R. Williams, Analysis of ethylene-vinyl acetate copolymers: a combined TGA/FTIR experiment, J. Chem. Educ. 71 (8) (1994) A195.
[48] A. Beeldens, D. Van Gemert, H. Schorn, Y. Ohama, L. Czarnecki, From microstructure to macrostructure: an integrated model of structure formation in polymer-modified concrete, Mater. Struct. 38 (2005) 601–607.
[49] R. Wang, J. Li, T. Zhang, L. Czarnecki, Chemical interaction between polymer and cement in polymer-cement concrete, Bull. Pol. Acad. Sci. (4) (2016).
[50] D.A. Silva, H.R. Roman, P.J.P. Gleize, Evidences of chemical interaction between EVA and hydrating Portland cement, Cem. Concr. Res. 32 (9) (2002) 1383–1390.
[51] B.C. Lyu, L.P. Guo, J.D. Wu, X.P. Fei, R.S. Bian, The impacts of calcium acetate on reaction process, mechanical strength and microstructure of ordinary Portland cement paste and alkali-activated cementitious paste, Constr. Build. Mater. 359 (2022) 129492.
[52] J.A. Larbi, J. Bijen, Interaction of polymers with Portland cement during hydration: a study of the chemistry of the pore solution of polymer-modified cement systems, Cem. Concr. Res. 20 (1) (1990) 139–147.
[53] H.F.W. Taylor, P. Barret, P.W. Brown, D.D. Double, G. Frohnsdorff, V. Johansen, D. Ménétrier-Sorrentino, I. Odler, L.J. Parrott, J.M. Pommersheim, The hydration of tricalcium silicate: RILEM committee 68-MMH, Task Group 3, Mater. Struct. 17 (1984) 457–468.
[54] D. Bülichen, J. Kainz, J. Plank, Working mechanism of methyl hydroxyethyl cellulose (MHEC) as water retention agent, Cem. Concr. Res. 42 (7) (2012) 953–959.
[55] C. Shi, X. Zou, P. Wang, Influences of EVA and methylcellulose on mechanical properties of Portland cement-calcium aluminate cement-gypsum ternary repair mortar, Constr. Build. Mater. 241 (2020) 118035.
[56] M.C. Baptista, M. da Luz Garcia, S.C. Pinho, M. Ascensao Lopes, M.F. Almeida, C. Coelho, C. Fonseca, Valorization of EVA waste from footwear industry as natural aggregates substitutes in mortar: the effect of granulometry, J. Mater. Cycles Waste Manag. 23 (2021) 1445–1455.
[57] F.A. Shaker, A.S. El-Dieb, M.M. Reda, Durability of styrene-butadiene latex modified concrete, Cem. Concr. Res. 27 (5) (1997) 711–720.
[58] G. Barluenga, F. Hernández-Olivares, SBR latex modified mortar rheology and mechanical behaviour, Cem. Concr. Res. 34 (3) (2004) 527–535.
[59] R. Wang, P.M. Wang, X.G. Li, Physical and mechanical properties of styrene–butadiene rubber emulsion modified cement mortars, Cem. Concr. Res. 35 (5) (2005) 900–906.
[60] R. Dennis, Latex in the construction industry, Chem. Ind. 15 (1985) 505.
[61] C.L. Page, M.M. Page, Durability of concrete and cement composites, Elsevier, 2007.
[62] J. Xu, B. Hong, G. Lu, T. Li, S. Wang, C. Wang, D. Wang, Carboxylated styrene-butadiene latex (XSB) in asphalt modification towards cleaner production and enhanced performance of pavement in cold regions, J. Clean. Prod. 372 (2022) 133653.
[63] M. Alimardani, F. Abbassi-Sourki, G.R. Bakhshandeh, Preparation and characterization of carboxylated styrene butadiene rubber (XSBR)/multiwall carbon nanotubes (MWCNTs) nanocomposites, Iran. Polym. J. 21 (11) (2012) 809–820.
[64] S. Chandra, P. Flodin, Interactions of polymers and organic admixtures on portland cement hydration, Cem. Concr. Res. 17 (6) (1987) 875–890.
[65] Z. Yang, X. Shi, A.T. Creighton, M.M. Peterson, Effect of styrene–butadiene rubber latex on the chloride permeability and microstructure of Portland cement mortar, Constr. Build. Mater. 23 (6) (2009) 2283–2290.
[66] J. Plank, M. Gretz, Study on the interaction between anionic and cationic latex particles and Portland cement, Colloids Surf. A: Physicochem. Eng. Asp. 330 (2-3) (2008) 227–233.
[67] Z. Lu, X. Kong, C. Zhang, F. Xing, Y. Cai, L. Jiang, Y. Zhang, B. Dong, Effect of surface modification of colloidal particles in polymer latexes on cement hydration, Constr. Build. Mater. 155 (2017) 1147–1157.
[68] Z. Lu, X. Kong, C. Zhang, Y. Cai, Effect of highly carboxylated colloidal polymers on cement hydration and interactions with calcium ions, Cem. Concr. Res. 113 (2018) 140–153.
[69] C. Schröfl, K.A. Erk, W. Siriwatwechakul, M. Wyrzykowski, D. Snoeck, Recent progress in superabsorbent polymers for concrete, Cem. Concr. Res. 151 (2022) 106648.
[70] C.J. Adams, B. Bose, J. Olek, K.A. Erk, Evaluation of mix design strategies to optimize flow and strength of mortar internally cured with superabsorbent polymers, Constr. Build. Mater. 324 (2022) 126664.
[71] R. Liang, Q. Liu, D. Hou, Z. Li, G. Sun, Flexural strength enhancement of cement paste through monomer incorporation and in situ bond formation, Cem. Concr. Res. 152 (2022) 106675.

[72] Q. Zhu, C.W. Barney, K.A. Erk, Effect of ionic crosslinking on the swelling and mechanical response of model superabsorbent polymer hydrogels for internally cured concrete, Mater. Struct. 48 (2015) 2261–2276.
[73] A. Nowbahar, A.O. Connor, V. Mansard, P. Spicer, T.M. Squires, Salt comets in hand sanitizer: A simple probe of microgel collapse dynamics, Phys. Rev. Fluids 4 (6) (2019) 061301.
[74] C.J. Adams, B. Bose, E. Mann, K.A. Erk, A. Behnood, A. Castillo, F.B. Rodriguez, Y. Wang, J. Olek, Superabsorbent Polymers for Internally Cured Concrete (Joint Transportation Research Program Publication No. FHWA/IN/JTRP-2022/04), Purdue University, West Lafayette, IN, 2022.
[75] V. Afroughsabet, T. Ozbakkaloglu, Mechanical and durability properties of high-strength concrete containing steel and polypropylene fibers, Constr. Build. Mater. 94 (2015) 73–82.
[76] Z. Sun, Q. Xu, Microscopic, physical and mechanical analysis of polypropylene fiber reinforced concrete, Mater. Sci. Eng. A. 527 (1-2) (2009) 198–204.
[77] A.A. Ramezanianpour, M. Esmaeili, S.A. Ghahari, M.H. Najafi, Laboratory study on the effect of polypropylene fiber on durability, and physical and mechanical characteristic of concrete for application in sleepers, Constr. Build. Mater. 44 (2013) 411–418.
[78] J.Y. Wang, K.S. Chia, J.Y.R. Liew, M.H. Zhang, Flexural performance of fiber-reinforced ultra lightweight cement composites with low fiber content, Cem. Concr. Compos. 43 (2013) 39–47.
[79] H.R. Pakravan, M. Latifi, M. Jamshidi, Hybrid short fiber reinforcement system in concrete: a review, Constr. Build. Mater. 142 (2017) 280–294.
[80] S. Guler, The effect of polyamide fibers on the strength and toughness properties of structural lightweight aggregate concrete, Constr. Build. Mater. 173 (2018) 394–402.
[81] J.H.J. Kim, C.G. Park, S.W. Lee, S.W. Lee, J.P. Won, Effects of the geometry of recycled PET fiber reinforcement on shrinkage cracking of cement-based composites, Compos. B. Eng. 39 (3) (2008) 442–450.
[82] M. Cao, C. Xie, J. Guan, Fracture behavior of cement mortar reinforced by hybrid composite fiber consisting of CaCO3 whiskers and PVA-steel hybrid fibers, Compos. Part A Appl. Sci. 120 (2019) 172–187.
[83] R.F. Zollo, Fiber-reinforced concrete: an overview after 30 years of development, Cem. Concr. Compos. 19 (2) (1997) 107–122.
[84] A. Mardani-Aghabaglou, M. Ilhan, S. Ozen, The effect of shrinkage reducing admixture and polypropylene fibers on drying shrinkage behaviour of concrete, Cem. Wapno Beton 24 (3) (2019), 227-22+.
[85] A.M. López-Buendía, M.D. Romero-Sánchez, V. Climent, C. Guillem, Surface treated polypropylene (PP) fibres for reinforced concrete, Cem. Concr. Res. 54 (2013) 29–35.
[86] D. Hernández-Cruz, C.W. Hargis, S. Bae, P.A. Itty, C. Meral, J. Dominowski, M. J. Radler, D.A. Kilcoyne, P.J. Monteiro, Multiscale characterization of chemical–mechanical interactions between polymer fibers and cementitious matrix, Cem. Concr. Compos. 48 (2014) 9–18.
[87] C. Signorini, A. Sola, B. Malchiodi, A. Nobili, A. Gatto, Failure mechanism of silica coated polypropylene fibres for Fibre Reinforced Concrete (FRC), Constr. Build. Mater. 236 (2020) 117549.
[88] C. Thiyagu, I. Manjubala, U. Narendrakumar, Thermal and morphological study of graphene based polyurethane composites, Mater. Today.: Proc. 45 (2021) 3982–3985.
[89] R.-M. Pellenq, N. Lequeux, H. Van Damme, Engineering the bonding scheme in C–S–H: the iono-covalent framework, Cem. Concr. Res. 38 (2) (2008) 159–174.
[90] P.K. Mehta, P.J. Monteiro, Concrete: microstructure, properties, and materials, McGraw-Hill Education, 2014.
[91] Z. Li, X. Zhou, H. Ma, D. Hou, Advanced concrete technology, John Wiley & Sons, 2022.
[92] H. Pan, W. She, W. Zuo, Y. Zhou, J. Huang, Z. Zhang, Z. Geng, Y. Yao, W. Zhang, L. Zheng, Hierarchical toughening of a biomimetic bulk cement composite, ACS Appl. Mater. Interfaces 12 (47) (2020) 53297–53309.
[93] Y. Chen, Y. Zheng, Y. Zhou, W. Zhang, W. Li, W. She, J. Liu, C. Miao, Multi-layered cement-hydrogel composite with high toughness, low thermal conductivity, and self-healing capability, Nat. Commun. 14 (1) (2023) 3438.
[94] H. Pretorious, L. Brower, F. Apicella Polymeric structural support membrane, Google Patents, 2002.
[95] N. Dulzer, J. Champa, M. Porsch Polymeric structural support membrane, Google Patents, 2003.
[96] F.M. de Souza, P.K. Kahol, R.K. Gupta, Introduction to polyurethane chemistry, ACS Publications, 2021.
[97] E. Sharmin, F. Zafar, Polyurethane: an introduction, InTech, 2012.
[98] F.E. Golling, R. Pires, A. Hecking, J. Weikard, F. Richter, K. Danielmeier, D. Dijkstra, Polyurethanes for coatings and adhesives–chemistry and applications, Polym. Int. 68 (5) (2019) 848–855.
[99] J.O. Akindoyo, M.D.H. Beg, S. Ghazali, M.R. Islam, N. Jeyaratnam, A.R. Yuvaraj, Polyurethane types, synthesis and applications–a review, RSC Adv. 6 (115) (2016) 114453–114482.
[100] D.J. Primeaux, Polyurea elastomer technology: history, chemistry & basic formulating techniques, Primeaux Associates LLC, 2004, pp. 1–20.
[101] D. Primeaux, J. Dudley, Polyurea vs. polyurethane & polyurethane/polyurea: What's the difference?. Proceedings of the Polyurea Linings Annual Conference Polyurea Development Assocaition (PDA), Tampa, FL, USA, 2004, pp. 2–4.
[102] N. Iqbal, M. Tripathi, S. Parthasarathy, D. Kumar, P.K. Roy, Polyurea coatings for enhanced blast-mitigation: a review, RSC Adv. 6 (111) (2016) 109706–109717.
[103] P.S. Mehta, A.S. Mehta, S.J. Mehta, A.B. Makhijani, Bhopal tragedy's health effects: a review of methyl isocyanate toxicity, Jama 264 (21) (1990) 2781–2787.
[104] E. Coureau, L. Fontana, C. Lamouroux, C. Pélissier, B. Charbotel, Is isocyanate exposure and occupational asthma still a major occupational health concern? Systematic literature review, Int. J. Environ. Res. Public Health 18 (24) (2021) 13181.
[105] D.M. Wild, C.A. Redlich, A.D. Paltiel, Surveillance for isocyanate asthma: a model based cost effectiveness analysis, Occup. Environ. Med. 62 (11) (2005) 743–749.
[106] G. Rokicki, P.G. Parzuchowski, M. Mazurek, Non-isocyanate polyurethanes: synthesis, properties, and applications, Polym. Adv. Technol. 26 (7) (2015) 707–761.
[107] V. Froidevaux, C. Negrell, S. Caillol, J.P. Pascault, B. Boutevin, Biobased amines: from synthesis to polymers; present and future, Chem. Rev. 116 (22) (2016) 14181–14224.
[108] M. Bîlen, T.U.Z. Caner, Analysis and recommendations on the use of polymer and phenol-based materials for coal mines, Sci. Min. J. 62 (1) (2023) 31–36.
[109] D. Krizan, B. Zivanovic, Effects of dosage and modulus of water glass on early hydration of alkali–slag cements, Cem. Concr. Res. 32 (8) (2002) 1181–1188.
[110] A. Satoh, Water glass bonding, Sens. Actuator A Phys. 72 (2) (1999) 160–168.
[111] X.M. Guan, Z.P. Yang, C.J. Zhang, Bonding mechanism between waterglass/polyurethane adhesive and coal, J. Adhes. 88 (9) (2012) 802–811.
[112] Z. He, Q. Li, J. Wang, N. Yin, S. Jiang, M. Kang, Effect of silane treatment on the mechanical properties of polyurethane/water glass grouting materials, Constr. Build. Mater. 116 (2016) 110–120.
[113] Y. Liang, A. Gao, Y. Sun, F. Tian, W. Sun, W. Lu, Z. He, Mechanism confirmation of organofunctional silanes modified sodium silicate/polyurethane composites for remarkably enhanced mechanical properties, Sci. Rep. 11 (1) (2021) 9407.
[114] Q. Zhang, X.M. Hu, M.Y. Wu, Y.Y. Zhao, C. Yu, Effects of different catalysts on the structure and properties of polyurethane/water glass grouting materials, J. Appl. Polym. Sci. 135 (27) (2018) 46460.
[115] K.M. Zierold, C. Odoh, A review on fly ash from coal-fired power plants: chemical composition, regulations, and health evidence, Rev. Environ. Health 35 (4) (2020) 401–418.
[116] M. Ahmaruzzaman, A review on the utilization of fly ash, Prog. Energy Combust. Sci. 36 (3) (2010) 327–363.
[117] Z.T. Yao, X.S. Ji, P.K. Sarker, J.H. Tang, L.Q. Ge, M.S. Xia, Y.Q. Xi, A comprehensive review on the applications of coal fly ash, Earth-Sci. Rev. 141 (2015) 105–121.
[118] C. Qin, W. Lu, Z. He, G. Qi, J. Li, X. Hu, Effect of silane treatment on mechanical properties of polyurethane/mesoscopic fly ash composites, Polymers 11 (4) (2019) 741.
[119] S. Zhang, W. Liu, K. Yang, W. Yu, F. Zhu, Q. Zheng, The influence of fly ash on the foaming behavior and flame retardancy of polyurethane grouting materials, Polymers 14 (6) (2022) 1113.
[120] A.R. Tarakcılar, The effects of intumescent flame retardant including ammonium polyphosphate/pentaerythritol and fly ash fillers on the physicomechanical properties of rigid polyurethane foams, J. Appl. Polym. Sci. 120 (4) (2011) 2095–2102.
[121] N. Usta, Investigation of fire behavior of rigid polyurethane foams containing fly ash and intumescent flame retardant by using a cone calorimeter, J. Appl. Polym. Sci. 124 (4) (2012) 3372–3382.
[122] A.K. Geim, Graphene: status and prospects, Science 324 (5934) (2009) 1530–1534.
[123] K.S. Novoselov, V.I. Falʹko, L. Colombo, P.R. Gellert, M.G. Schwab, K. Kim, A roadmap for graphene, nature 490 (7419) (2012) 192–200.
[124] W. Yu, L. Sisi, Y. Haiyan, L. Jie, Progress in the functional modification of graphene/graphene oxide: a review, RSC Adv. 10 (26) (2020) 15328–15345.
[125] Y. Fadil, S.C. Thickett, V. Agarwal, P.B. Zetterlund, Synthesis of graphene-based polymeric nanocomposites using emulsion techniques, Prog. Polym. Sci. 125 (2022) 101476.
[126] C. Thiyagu, U. NarendraKumar, Effect of graphene on thermal, mechanical, and shape memory properties of polyurethane nanocomposite, Appl. Phys. A 128 (10) (2022) 937.
[127] Z. Chen, H. Lu, Constructing sacrificial bonds and hidden lengths for ductile graphene/polyurethane elastomers with improved strength and toughness, J. Mater. Chem. 22 (25) (2012) 12479–12490.
[128] H. Kim, Y. Miura, C.W. Macosko, Graphene/polyurethane nanocomposites for improved gas barrier and electrical conductivity, Chem. Mater. 22 (11) (2010) 3441–3450.
[129] Chryso Southern Africa, Thin-Skin Liner from CHRYSO Stabilises Tweefontein Highwall. ⟨https://www.claybrick.org/profile/chryso-southern-africa⟩.
[130] L. CCTEG Nanjing Design & Research Institute Co., Thin spray (sealing) materials and equipment. ⟨https://zmnjy.ccteg.cn/contents/4115/48202.html⟩.
[131] RockWeb T.S.L., Case Studies. ⟨http://sprayonplastics.com/RWTailings.html⟩.
[132] D. Hill, Trials of the Thin Sprayed Liner "Silcrete" for Rib Control Purposes (2021).
[133] Carbontech, Projects. ⟨https://www.web.carbontech.co.za/projects⟩.
[134] J.S. Kuijpers, E.J. Sellers, A.Z. Toper, T. Rangasamy, T. Ward, A.J. Van Rensburg, H. Yilmaz, R. Stacey, Required technical specifications and standard testing methodology for thin sprayed linings, SIMRAC Final Report. Research agency: CSIR Division of Mining Technology. Project No: SIM 20206 (2004), 2004-0404.
[135] H. Ozturk, D.D. Tannant, Thin spray-on liner adhesive strength test method and effect of liner thickness on adhesion, Int. J. Rock. Mech. Min. Sci. 47 (5) (2010) 808–815.
[136] H. Ozturk, D.D. Tannant, Influence of rock properties and environmental conditions on thin spray-on liner adhesive bond, Int. J. Rock. Mech. Min. Sci. 48 (7) (2011) 1196–1198.

[137] E. Morton, A. Thompson, E. Villaescusa, Static testing of shotcrete and membranes for mining applications, Proceedings of the 6th International Conference on Ground Support (2008) 195–212.
[138] T.R. Stacey, Review of membrane support mechanisms, loading mechanisms, desired membrance performance, and appropriate test methods, J. South. Afr. Inst. Min. Metall. 101 (7) (2001) 343–351.
[139] D.J. Finn, P. Teasdale, C.R. Windsor, In-situ trials and field testing of two polymer restraint membranes. Rock Support and Reinforcement Practice in Mining, Routledge, 2018, pp. 139–153.
[140] Q. Qiao, Experimental and numerical analysis of thin spray-on liner materials for use in underground mines (2015).
[141] H. Yilmaz, S. Saydam, D. Henderson, Torque testing of thin spray-on liner coated cores, 3rd International Seminar on Surface Support Liners: Thin Spray-On Liners, Shotcrete and Mesh (2003).
[142] J. Dube, Investigations Into the Mechanisms of Rock Support Provided by Sprayed Liners, University of the Witwatersrand, 2009.
[143] D. Guner, H. Ozturk, Experimental and numerical analysis of the effects of curing time on tensile mechanical properties of thin spray-on liners, Rock. Mech. Rock. Eng. 49 (2016) 3205–3222.
[144] D. Guner, H. Ozturk, Creep behaviour investigation of a thin spray-on liner, Int. J. Rock. Mech. Min. Sci. 108 (2018) 58–66.
[145] P.K. Boeg-Jensen, G. Swan, The operational and laboratory aspects of a thin spray-on liner. Deep Mining 2014: Proceedings of the Seventh International Conference on Deep and High Stress Mining, Australian Centre for Geomechanics, 2014, pp. 241–251.
[146] Z. Li, S. Saydam, R. Mitra, D. Chalmers, Investigation on adhesion strength of thin spray-on liners in an underground coal mine, 15th Coal Operator's Conference. The Australasian Institute of Mining and Metallurgy and Min Managers Association of Australia, Univesity of Wollongong, Australia, 2015.
[147] S. Saydam, H. Yilmaz, T.R. Stacey, A new testing approach for thin spray-on liners: double-sided shear strength (DSS) test, International Workshop and Seminar Surface Support Liners: Thin Spray-On Liners, Shotcrete and Mesh (2003) 25–26.
[148] Q. Qiao, J. Nemcik, I. Porter, Shear strength testing of glass fibre reinforced thin spray-on liner, Geotech. Lett. 4 (4) (2014) 250–254.
[149] L. Chen, J. Teng, G. Liu, Y. Zheng, X. Cui, Z. Zhou, Effect of high humidity on the initial mechanical properties and failure modes of thin spray-on liners (TSLs), Tunn. Undergr. Space Technol. 145 (2024) 105617.
[150] Y. Potvin, Towards a common understanding of TSL applications in mines, Proceedings of 2nd International Seminar on Surface Support Liners: Thin Sprayed Liners, Shotcrete, Mesh (2002).
[151] J.F. Archibald, Assessing acceptance criteria for and capabilities of liners for mitigating ground falls, Mining health and safety conference, Sudbury Ontario (2001) 1–31.
[152] EFNARC, Specification and Guidelines on Thin Spray-on Liners for Mining and Tunnelling (2008).
[153] D.D. Tannant, G. Swan, S. Espley, C. Graham, Laboratory test procedures for validating the use of thin sprayed-on liners for mesh replacement, Proc. Canadian Institute of Mining, Metallurgy and Petroleum 101st Annual General Meeting (1999).
[154] Z. Li, J. Tenney, D. Chalmers, R. Mitra, S. Saydam, Application of thin spray-on liners to enhance the pre-drained coal seam gas quality, Energy Explor. Exploit. 34 (5) (2016) 746–765.
[155] J. Hadjigeorgiou, M. Grenon, Towards a rational design methodology for thin sprayed on liners, Proc. 2nd Int. Seminar on Surface Support Liners: Thin Sprayed Liners, Shotcrete, Mesh. Sandton, South Africa, Section (2002) 1–16.
[156] H. Yilmaz, Comparison of mechanical properties of shotcrete and thin spray-on liner (TSL), Proc. Shotcrete for Africa Conf., Johannesburg (2009) 251–266.
[157] Q. Qiao, J. Nemcik, I. Porter, E. Baafi, Laboratory tests on thin spray-on liner penetrated rock joints in direct shear, Rock. Mech. Rock. Eng. 48 (2015) 2173–2177.
[158] B. Seymour, L. Martin, C. Clark, M. Stepan, R. Jacksha, R. Pakalnis, M. Roworth, C. Caceres, A practical method of measuring shotcrete adhesion strength, SME-annual meeting and exhibit (2010).
[159] D.P. Mason, T.R. Stacey, Support to rock excavations provided by sprayed liners, Int. J. Rock. Mech. Min. Sci. 45 (5) (2008) 773–788.
[160] D.P. Mason, H. Abelman, Support provided to rock excavations by a system of two liners, Int. J. Rock. Mech. Min. Sci. 46 (7) (2009) 1197–1205.
[161] H. Ozturk, Fracture mechanics interpretation of thin spray-on liner adhesion tests, Int. J. Adhes. Adhes. 34 (2012) 17–23.
[162] L. Li, P.C. Hagan, S. Saydam, B. Hebblewhite, Shear resistance contribution of support systems in double shear test, Tunn. Undergr. Space Technol. 56 (2016) 168–175.
[163] J. Richardson, R. Mitra, S. Saydam, Investigation of thin spray-on liners using numerical modeling. 43rd US Rock Mechanics Symposium & 4th US-Canada Rock Mechanics Symposium, OnePetro, 2009.
[164] Q. Qiao, J. Nemcik, I. Porter, A new approach for determination of the shear bond strength of thin spray-on liners, Int. J. Rock. Mech. Min. Sci. 73 (2015) 54–61.
[165] Z. Zhang, X. Shi, X. Qiu, J. Ouyang, W. Wang, In situ tests comparing the support effects of thin spray-on liner and shotcrete on a roadway subjected to blasting, Rock. Mech. Rock. Eng. (2023) 1–25.
[166] S. Espley, D.D. Tannant, G. Baiden, P.K. Kaiser, Design criteria for thin spray-on membrane support for underground hardrock mining, Canadian Ins. Of Mining and Metallurgy Annual Meeting, Calgary (1999).
[167] S. Zhenjun, I. Porter, J. Nemcik, E. Baafi, Comparing the reinforcement capacity of welded steel mesh and a thin spray-on liner using large scale laboratory tests, Int. J. Min. Sci. Technol. 24 (3) (2014) 373–377.
[168] Z. Shan, I. Porter, J. Nemcik, E. Baafi, Z. Zhang, Investigation on the rock surface support performance of welded steel mesh and thin spray-on liners using full-scale laboratory testing, Rock. Mech. Rock. Eng. 53 (2020) 171–183.
[169] Q. Qiao, J. Nemcik, I. Porter, E. Baafi, Laboratory investigation of support mechanism of thin spray-on liner for pillar reinforcement, Géotechnique Lett. 4 (4) (2014) 317–321.
[170] H. Ozturk, D. Guner, Failure analysis of thin spray-on liner coated rock cores, Eng. Fail. Anal. 79 (2017) 25–33.
[171] D. Guner, H. Ozturk, Experimental and modelling study on nonlinear time-dependent behaviour of thin spray-on liner, Tunn. Undergr. Space Technol. 84 (2019) 306–316.
[172] M.J. Kanda, T.R. Stacey, Review of the practical effectiveness of thin spray-on liners based on information from suppliers and observations from the mining industry, MGR 2019: Proceedings of the First International Conference on Mining Geomechanical Risk, Australian Centre for Geomechanics (2019) 443–458.
[173] G.K. Dondapati, D. Deb, I. Porter, S. Karekal, Improvement of strength-deformability behaviour of rock-like materials and coal using fibre-reinforced thin spray-on liner (FR-TSL), Rock. Mech. Rock. Eng. 55 (7) (2022) 3997–4013.
[174] Q. Dong, L. Chen, W. Cheng, Z. Liu, X. Cui, G. Liu, Z. Shi, Z. Sun, Y. Zhang, Material performance tests of the polymer-cement thin spray-on liner, Geofluids 2020 (2020) 1–14.
[175] Y. Zhao, X. Fu, Y. Shi, B. Zhao, X. Fu, X. Zhang, Y. Chen, Research on mechanical behavior and energy evolution of coal and rocks with different thin spray-on liners thickness under uniaxial compressive loading, Sustainability 14 (10) (2022) 5909.
[176] M.P. Tibbs, O.K. Tyler, S. Van Duin, E. Baafi, Autonomous thin spray-on liner application in irregular tunnel and mine roadway surfaces. 30th International Symposium on Automation and Robotics in Construction, Mining & Petroleum Industries, Canadian Institute of Mining, Metallurgy and Petroleum, Canada, 2013, pp. 1456–1463.
[177] J. Zhang, Q.S. Zhuo, S. Yang, T. Yang, B. Wang, W.Y. Bai, J.J. Wu, Y.F. He, H. R. Li, Study on antiweathering support technology of thin spray-on liners in shallowly buried coal seam roadway under corrosion condition, Shock. Vib. 2022 (2022).
[178] M. Mukhopadhyay, Innovative materials and methods for ground support, consolidation and water sealing for the mining industry, Water Energy Int. 58 (9) (2015) 67–69.
[179] G.A. Khan, E.S. Singh, Use of geosynthetic materials in road construction, IJSDR 5 (8) (2020) 1–9.
[180] H. Birgisdóttir, Life cycle assessment model for road construction and use of residues from waste incineration, Institute of Environment & Resources, Technical University of Denmark Lyngby, 2005.
[181] E. Komurlu, Support performances of elastomer thin spray-on liners (TSLS) against the rock burst: a case study, Traban, Turkey, 12th regional rock mechanics symposium (2018).
[182] J. Archibald, P. Dirige, Development of thin, spray-on liner and composite superliner area supports for damage mitigation in blast-and rockburst-induced rock failure events, WIT Transactions on The Built Environment 87 (2006).
[183] M. Son, E.J. Cording, Ground–liner interaction in rock tunneling, Tunn. Undergr. Space Technol. 22 (1) (2007) 1–9.
[184] E. Bernard, A. Thomas, Fibre reinforced sprayed concrete for ground support, Tunn. Undergr. Space Technol. 99 (2020) 103302.
[185] H. Yu, Z. Zhang, J. Chen, A. Bobet, M. Zhao, Y. Yuan, Analytical solution for longitudinal seismic response of tunnel liners with sharp stiffness transition, Tunn. Undergr. Space Technol. 77 (2018) 103–114.
[186] T. Ahn, Thermal and mechanical studies of thin spray-on liner (TSL) for concrete tunnel linings, The University of Western Ontario, Canada, 2011.
[187] J. Zhang, Q.-S. Zhuo, S. Yang, T. Yang, B. Wang, W.-Y. Bai, J.-J. Wu, Y.-F. He, H.-R. Li, Study on antiweathering support technology of thin spray-on liners in shallowly buried coal seam roadway under corrosion condition, Shock Vib. 2022 (2022).
[188] DSI Underground Product Development Update, 2013. http://bbugs.org.au/wp-content/uploads/2013/04/DSI.pdf. (Accessed 24/11 2003).
[189] E. Komurlu, A. Kesimal, Usability of thin spray-on liners (TSL) for akarsen underground mine in Murgul, 25th International Congress and Exhibition of Turkey (IMCET 2017) (2017) 89–104.
[190] H. Kang, Support technologies for deep and complex roadways in underground coal mines: a review, Int. J. Coal Sci. Technol. 1 (2014) 261–277.
[191] N. Hepworth, J. Lobato, Tekflex resin spray field trials-Neves Corvo Mine Portugal, 2nd international seminar on surface support liners: thin spray liners, shotcrete, Mesh, 2002.
[192] D.M. Pappas, T.M. Barton, E.S. Weiss, The Long-Term Performance of Surface Support Liners for Ground Control in a Underground Mine, Third International Seminar on Surface Support Liners: Thin Spray-On Liners, Shotcrete, and Mesh, Department of Mining, Metallurgical and Materials Engineering, Quebec City, Queber, Canada, 2003.
[193] P.H. Ferreira, A. Piroddi, The application of GRP and thin spray liner support products in a typical block cave mining method to enhance safety and productivity, J. South. Afr. Inst. Min. Metall. 112 (2) (2012) 141–150.
[194] S. Akdag, M. Karakus, A. Taheri, G. Nguyen, H. Manchao, Effects of thermal damage on strain burst mechanism for brittle rocks under true-triaxial loading conditions, Rock. Mech. Rock. Eng. 51 (2018) 1657–1682.